

NAG 3-87

Discrete-Time Blade Pitch Control for Wind Turbine Torque  
Regulation with Digitally Simulated Turbulence Excitation

by

Ali-Reza Sharif-Razi

7N-37-CR

192952

p-183

A THESIS

submitted to

Oregon State University

(NASA-CR-184807) DISCRETE-TIME BLADE PITCH  
CONTROL FOR WIND TURBINE TORQUE REGULATION  
WITH DIGITALLY SIMULATED TURBULENCE  
EXCITATION Ph.D. Thesis (Oregon State  
Univ.) 183 p

N89-70361

00/37 Unclas  
0192952

in partial fulfillment of  
the requirements for the  
degree of

Doctor of Philosophy

Completed June 6, 1986

Commencement June 1987

Discrete-Time Blade Pitch Control for Wind Turbine Torque  
Regulation with Digitally Simulated Turbulence Excitation

by

Ali-Reza Sharif-Razi

A THESIS

submitted to

Oregon State University

in partial fulfillment of  
the requirements for the  
degree of

Doctor of Philosophy

Completed June 6, 1986

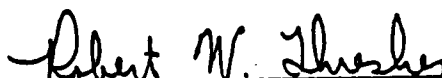
Commencement June 1987

AN ABSTRACT OF THE THESIS OF

Ali-Reza Sharif-Razi for the degree of Doctor of Philosophy in Mechanical Engineering presented on June 6, 1986.

Title: Discrete-Time Blade Pitch Control for Wind Turbine Torque Regulation with Digitally Simulated Random Turbulence Excitation

Abstract approved:



Robert W. Thresher



William E. Holley

A time domain simulation model which approximates the three-dimensional velocity fluctuations of wind turbulence has been developed. This model is used in a discrete time control algorithm to regulate the output torque of a wind turbine by changing the pitch angle of the turbine blade. The wind model provides a velocity field which varies randomly with time and space and gives the proper correlation between spatial locations and velocity components. In addition, the spectral representations approximate those observed from a rotating reference frame. The version of the model described in this report is a time domain simulation. It makes use of a random number gener-

ator to construct a white noise time series with a uniform power spectral density over the frequency range of interest. This noise source is then passed through a set of appropriate linear filters to obtain the various wind velocity fluctuations which would be experienced by a rotating wind turbine blade. The blade pitch angle remains fixed in the computation of average torque values for each revolution which does not permit a continuous control action to be implemented. Therefore, a discrete control model with a time interval equal to the period of the rotor revolution is chosen. A control action which compensates for the flapping oscillation and induces a torque step response with a small overshoot which reaches steady state in a minimum number of steps is desirable. To achieve this, an integral control action is combined with a digital narrow band rejection filter. The integral control action eliminates the steady error in the resulting torque response.

Discrete-Time Blade Pitch Control for Wind Turbine  
Torque Regulation with Digitally Simulated Random  
Turbulence Excitation

by

Ali-Reza Sharif-Razi

A THESIS

submitted to

Oregon State University

in partial fulfillment of  
the requirements for the  
degree of

Doctor of Philosophy

Completed June 6, 1986

Commencement June 1987

APPROVED:

Robert W. Thresher

Professor of Mechanical Engineering in charge of major

William E. Holley

Professor of Mechanical Engineering in charge of major

Gordon M. Keistak

Head of Mechanical Engineering Department

\_\_\_\_\_  
Dean of Graduate School

Date thesis is presented June 6, 1986

Typed by Peggy Offutt for Ali-Reza Sharif-Razi

## ACKNOWLEDGEMENTS

I would sincerely like to thank Dr. R.W. Thresher and Dr. W.E. Holley for their valuable and continuing help and support in the preparation of this thesis. I also would like to thank NASA Lewis Research Center Wind Power Office for funding the first part of this work under Grant NAG 3-87. I am very grateful to Ms. Bea Bjornstad from the Mechanical Engineering Department for her everlasting support and help during the years I spent at OSU. I am also grateful to Ms. Peggy Offutt for her efforts in putting this work into final form.

## TABLE OF CONTENTS

	<u>Page</u>
INTRODUCTION .....	1
I. DIGITAL SIMULATION OF TURBULENCE EXCITATION FOR DYNAMIC ANALYSIS OF WIND TURBINES	
CHAPTER I.1 TURBULENCE MODEL.....	3
I.1.1 Introduction.....	3
I.1.2 Model Assumptions and Approximations	4
I.1.3 Series Approximation to the Turbulent Velocity Field.....	6
I.1.4 Filtered Noise Model For Turbulence..	12
I.1.5 References.....	26
CHAPTER I.2. NUMERICAL SIMULATION.....	28
I.2.1 Introduction.....	28
I.2.2 Generation of Uniformly Distributed Random Numbers.....	28
I.2.3 Construction of a White-Noise Time Series.....	31
I.2.4 Filter Model.....	33
I.2.5 References.....	39
CHAPTER I.3. DIGITAL COMPUTER IMPLEMENTATION.....	40
I.3.1 Introduction.....	40
I.3.2 Input Data.....	40
I.3.3 Computer Algorithm for Turbulence Simulation.....	40
I.3.4 Tool Kit for Signal Analysis.....	43
I.3.5 References.....	49



CHAPTER I.4	RESULTS AND CONCLUSIONS.....	50
I.4.1	Introduction.....	50
I.4.2	Comparison of Simulation .....	50
I.4.3	Concluding Remarks.....	54
I.4.4	Reference.....	63
II.	DISCRETE-TIME BLADE PITCH CONTROL FOR WIND TURBINE TORQUE REGULATION	
CHAPTER II.1	TURBINE MODEL.....	64
II.1.1	Description of the Turbine Model....	64
II.1.2	References.....	68
CHAPTER II.2	CONTROL MODEL.....	69
II.2.1	Introduction.....	69
II.2.2	Development of the Transfer Function	69
II.2.3	Development of the Controller.....	71
II.2.4	References.....	92
CHAPTER II.3	IMPLEMENTATION OF THE CONTROL MODEL.	93
II.3.1	Controller Implementation.....	93
II.3.2	Reference.....	96
CHAPTER II.4	RESULTS AND CONCLUSIONS.....	99
BIBLIOGRAPHY.....		112
APPENDIX I.A	LINEAR LEAST-SQUARES REGRESSION.....	114
APPENDIX I.B	DIGITAL SPECTRAL ANALYSIS.....	120
APPENDIX I.C	COMPUTER CODE LISTING.....	124
APPENDIX I.D	INPUT DATA FILE.....	150
APPENDIX I.E	PROCEDURAL EXAMPLE OF THE PROGRAM SIMULX INTERACTIVE RUN.....	152
APPENDIX I.F	RESULTS OF THE SAMPLE RUN FOR Mod-0A TURBINE.....	154

APPENDIX II.A	PADÉ APPROXIMATION FOR MOVING AVERAGE PROCESS.....	160
APPENDIX II.B	.....	162

# LIST OF FIGURES

<u>Figure</u>		<u>Page</u>
I.1.1	Rotor disk coordinate system.....	24
I.1.2	Streamlines for in-plane velocity gradient terms.....	25
I.2.1	Time series constructed from a sequence of uniformly distributed random numbers.....	37
I.2.2	Autocorrelation function and spectral density function for the constructed time series.....	38
I.3.1	Flow chart of the program SIMULX.....	47
I.3.2	Flow chart of the subroutine TURBS.....	48
I.4.1	Simulated series for the longitudinal velocity component $V_y$ , as observed from the tip of a rotating MOD-0A blade with $V_w = 26.25$ ft/s, $\sigma/V_w = 0.10$ and $L = 400$ ft.	56
I.4.2	Spectral density plot of the $V_y$ simulated time series as observed from the tip of a MOD-0A wind turbine blade.....	57
I.4.3	Probability density for the MOD-0A turbulence simulation, $V_y$ component.....	58
I.4.4	Spectral density plot of the $V_z$ simulated time series as observed from the tip of a MOD-0A wind turbine blade.....	59
I.4.5	Probability density for the MOD-0A turbulence simulation, $V_z$ component.....	60
I.4.6	Spectral density plot of the $V_y$ turbulence component as observed from a MOD-2 rotor blade at different radial stations.....	61
I.4.7	Probability density for the $V_y$ component of Mod-2 simulation at 70% span.....	62
II.1.1	Illustration of the rotor system coordinates.....	67
II.2.1	Power regulation curve.....	80

II.2.2	Transient torque response to step change in pitch angle: a) -0.5 deg pitch change, b) +0.5 deg pitch change.....	81
II.2.3a	Block diagram of the wind turbine blade transfer function and proportional and integral feedback control model.....	82
II.2.3b	System block diagram of the zero order hold and sampler.....	82
II.2.3c	System discrete time block diagram.....	83
II.2.3d	Location of poles and zeros of the wind turbine blade transfer function.....	84
II.2.3e	Root locus illustration of the system inner loop with proportional feedback controller..	84
II.2.3f	Root locus illustration of the system closed loop transfer function for gain a) $k_1 = 0.0$ , b) $k_1 = -0.1$ deg/ft-lb.....	85
II.2.4a	Discrete block diagram of the wind turbine blade and notch filter feedback controller..	86
II.2.4b	Root locus illustration of the system inner loop with notch filter feedback controller.....	87
II.2.4c	Root locus illustration of the system closed loop transfer function for gain $k_1 = -0.1$ deg/ft-lb.....	87
II.2.5a	Discrete block diagram of the wind turbine blade and notch filter feedback controller with integral action.....	88
II.2.5b	Root locus illustration of the system closed loop transfer function with notch filter and dead beat controller.....	89
II.2.5c	Location of poles and zeros of the system closed loop transfer function.....	89
II.2.5d	Location of poles and zeros of the system closed loop a) positive step transfer function, b) negative step transfer function.....	90
II.2.6	Torque step response to a unit change in reference torque.....	91

II.3.1	Static pitch control gain for different wind speeds.....	98
II.4.1a	Average torque response for 20% step reduction in reference torque for wind speed = 20 mph.....	102
II.4.1b	Blade pitch angle control for 20% step reduction in reference torque for wind speed = 20 mph.....	103
II.4.2a	Average torque response for 20% step reduction in reference torque for wind speed = 35 mph.....	104
II.4.2b	Blade pitch angle control for 20% step reduction in reference torque for wind speed = 35 mph.....	105
II.4.3	Fixed pitch operation for wind speed = 20 mph.....	106
II.4.4	Active pitch control operation for wind speed = 20 mph.....	107
II.4.5	Average single blade torque over each revolution for wind speed = 20 mph.....	108
II.4.6	Fixed pitch operation for wind speed = 35 mph.....	109
II.4.7	Active pitch control operation for wind speed = 35 mph.....	110
II.4.8	Average single blade torque over each revolution for wind speed = 35 mph.....	111

## LIST OF TABLES

<u>Table</u>		<u>Page</u>
I.1.1	Relative approximation error for series approximation.....	20
I.1.2	Description of turbulence input terms.....	21
I.1.3	Regression parameters for uniform turbulence terms.....	22
I.1.4	Regression parameters for shear and quadratic turbulence terms.....	23
I.3.1	List of input variables.....	46
II.3.1	Control algorithm logic.....	97
II.4.1	Single blade torque response in turbulence..	101

# LIST OF SYMBOLS

$a$	dimensional atmospheric coefficient
$a_*$	dimensionless atmospheric coefficient
$A$	area of rotor disk
$[A]$	12x12 diagonal atmospheric coefficient matrix containing $a_*$ coefficients
$b$	dimensional atmospheric coefficient
$b_*$	dimensionless atmospheric coefficient
$[B]$	12x12 diagonal atmospheric coefficient matrix containing $b_*$ coefficients
$e(i)$	value of the output error at $i$ th step
$E(\cdot)$	expectation operator
$F(\cdot)$	probability density function
$f_i$	weight function
$g(\cdot)$	unit impulse response
$G(\cdot)$	transfer function
$i$	$\sqrt{-1}$
$k$	the $k^{\text{th}}$ stage or $k^{\text{th}}$ component
$k_1, k_2, K, K^*$	control action gain
$L$	turbulence integral scale
$m$	range of the random numbers
$r$	radial position on the rotor disk
$R$	rotor disk radius
$[R]$	state correlation matrix
$R_f$	autocorrelation function
$R_*$	$R/L$

$S_w$	power spectral density of white noise excitation
$t$	time
$T$	period of one rotor revolution in sec
$TI$	turbulence intensity in percent
$TQ_r$	reference torque in in-lb
$v_i$	the turbulence velocity component
$V_i$	turbulence uniform term
$V_{i,j}$	turbulence gradient term
$V_{i,kj}$	turbulence quadratic term
$V_w, V$	mean wind speed
$w$	12x1 nondimensional vector of independent white noise
$\bar{w}$	equivalent discrete time noise input
$x$	12x1 vector of system states
$x$	lateral coordinate
$x$	pseudorandom number
$y$	longitudinal coordinate
$z$	vertical coordinate

#### Greek Symbols:

$\mu$	expected mean value
$\tau$	time interval
$\sigma^2$	turbulent velocity component variance
$\gamma_{xz}$	swirl about mean wind axis (in-plane)
$\bar{\gamma}_{xz}$	shear strain rate (in-plane)
$\epsilon(i)$	filtered control error at ith step
$\epsilon_{xz}$	shear strain rate (in-plane)



$\bar{\epsilon}_{xz}$	dilation (in-plane)
$\Delta T$	time interval
$\theta(i)$	pitch angle command to actuator at ith step
$\phi$	transition matrix
$\psi$	azimuthal angular position in the rotor disk
$\xi$	damming ratio
$\omega$	frequency in radians/sec
$\omega_d$	forced frequency in radians/sec
$\omega_n$	natural frequency in radians/sec

Mathematical Symbols:

$\underline{A}$	defined equal to
$\approx$	approximately equal to
$L^{-1}$	inverse laplace transform
$z$	$z$ transform

# DISCRETE-TIME BLADE PITCH CONTROL FOR WIND TURBINE TORQUE REGULATION WITH DIGITALLY SIMULATED TURBULENCE EXCITATION

## INTRODUCTION

The objective of this report is twofold. In the first part a time domain simulation model which approximates the three-dimensional velocity fluctuations of wind turbulence is developed. In the second part a control algorithm is developed and incorporated into an existing simulation model of a wind turbine. The torque on the wind turbine rotating shaft is controlled by changing the pitch angle of the wind turbine blade. The input disturbances to the wind turbine are composed of steady and turbulence parts. The varying turbulent wind fluctuations are digitally simulated using the reports of the analysis in Part I.

The wind model provides a velocity field which varies randomly with time and space and gives the proper correlation between spatial locations and velocity components. In addition, the spectral representations approximate those observed for a rotating reference frame. It makes use of a random number generator to construct a white noise series with a uniform power spectral density over the frequency range of interest. This noise source is then passed through a set of appropriate linear filters to

obtain the various wind velocity fluctuations which would be experienced by a rotating wind turbine blade.

The program is written in Fortran V on the CDC Cyber 170/720 series. It is designed in a block-structured form so various tasks performed within the program are essentially separate routines and are linked together by an executive program. Appendices I.C. through I.F include a complete program listing, a sample input data file, a procedural example of the interactive features, and results of the sample run as observed from the tip of a Mod-0A wind turbine blade.

## CHAPTER I.1 TURBULENCE MODEL

### I.1.1 Introduction

Fluctuations in the aerodynamic forces on a wind turbine blade are generated by the relative motions of the air with respect to the blade. These relative motions are comprised of two parts: the motions of the blade and the motions of the air. The motions of the air can further be divided into the undisturbed turbulent flow and the "induced flow" due to the presence of the wind turbine wake. The terms comprising the undisturbed turbulent flow will be characterized in this chapter. More precisely, for a horizontal axis wind turbine, the aerodynamic forces are determined by the instantaneous air velocity distribution along each of the turbine blades. These blades, in turn, are rotating through the turbulence field which is being convected past the turbine rotor disk. It is thus necessary to characterize the wind turbulence field by a three-dimensional velocity vector which varies randomly with time and with the position in space. A complete statistical description of this turbulent velocity field requires the determination of all possible joint probability distributions between different velocity components at different times and positions in space. Clearly, such a description will not be possible without considerable simplification. The validity of the resulting simplified

model will depend upon a comparison of the characteristics predicted by the model and those observed in the atmosphere and more importantly, those observed in actual wind turbine field tests (1). The turbulence model used in this report is discussed in detail in reference (2) and is briefly described in this chapter for clarity.

### I.1.2 Model Assumptions and Approximations

The wind turbulence inputs used in the model are determined in three basic modeling steps. First, the turbulent velocity field is characterized by a model which gives the correlations between velocity components at different spatial points and at different time instants. Second, the velocity field is approximated in the rotor disk by a series which varies with time. A correlation model for these components is derived from the original field model. Third, simple rational spectral representations are determined which approximate the derived correlation model. A brief discussion of the assumptions and approximations used in these steps follows.

The turbulent velocity field is assumed to be stationary, locally homogeneous, isotropic (3), and satisfying Taylor's frozen field hypothesis (4). The Von Karman model (5) is used to characterize the correlations between velocities of spatially separated points. This model is widely used in aircraft turbulence response analysis

(6,7). However, due to the anisotropic nature of the atmospheric boundary layer, the use of the model for wind turbines can be questioned. Frost (8) has estimated that the deviation from isotropy is of secondary importance. However, one should not rely heavily on design calculations which use this model until more complete experimental verification is available.

Once the correlation model of the turbulence field is established, the velocity is approximated over the rotor disk by a series which varies with time. This is done to simplify the statistical nature of the random field to that of several stochastic processes.

In order to further simplify the model, the power spectral densities are approximated by a simple rational form, and nondimensional parameters are determined which match the low frequency power spectral density and the total variance for the computed spectra and the rational approximation. The rational form chosen corresponds to an exponentially correlated random process which is particularly easy to handle both analytically and in simulation. The following section describes the resulting model in more detail.

### I.1.3 Series Approximation to the Turbulent Velocity Field

The longitudinal component of turbulence (normal to the rotor disk) generally provides the most important aerodynamic effect on wind turbines (5). In order to provide an accurate determination of these effects, it is proposed to approximate the variation of the velocity across the rotor disk by a series which includes up to quadratic terms. Using Taylor's frozen field hypothesis relating the spatial and time dependency, the velocity across the rotor disk can be written as follows:

$$\begin{aligned}
 v_y(x, -V_w t, z) = & v_{y,0}(t) + v_{y,z}(t)z + v_{y,x}(t)x \\
 & + v_{y,zz}(t)\left(z^2 - \frac{1}{4} R^2\right) \\
 & + v_{y,xx}(t)\left(x^2 - \frac{1}{4} R^2\right) + v_{y,zx}(t)zx
 \end{aligned}
 \tag{1.1}$$

where  $v_y(x,y,z)$  is the velocity component depending on the  $x,y,z$  coordinates shown in Figure I.1.1 and  $R$  is the radius of the rotor disk. The series of functions:

$$f_0 = 1$$

$$f_1 = z$$

$$f_2 = x \quad (1.2)$$

$$f_3 = z^2 - \frac{1}{4} R^2$$

$$f_4 = x^2 - \frac{1}{4} R^2$$

$$f_5 = zx$$

were found by choosing polynomials with successively higher powers of  $x$  and  $z$  and enforcing conditions of mutual orthogonality over the rotor disk, i.e.,

$$\int f_j(x,z) f_k(x,z) dA = 0 ; \text{ for } j \neq k \quad (1.3)$$

Thus, the least-square functional approximation (i.e., the terms  $V_y, \dots$  which minimize the difference between  $v_y$  and the approximate value) is given using the usual generalized Fourier expansion formulas (6):

$$V_{y,0} = \int (1) v_y dA / \int (1)^2 dA$$

$$V_{y,z} = \int z v_y dA / \int z^2 dA$$

$$V_{y,x} = \int x v_y dA / \int x^2 dA \quad (1.4)$$

$$V_{y,zz} = \int (z^2 - \frac{1}{4} R^2) v_y dA / \int (z^2 - \frac{1}{4} R^2)^2 dA$$

$$V_{y,xx} = \int (x^2 - \frac{1}{4} R^2) v_y dA / \int (x^2 - \frac{1}{4} R^2)^2 dA$$

$$V_{y,zx} = \int zx v_y dA / \int (zx)^2 dA$$



Note that the time argument has been dropped for these equations. It should be understood that these equations apply at any instant of time. Now, when the statistics of the terms  $V_{y,zz}$  and  $V_{y,xx}$  are considered it is found that correlation between the terms exists which complicates the statistical modeling. To alleviate this problem, linear combinations of the last three terms are defined so that the resulting six terms are all mutually uncorrelated. Thus, we define

$$\begin{aligned} V_{y,rr} &= \frac{1}{2} (V_{y,zz} + V_{y,xx}) \\ V_{y,rc} &= \frac{1}{2} (V_{y,zz} - V_{y,xx}) \\ V_{y,rs} &= \frac{1}{2} V_{y,zx} \end{aligned} \tag{1.5}$$

Converting to polar coordinates and substituting Eqs. (1.5) into Eqs. (1.1) and (1.4) gives the following form for the series

$$\begin{aligned} v_y &= V_{y,o} + V_{y,z} r \cos\psi + V_{y,x} r \sin\psi \\ &\quad + V_{y,rr}(r^2 - \frac{1}{2} R^2) + V_{y,rc} r^2 \cos 2\psi \\ &\quad + V_{y,rs} r^2 \sin 2\psi \end{aligned} \tag{1.6}$$

where the six relations:

$$\begin{aligned}
V_{y,o} &= \frac{1}{\pi R^2} \int_0^R \int_0^{2\pi} v_y r dr d\psi \\
V_{y,z} &= \frac{4}{\pi R^4} \int_0^R \int_0^{2\pi} v_y (r \cos \psi) r dr d\psi \\
V_{y,x} &= \frac{4}{\pi R^4} \int_0^R \int_0^{2\pi} v_y (r \sin \psi) r dr d\psi \\
V_{y,rr} &= \frac{12}{\pi R^6} \int_0^R \int_0^{2\pi} v_y (r^2 - \frac{1}{2} R^2) r dr d\psi \\
V_{y,rc} &= \frac{6}{\pi R^6} \int_0^R \int_0^{2\pi} v_y (r^2 \cos 2\psi) r dr d\psi \\
V_{y,rs} &= \frac{6}{\pi R^6} \int_0^R \int_0^{2\pi} v_y (r^2 \sin 2\psi) r dr d\psi
\end{aligned} \tag{1.7}$$

Given a three-dimensional correlation model for the velocity component  $v_y$ , it is then possible to utilize Eqs. (1.7) to compute the correlation statistics or power spectral densities for the six "indicial" velocity terms:  $V_{y,o}$ ,  $V_{y,z}$ , etc. Before proceeding to do this, however, we will first consider the convergence properties of the series.

In general, the convergence of a series based on orthogonal functions requires that the true function be square integrable over the domain of interest (7). The turbulent velocity component,  $v_y$ , is a random variable depending on space and time, so that the usual Riemann integration does not apply. The theorems of stochastic integration (8) can be used instead, and the concept of

convergence of the series can be defined so that the variance of the difference between the true value and that given by the truncated series goes to zero as more and more terms in the series are included (9). Since the variance of this approximation error is positive over the whole domain, a necessary and sufficient condition for convergence of the series is that the error variance, averaged over the domain, goes to zero. This averaged error variance is then a measure of the convergence properties of the series. Table I.1.1 shows the relative approximation error for the truncated series defined by Eq. (1.6).

$$\epsilon_2 = \frac{1}{\sigma^2 A} \int E[(v_y - \hat{v}_y)^2] dA \quad (1.8)$$

where  $\hat{v}_y$  = truncated series representation of  $v_y$

$\sigma^2$  = variance of  $v_y$

A = area of rotor disk.

The relative approximation error is seen to depend on the dimensionless parameter  $R/L$  where  $R$  is the disk radius and  $L$  is the turbulence integral scale. The computation was carried out using the three-dimensional Von Karman correlation function for isotropic turbulence (10).

Also shown in Table I.1.1 are the relative approximation errors when only the uniform term  $V_{y,o}$  is retained and when the uniform and shear terms  $V_{y,o}$ ,  $V_{y,z}$ , and  $V_{y,x}$  are retained. These relative approximation errors are

designated  $\epsilon_0$  and  $\epsilon_1$ , respectively. It can immediately be seen from the table that the quadratic terms improve the approximation and that the approximation is relatively poor when the disk radius approaches the turbulence integral scale. It must be remembered, however, that the Von Karman model does not account for the effects of high wave number viscous dissipation and that the aerodynamic wind turbine rotor forces are always given by spatial integrations which also provide low-pass wave number filtering. Thus, it is expected that these aerodynamic forces will be computed more accurately using the truncated series approximation than is indicated by the data in Table I.1.1.

Using uniform and linear gradient terms to approximate the in-plane velocity components yields six turbulence input terms which vary with time. The complete turbulence model can then be written in the following form:

Normal Velocity Components:

$$\begin{aligned}
 v_y(x, -V_w t, z) = & V_{y,0} + V_{y,z}(z) + V_{y,x}(x) \\
 & + V_{y,rr}(z^2 + x^2 - \frac{1}{2} R^2) \\
 & + V_{y,rc}(z^2 - x^2) + V_{y,rs}(2zx) \quad (1.9)
 \end{aligned}$$

### In-Plane Velocity Components:

$$\begin{aligned} v_z(x, -V_w t, z) &= V_{z,0} + \gamma_{zx} x + \bar{\gamma}_{zx} x + \epsilon_{zx} z + \bar{\epsilon}_{zx} z \\ v_x(x, -V_2 t, z) &= V_{x,0} - \gamma_{zx} z + \bar{\gamma}_{zx} z - \epsilon_{zx} x + \bar{\epsilon}_{zx} x \end{aligned} \quad (1.10)$$

where the time-dependent linear gradient turbulence parameters are given by

$$\begin{aligned} \gamma_{zx} &= \frac{1}{2} (V_{z,x} - V_{x,z}) \\ \bar{\gamma}_{zx} &= \frac{1}{2} (V_{z,x} + V_{x,z}) \\ \epsilon_{zx} &= \frac{1}{2} (V_{z,z} - V_{x,x}) \\ \bar{\epsilon}_{zx} &= \frac{1}{2} (V_{z,z} + V_{x,x}) \end{aligned}$$

There are twelve turbulence inputs which define the turbulence model. These twelve terms are described in Table I.1.2. Drawings of typical fluid streamlines are shown in Figure I.1.2 for the in-plane gradient terms.

#### I.1.4 Filtered Noise Model For Turbulence

Each of these twelve terms are modeled as a stationary exponentially correlated random process, and they are assumed to be uncorrelated with each other; although it can be shown using mass continuity that  $V_{y,0}$ ,  $\bar{\epsilon}_{zx}$  and  $V_{y,rr}$  must be correlated. The  $\bar{\epsilon}_{zx}$  and  $V_{y,rr}$  terms are relatively small compared with  $V_{y,0}$ , and are not associated with large aerodynamic forces allowing this simplification.

tion without introducing large error. This makes it possible to represent the turbulence inputs in the following way

$$\frac{dx}{dt} = Ax + Bw \quad (1.11)$$

where  $x$  = the vector of system states

$w$  = the vector of independent white noise  
excitations

$A, B$  = matrices.

The state correlation matrix is defined by

$$R(\tau) = E[x(t + \tau)x^T(t)] \quad (1.12)$$

and is computed from the differential equation (for  $\tau > 0$ )

$$\frac{d}{d\tau} R = AR, \quad R(0) = X \quad (1.13)$$

where the covariance matrix  $X$  (assuming zero mean) is given by the solution to the Lyapunov equation (11)

$$AX + XA^T + B S_w B^T = 0 \quad (1.14)$$

and  $S_w$  is the diagonal matrix of noise power spectral densities.

Assuming that the turbulence terms  $V_{y,o}$ ,  $V_{y,z}$ , etc. form the state of a system in the form of Eq. (1.11), the correlation matrix  $R(\tau)$  is given by the various cross correlations among the individual terms. For example,

$$\begin{aligned}
E[V_{y,z}(t+\tau)V_{y,z}(t)] = & \\
& \left(\frac{1}{\pi R^2}\right)^2 \iint E[x_1, -V_w(t+\tau), z_1] v_y(x_2, -V_w t, z_2)] \\
& \cdot z_1 z_2 dA_1 dA_2
\end{aligned} \tag{1.15}$$

where the integration is over two disks of radius  $R$ . The subscripts 1 and 2 refer to coordinates in the two disks, respectively. Given the correlation matrix  $R(\tau)$ , the matrix  $A$  can be computed by integrating Eq. (1.13)

$$R(\infty) - R(0) = A \int_0^{\infty} R(\tau) d\tau \tag{1.16}$$

or

$$A = -X[S_+]^{-1} \tag{1.17}$$

$$\begin{aligned}
\text{where } S_+ &= \int_0^{\infty} R(\tau) d\tau \\
X &= R(0)
\end{aligned}$$

$$\text{and } R(\infty) = 0.$$

The  $B$  matrix then must satisfy Eq. (1.14) so that

$$B S_w B^T = - (AX + XA^T) \tag{1.18}$$

If the noise terms are chosen (for simplicity) to have identical power spectral densities, then

$$BB^T = - \frac{1}{S_w} (AX + XA^T) \tag{1.19}$$

where  $S_w$  is now the scalar PSD of each noise excitation.

A unique matrix  $B$  can be determined if it is also required

to be triangular, the result of which is called the Chloeskii square root matrix (12).

In cases where  $R(\tau)$  is diagonal, considerable simplification results. In this case, A and B will both be diagonal and the resulting scalar equations apply:

$$\begin{aligned} A_k &= - \frac{X_k}{S_{+k}} \\ B_k &= \sqrt{- \frac{2A_k X_k}{S_w}} \end{aligned} \quad (1.20)$$

where the subscript indicates the  $k^{\text{th}}$  diagonal element.

It is convenient to choose the noise power spectral density

$$S_w = \frac{\sigma^2 L}{V_w^3} \quad (1.21)$$

thereby defining the noise vector to be dimensionless.

Also, dimensionless parameters can be chosen so that

$$a_* = - \frac{L A_k}{V_w} \quad (1.22)$$

$$\frac{L B_k}{V_w^2} \quad \text{for uniform terms}$$

$$b_* = \frac{RL B_k}{V_w^2} \quad \text{for shear terms} \quad (1.23)$$

$$\frac{R^2 L B_k}{V_w^2} \quad \text{for quadratic terms}$$

These parameters only depend on the dimensionless ratio  $R/L$ , where again  $R$  is the disk radius and  $L$  is the turbu-



lence integral scale. The previous work (13) gives a table of values for the  $a_*$  and  $b_*$  parameters for the uniform and shear values, while the quadratic terms are found in (14). In summary, then, for a given turbine rotor size and turbulence scale, the  $a_*$  and  $b_*$  parameters are given. Then using the steady wind speed  $V_w$  and the turbulent velocity variance  $\sigma^2$ , the dimensional parameters governing the model are then computed.

In order to avoid the inconvenient interpolation necessary in evaluating the model parameters when  $R/L$  is not a tabulated value, a regression procedure was utilized to give a formula for calculating the dimensionless parameters. For the uniform terms, the following form was found to describe the data:

$$a_* \text{ or } b_* = k_1 - \frac{k_2 R_* (1 + k_3 R_*)}{(1 + k_4 R_*)} \quad (1.24)$$

where  $R_* = \frac{R}{L}$ .

The parameters  $k_1$ , etc. were determined as follows:

1.  $k_1$  is given by the limit as  $R_* \rightarrow 0$ , which is either 1, 2 or  $\sqrt{2}$ .
2. Assuming  $k_3 = 0$  and  $R_*$  is small, Eq. (1.24) can be rearranged so that

$$a_* \text{ or } b_* = k_1 - k_2 R_* + k_2 k_4 R_*^2 \quad (1.25)$$

the parameters  $k_2$  and  $k_4$  can be found using standard linear regression using the data for small  $R_*$ .

3. The equation is then rearranged into the form

$$a_* \text{ or } b_* = k_1 + c_1 \frac{k_4 R_*}{1 + k_4 R_*} + c_2 R \quad (1.26)$$

and the parameters  $c_1$  and  $c_2$  are again determined using standard linear regression with  $k_1$  and  $k_4$  fixed. These values then give the final values of  $k_2$  and  $k_3$  parameters.

Table I.1.3 shows the resulting regression parameters for the uniform turbulence terms including the in-plane velocity components described in the previous work (14).

For the shear and quadratic terms a different form was found to fit the data. In this case,

$$a_* \text{ or } b_* = k_1 R_*^{-k_2} + k_3 + k_4 R_* \quad (1.27)$$

The parameter  $k_2$  was chosen to match the slope of a log-log plot of  $a_*$  or  $b_*$  vs.  $R_*$ . A value of  $k_2 = 1$  was found to give good results for  $a_*$  and  $k_2 = 1/4$  for  $b_*$ . The remaining parameters,  $k_1$ ,  $k_3$  and  $k_4$ , were determined by standard linear regression. Table I.1.4 gives the resulting values for both the normal and in-plane components for the shear terms and for the normal component quadratic

terms. Again the data for the in-plane terms were taken from reference (15). In all cases the maximum deviation of the data from the regression curves was less than 5%.

The model describing the turbulent velocity fluctuations can be summarized in polar coordinates in the following manner

#### Normal Velocity

$$\begin{aligned} v_y(r, t, \psi) = & V_{y,o} + V_{y,x}(r \sin \psi) + V_{y,z}(r \cos \psi) \\ & + V_{y,rr}(r^2 - R^2/R) + V_{y,rc}(r^2 \cos 2\psi) \\ & + V_{y,rs}(r^2 \sin 2\psi) \end{aligned} \quad (1.28)$$

#### In-Plane Velocities

$$\begin{aligned} v_x(r, t, \psi) = & V_{x,o} + (\bar{\gamma}_{zx} - \gamma_{zx}) r \cos \psi \\ & + (\bar{\epsilon}_{zx} - \epsilon_{zx}) r \sin \psi \\ v_z(r, t, \psi) = & V_{z,o} + (\gamma_{zx} + \bar{\gamma}_{zx}) r \sin \psi \\ & + (\epsilon_{zx} + \bar{\epsilon}_{zx}) r \cos \psi \end{aligned} \quad (1.29)$$

where from Figure I.1.1,  $z = r \cos \psi$  and  $x = r \sin \psi$ .

Each of the turbulence terms ( $V_{y,o}$ ,  $V_{x,o}$ , ...,  $V_{y,rs}$ ) is given by an equation of the form

$$\frac{d}{dt} [v_{y,.}] + a v_{y,.} = bw \quad (1.30)$$

where  $a$  and  $b$  are defined by

$$a = - \frac{V_w}{L} a_* \quad (1.31)$$

$$b = \begin{array}{ll} (V_w^2/L) b_* & \text{for uniform terms} \\ (V_w^2/RL) b_* & \text{for shear terms} \\ (V_w^2/R^2L) b_* & \text{for quadratic terms} \end{array} \quad (1.32)$$

where  $a_*$  and  $b_*$  are given by the regression Eqs. (1.24) or (1.26) and depend on the ratio  $R/L$ . The white noise term  $w$  for each of the twelve turbulence terms is an independent noise source with  $\text{PSD} = \frac{\sigma^2 L}{V_w^3}$ . A computer program which calculates the values of  $a$  and  $b$  in Eqs. (1.30) is given as the subroutine ATMOS in Appendix I.C.

Table I.1.1. Relative Approximation Error for Series Approximation.

R/L	$\epsilon_0$	$\epsilon_1$	$\epsilon_2$
.01	.044	.026	.020
.054	.135	.081	.060
.1	.201	.121	.091
.3	.397	.250	.189
.5	.527	.348	.264
1.0	.724	.527	.411
2.0	.889	.737	.608

Table I.1.2. Description of Turbulence Input Terms.

Component	Description
$V_{x,o}$	uniform lateral or side component (in plane)
$V_{y,o}$	uniform longitudinal component along mean wind
$V_{z,o}$	uniform vertical component (in plane)
$V_{y,x}$	lateral gradient of longitudinal velocity
$V_{y,z}$	vertical gradient of longitudinal velocity
$\gamma_{zx}$	swirl about mean wind axis (in plane)
$\bar{\gamma}_{zx}$	shear strain rates (in plane)
$\epsilon_{zx}$	
$\bar{\epsilon}_{zx}$	dilation (in plane)
$V_{y,rr}$	symmetric quadratic variation
$V_{y,rc}$	quadratic with $\cos 2\psi$ azimuthial variation
$V_{y,rs}$	quadratic with $\sin 2\psi$ azimuthial variation

Table I.1.3. Regression Parameters for Uniform Turbulence Terms.

		$k_1$	$k_2$	$k_3$	$k_4$
$V_z$ & $V_x$	$a^*$	2.0	2.894	-.1383	2.049
	$b^*$	2.0	3.290	+.0270	2.054
$V_y$	$a^*$	1.0	1.713	-.0790	2.048
	$b^*$	$\sqrt{2.0}$	2.713	+.01591	2.051

Table I.1.4. Regression Parameters for Shear and Quadratic Turbulence Terms.

		$k_1$	$k_2$	$k_3$	
$k_4$					
$V_{y,z}$ & $V_{y,x}$	$a^*$	.3266	1.0	.5953	-.1142
	$b^*$	.2811	.25	.6450	-.1500
$\gamma_{zx}$	$a^*$	.4343	1.0	.9170	-.1532
	$b^*$	.2579	.25	.6467	-.1093
$\bar{\gamma}_{zx}$ & $\epsilon_{zx}$	$a^*$	.5342	1.0	1.276	-2.147
	$b^*$	.1167	.25	.7733	-.1284
$\bar{\epsilon}_{zx}$	$a^*$	1.654	1.0	1.069	+2.154
	$b^*$	.3546	.25	.3951	+.2593
$V_{y,rr}$	$a^*$	1.091	1.0	.0276	+.0686
	$b^*$	.5508	.25	.6473	-.1365
$V_{y,rc}$ & $V_{y,rs}$	$a^*$	1.081	1.0	.0279	+.0685
	$b^*$	.3897	.25	.4567	-.0948



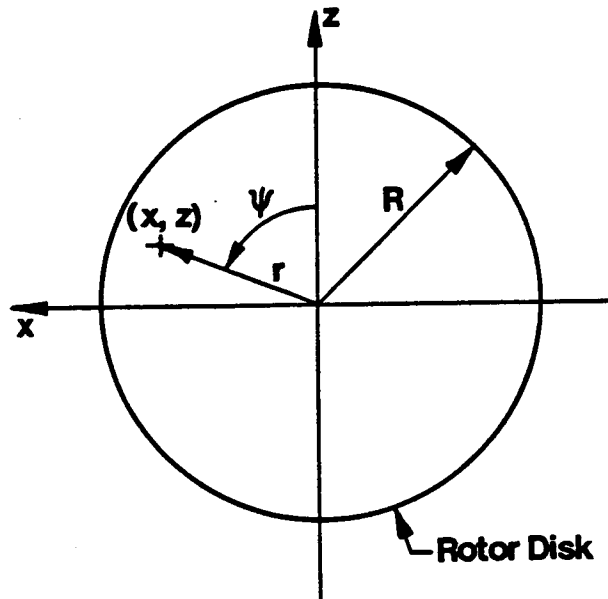


Figure I.1.1. Rotor disk coordinate system.

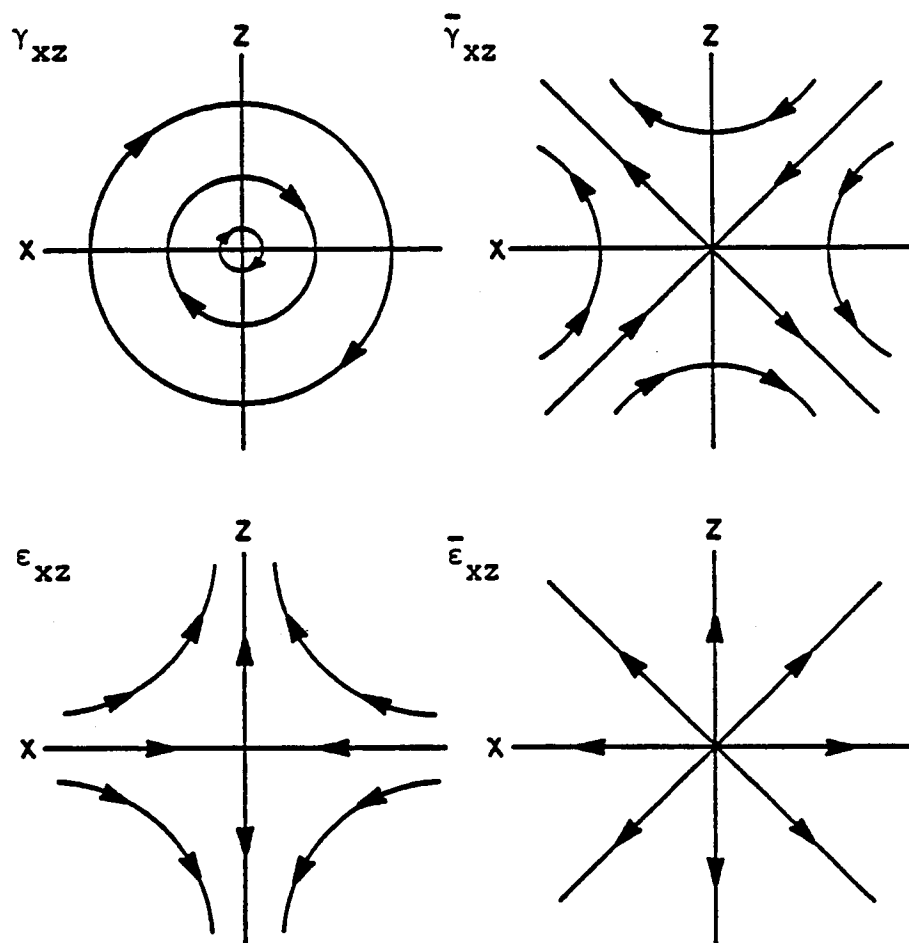


Figure I.1.2. Streamlines for in-plane velocity gradient terms.

## I.1.5 References

1. Connell, J.R., The Spectrum of Wind Speed Fluctuations Encountered by a Rotating Blade of a Wind Energy Conversion System: Observation and Theory, Battelle Pacific Northwest Laboratory, Report PNL 4083, 1981.
2. Thresher, R.W., et al., Modeling the Response of Wind Turbines to Atmospheric Turbulence, Oregon State University, Dept. of Mechanical Engineering, Report RLO/2227-81/2, Aug. 1981.
3. Kristensen, L. and Frandsen, Sten, "Model for Power Spectra Measured from the Moving Frame of Reference of the Blade of a Wind Turbine," Journal of Wind Engineering and Industrial Aerodynamics, V. 10, 1982, pp. 249-262.
4. Rosenbrock, H.H., Vibration and Stability Problems in Large Turbines Having Hinged Blades, ERA Technology Ltd., Surrey, England, Report C/T 133, 1955.
5. Thresher, R.W. and Holley, W.E., The Response Sensitivity of Wind Turbines to Atmospheric Turbulence, Oregon State University, Dept. of Mechanical Engineering, Report RLO/2227-81/1, May 1981.
6. Abroamowitz, M.A. and Segun, I.A., Handbook of Mathematical Functions, U.S. Nat. Bureau Standards, 1964, p. 790.

7. Isaacson, E. and Keller, H.B., Analysis of Numerical Methods, Wiley, 1966, p. 194.
8. Papoulis, A., Probability Random Variables and Stochastic Processes, McGraw-Hill, 1965, pp. 323-325.
9. Ibid, pp. 260-263.
10. Von Karman, T., "Sur la Theorie Statistique de la Turbulence," Comptes Rendus des Seanes de l'Acadamie de Sciences, v. 226, 1948, pp. 2108-2111.
11. Kwakernaak, H. and Sivan, R., Linear Optimal Control Systems, Wiley, 1972, p. 104.
12. Isaacson (1966) op. cit. p. 54.
13. Thresher, et al., (1981), op cit., pp. 142-145.
14. Ibid, pp. 138-146.
15. Ibid.
16. Ibid.

## CHAPTER I.2 NUMERICAL SIMULATION

### I.2.1 Introduction

The objective of this chapter is to outline the development for the digital simulation of the turbulence velocity terms. It consists of two parts. First, generation of uniformly distributed random numbers using the multiplicative congruential method to approximate a white-noise time series. Second, generation of the turbulence velocity terms by filtering the white-noise time series to obtain the required shape of the spectral density to produce the appropriate statistics for velocity fluctuations.

### I.2.2 Generation of Uniformly Distributed Random Numbers

There are a number of techniques for generating random variables by digital computers for simulation purposes. Most of these are reproducible and therefore the same sequence of numbers will be generated over and over again given the same starting input. It may be argued that such repeatable random numbers are, in the true statistical sense, deterministic, and not random. Since the digital computer consists of a finite, though large, number of states, the use of an algorithm for the generation of random variables also implies that eventually the computer must return to a state that had existed at the time of some previous implementation of the algorithm which starts the repetition cycle. However, as long as several

conditions are met random numbers generated by an algorithm on digital computers can be used for simulation problems. Numbers that are generated by means of a stored algorithm are accordingly referred to as pseudorandom.

Four criteria are usually employed to evaluate the suitability of random number generation method:

1. length of the sequence of the generated random variates,
2. uniformity of amplitude-density spectrum,
3. small degree of autocorrelation, and
4. speed of computer execution.

The first criterion simply means that the period of repetition should be much larger than the intended simulation period. The second implies that a uniform probability density is to be obtained and the degree of the true uniformity is to be a measure of quality. The third condition, if met perfectly, would mean that zero correlation would result, corresponding to true white noise. This is never the case and a reasonably small degree of correlation (and consequent deviation of the power-spectral density from a flat spectrum of white-noise) should be considered allowable.

However, the best criterion is the applicability of the method used to the problem at hand. Methods that are very satisfactory for some applications are found unsuitable when applied to others. With these considerations in

mind, the method to be suggested here is the one known either as the multiplicative congruential technique, or as the power residue method. It selects as the  $k^{\text{th}}$  pseudorandom number the remainder of the division of the product of a constant integer  $c$ , and the  $(k-1)^{\text{st}}$  pseudorandom number by some second constant  $m$ . Denoting  $x_k$  the  $k^{\text{th}}$  variate so generated, the operation is described mathematically as follows:

$$x_k = cx_{k-1} \pmod{m} \quad (2.1)$$

where the relation " $x \pmod{m}$ " denotes the selection of the remainder from the division of  $x$  by  $m$ . This technique is ideally suited for implementation on a digital computer.

In practice it is recommended that the starting seed value,  $x_0$ , be some odd number less than  $m$ . For a binary computer, one selects  $m = 2^b$  where  $b$  is the number of bits per word. The value of the constant  $c$  should be of the order  $m$  and in the form

$$c = 8k \pm 3 \quad \text{for any integer } k > 0$$

Thus providing a maximum period of  $2^{(b-2)}$  pseudorandom numbers, each between zero and  $2^b (1,2)$ . Dividing the generated variates by  $m$  gives the numbers between zero and one. This scheme is used in subroutine RANDOM of Appendix I.C to generate a sequence of uniformly

distributed random numbers, starting with an arbitrary selected seed value.

### I.2.3 Construction of a White-Noise Time Series

By definition a set of uniformly distributed random numbers with a range of 0 to  $m$  will have a probability density function given by

$$\begin{aligned} \text{probability} \\ \text{density function} \equiv f(x) = \begin{cases} \frac{1}{m} & 0 \leq x < m \\ 0 & \text{otherwise} \end{cases} \end{aligned} \quad (2.2)$$

The mean value and variance of the random variates may be computed from its probability density function, Eq. (2.2), as follows

$$\begin{aligned} \mu_x = E[X] &= \int_{-\infty}^{\infty} x f(x) dx = \frac{m}{2} \\ \sigma_x^2 &= E[X^2] - [E[X]]^2 = \frac{m^2}{12} \end{aligned} \quad (2.3)$$

A random time series can be constructed using this set of uniformly distributed random numbers. First, subtract the mean value from each of the variates to obtain a zero mean process, with all values between  $-\frac{m}{2}$  and  $\frac{m}{2}$ . Construct the time series,  $x(t)$ , by assuming that each of the variates,  $x_i$  occurs at intervals  $\Delta t$  apart, and that the value of  $x(t)$  is a constant for the period  $\Delta t$ . This



produces a random time series  $x(t)$ , which is a piecewise continuous function of time as illustrated in Figure I.2.1. If each number generated,  $x_i$ , is statistically independent and therefore uncorrelated with other numbers in the sequence, then the autocorrelation function of  $x(t)$  can be determined as

$$\begin{aligned}
 R_x(\tau) &= E [x(t)x(t+\tau)] \\
 &= \int_0^{\Delta t} x(t)x(t+\tau)f(t)dt \\
 R_x(\tau) &= \sigma_x^2 \left(1 - \frac{|\tau|}{\Delta t}\right)
 \end{aligned} \tag{2.4}$$

This autocorrelation function is plotted in Figure I.2.2. Inevitable imperfections in the white-noise properties of the random number generation process are evident by the presence of some degrees of correlation for  $|\tau| < \Delta t$ .

The corresponding power-spectral density of  $x(t)$  may be obtained using the above autocorrelation function as

$$\begin{aligned}
 S_x(\omega) &\triangleq \int_{-\infty}^{\infty} R_x(\tau) e^{-i\omega\tau} d\tau \\
 &= \sigma_x^2 \Delta t \left[ \frac{1 - \cos\omega\Delta t}{\frac{1}{2}(\omega\Delta t)^2} \right]
 \end{aligned} \tag{2.5}$$

which is also plotted in Figure I.2.2. If the interval,  $\Delta t$  is sufficiently small (i.e.,  $\omega\Delta t \ll 1$ ), relationship (2.5) becomes approximately

$$S_x(\omega) = \frac{m^2 \Delta t}{12} \left[ 1 - \frac{(\omega \Delta t)^2}{12} \right] \quad (2.6)$$

Note that if  $\Delta t$  is selected small enough, with respect to the range of frequencies involved in the simulation problem, it may be considered that the process takes place on the flat part of the spectral curve near  $\omega = 0$  (3). For this situation the signal is approximately white-noise with a constant spectral density of

$$S_x(\omega) = \frac{m^2 \Delta t}{12} \quad (2.7)$$

#### I.2.4 Filter Model

It was shown in Chapter 1 that each of the twelve turbulence terms in the turbulence model can be approximated by an uncorrelated stationary random process. Each term was given by an equation of the form

$$\dot{u} + au = bw \quad (2.8)$$

where  $u$  = instantaneous value of one of the turbu

lence terms,  $V_{y,o}, V_{x,o}, \dots, V_{y,rs}$

$w$  = nondimensional zero mean white-noise with

power spectral density  $S_w = \frac{\sigma^2 L}{V_w^3}$

$\sigma^2$  = turbulent velocity component variance

$L$  = turbulence integral scale

$V_w$  = mean wind speed

$R$  = rotor disk radius.

$a$  and  $b$  are given by Eqs. (1.31) and (1.32). The desired power spectral density of the turbulence velocity term is

$$S_u(\omega) = |G(j\omega)|^2 S_w = \frac{b^2 S_w}{a^2 + \omega^2} \quad (2.9)$$

where  $G(s)$  is the transfer function between the input white-noise,  $w$  and output turbulence velocity specified by Eq. (2.8).

To generate a turbulence velocity term digitally let us consider samples of the white-noise forcing function at discrete times  $t_0, t_1, \dots, t_k$ . Following the procedure outlined in (4), the solution to Eq. (2.8) at time  $t_{k+1}$  may be written as

$$u(t_{k+1}) = \phi(t_{k+1}, t_k) u(t_k) + \int_{t_k}^{t_{k+1}} b\phi(t_{k+1}, \tau) w(\tau) d\tau$$

and in an abbreviated form

$$u_{k+1} = \phi_k u_k + \bar{w}_k \quad (2.10)$$

$\phi_k$  is the state transition matrix for the step  $t_k$  to  $t_{k+1}$ , and  $\bar{w}_k$  is the driven response at  $t_{k+1}$  due to the presence of the white-noise input during the  $(t_k, t_{k+1})$  interval. Note that the white-noise input required in the continuous model automatically assures that  $\bar{w}_k$  will be an uncorrelated white-noise sequence in the discrete model (4).

From Eq. (2.8) the transition matrix is easily determined as

$$\phi_k = e^{-a\Delta t} \quad (2.11)$$

The variance of  $\bar{w}_k$  is established by using the convolution integral as

$$\sigma_{\bar{w}}^2 = E[\bar{w}^2] = \int_0^{\Delta t} \int_0^{\Delta t} g(u)g(v)R_f(u-v) du dv \quad (2.12)$$

where  $g[\cdot]$  = unit impulse response

$$g(t) \triangleq \mathcal{L}^{-1} [G(s)] = be^{-at} \quad (2.13)$$

and  $R_f[\cdot]$  = autocorrelation function of the input white-noise. The autocorrelation function of the input white-noise can be established as

$$R_f[u-v] = E[w(u)w(v)] = S_w \delta(u-v) \quad (2.14)$$

where  $S_w$  is the power spectral density of the input.

Substituting Eqs. (2.13) and (2.14) in Eq. (2.12) and carrying out the integration, the variance of  $\bar{w}_k$  becomes

$$\sigma_{\bar{w}}^2 = E[\bar{w}^2] = \frac{b^2 S_w}{2a} (1 - e^{-2a\Delta t}) \quad (2.15)$$

If the generated random signal  $x(t)$  with zero mean and variance  $\sigma_x^2 = \frac{m^2}{12}$  is used to approximate  $\bar{w}(k)$  at the time intervals  $t_1, t_2, \dots, t_k$ , and if

$$\bar{w}(k) = cx(k) \quad (2.16)$$

then the mean square of both sides is

$$E[\bar{w}^2] = c^2 E[x^2]$$

$$\sigma_{\bar{w}}^2 = c^2 \sigma_x^2$$

Substitute for  $\sigma_x^2 = \frac{m^2}{12}$  and solving for  $c$  gives

$$c = \left\{ \frac{6b^2 S_w}{am^2} (1 - e^{-2a\Delta t}) \right\}^{1/2} \quad (2.17)$$

Substituting Eq. (2.17) in Eq. (2.16) and using the result and Eq. (2.11) in Eq. (2.10), gives the turbulence velocity term at  $t_{k+1}$  as

$$u_{k+1} = e^{-a\Delta t} u_k + \left\{ \frac{6b^2 S_w}{am^2} (1 - e^{-2a\Delta t}) \right\}^{1/2} x_k \quad (2.18)$$

If the range of the random numbers,  $m$ , is 1 then Eq. (2.18) can be written as

$$u_{k+1} = e^{-a\Delta t} u_k + \left\{ \frac{6b^2 S_w}{a} (1 - e^{-2a\Delta t}) \right\}^{1/2} x_k \quad (2.19)$$

Evaluating the variance of the generic turbulence term from Eq. (2.9) gives

$$\sigma_u^2 = E[u^2(t)] = R_u(\tau=0) = \frac{1}{2\pi} \int_{-\infty}^{\infty} S_u(w) dw$$

$$\sigma_u^2 = \frac{b^2 S_w}{2a}$$

Taking the mean square of both sides of Eq. (2.19) gives an identical result.

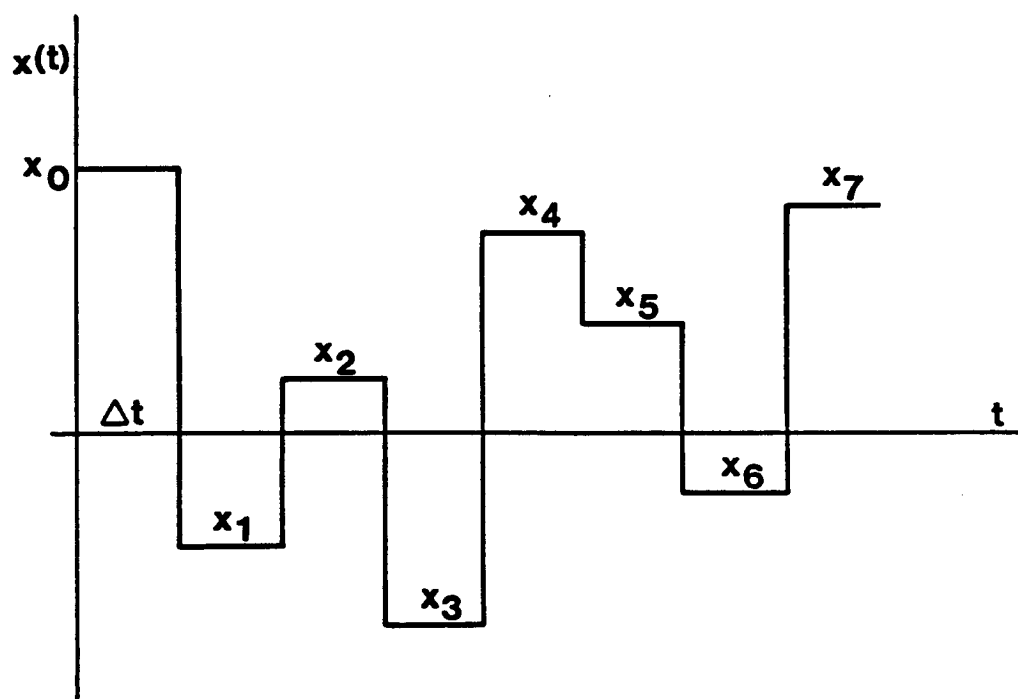
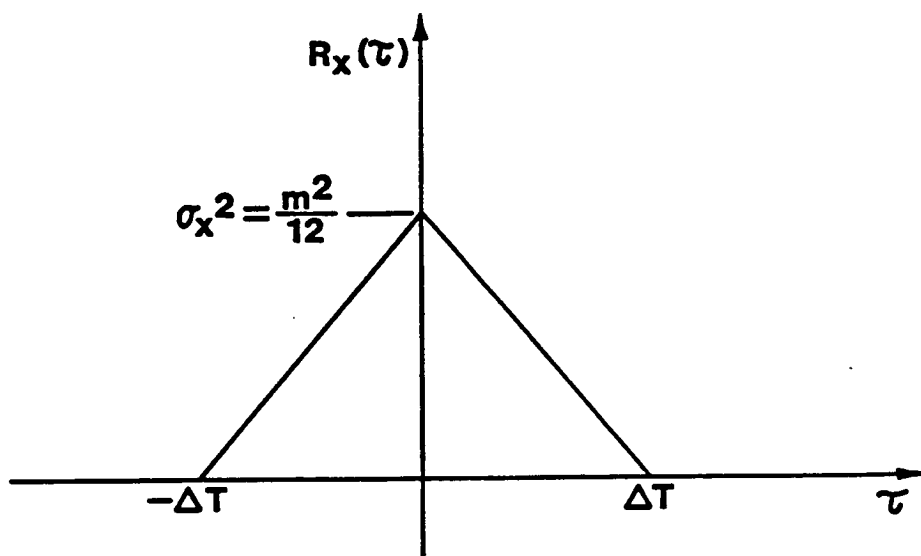
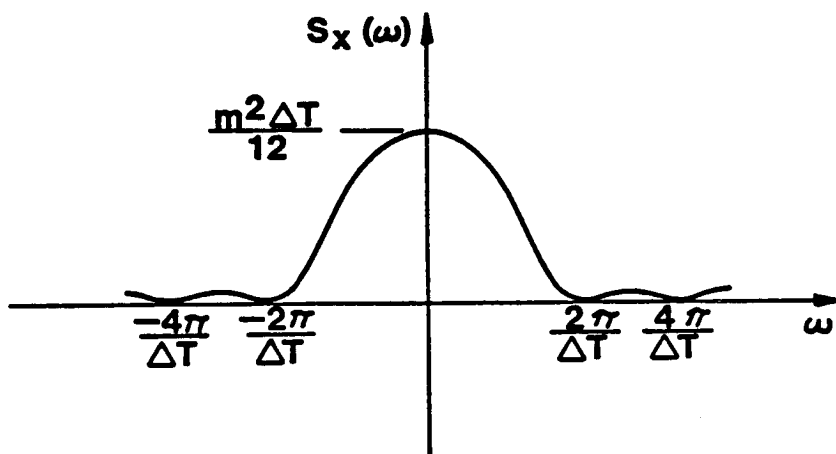


Figure I.2.1. Time series constructed from a sequence of uniformly distributed random numbers.



(a)



(b)

Figure I.2.2. (a) Autocorrelation function, and  
 (b) Spectral density function for the constructed time series.

### I.2.5 References

1. Mirham, G.A., Simulation, Statistical Foundations and Methodology, Academic Press, 1972, Ch. 2.
2. Hull, T.E. and Dobell, A.R., Random Number Generators, SIAM Rev. 4, 1962, pp. 230-254.
3. Kochenburger, R.J., Computer Simulation of Dynamic Systems, Prentice-Hall, 1972, pp. 405-445.
4. Brown, R.G., Random Signal Analysis and Kalman Filtering, John Wiley, 1983, pp. 181-211.



## CHAPTER I.3 DIGITAL COMPUTER IMPLEMENTATION

### I.3.1 Introduction

In this chapter the computer code for digital simulation of turbulence velocity components is discussed. The program is written in Fortran V on the CDC Cyber 170/720 series. It is designed in a block-structured form so the various tasks performed within the program are essentially separate routines and are linked together by an executive main program. It is run interactively but can be run in a batch mode with some prior preparation of response data.

### I.3.2 Input Data

A list of the input variables is given in Table I.3.1. The user has the opportunity to change any of the input variables listed in Table I.3.1 at execution time. When a run is completed the program allows the user to either end execution with the current data set, recycle the current data file with different values for the input variables, or employ a new data file.

### I.3.3 Computer Algorithm for Turbulence Simulation

It was shown in Chapter 1, Eqs. (1.28) and (1.29), that turbulence velocity components can be given in polar coordinates in the following form:

### Normal Velocity

$$\begin{aligned}
 v_y(r, \psi, t) = & V_{y,o} + V_{y,x} (r \sin \psi) + V_{y,z} (r \cos \psi) \\
 & + V_{y,rr} \left( r^2 - \frac{R^2}{2} \right) + V_{y,ro} (r^2 \cos 2\psi) \\
 & + V_{y,rs} (r^2 \sin 2\psi)
 \end{aligned} \tag{1.28}$$

### In-Plane Velocities

$$v_x(r, \psi, t) = V_{x,o} + (\bar{\gamma}_{zx} - \gamma_{zx}) r \cos \psi + (\bar{\epsilon}_{zx} - \epsilon_{zx}) r \sin \psi \tag{1.29}$$

$$v_z(r, \psi, t) = V_{z,o} + (\bar{\gamma}_{zx} + \gamma_{zx}) r \sin \psi + (\bar{\epsilon}_{zx} + \epsilon_{zx}) r \cos \psi$$

where each turbulence term ( $V_{y,o}$ ,  $V_{x,o}$ , ...,  $V_{y,rs}$ ) is given by an equation of the form

$$\frac{d}{dt} [v_{y,.}] + a v_{y,.} = b w$$

with  $a$  and  $b$  given by Eqs. (1.31) or (1.32).

The simulation routine SIMULX generates the appropriate  $a$  and  $b$  coefficients based on the given input data and the curve fitting contained in subroutine ATMOS. The procedure for obtaining these coefficients is described in Section 1, and the regression method is described in Appendix I.A. Next, the subroutine TURBS actually simulates the velocity fluctuations by first calling RANDOM to

generate a white noise time signal as discussed in Section 2.3. This signal is then filtered using Eq. (2.16) to obtain the twelve turbulence parameters of Table I.1.2,  $V_{x,o}$ ,  $V_{y,o}$ ,  $V_{z,o}$ ,  $V_{y,k}$ , etc. The values of these twelve turbulence parameters are then substituted into Eqs. (1.28) and (1.29) to obtain the resulting velocity fluctuations,  $v_x$ ,  $v_y$ , and  $v_z$ , at any desired radial station for the current time. As the procedure marches forward in time, the blade moves to a new azimuth angle and subroutine TURBS is called again to repeat the procedure. A flow chart of this process is shown in Figure I.3.1 for the executive program SIMULX, and Figure I.3.2 shows the flow chart for subroutine TURBS.

The number of points along the blade at which turbulence velocity is evaluated is given as the parameter, NPTS, in the program SIMULX, and can be easily changed. The turbulence velocity components then are computed at equally spaced points along the blade from an initial radius to a final radius which the user specifies. For the results presented here, only one radial position at the tip was considered (NPTS = 1). As much as possible, the code has been written to contain its own documentation through extensive use of comments within the program.

Appendices C through F include a complete program listing, a sample input data file, a procedural example of the interactive features, and the results of the sample

run as observed from the tip of a Mod-0A wind turbine blade.

#### I.3.4 Tool Kit for Signal Analysis

Analysis of random signals requires some basic mathematical tools. There are two general methods of describing random signals mathematically. The first, and more basic, is a probabilistic description in which the random quantity is characterized by a probability model. However, it tells very little about how the random signal varies with time, or how the amplitude varies as a function of frequency.

For this work dealing with atmospheric turbulence it is helpful to use some of the typical statistical measures to characterize the wind signal using the mean, variance, correlation function, and spectral density. These measures allow the signal which is being simulated to be compared with various theoretical models and with experimental data. This is essential because when comparing wind turbine responses generated using a simulated wind with responses obtained from field test measurements the comparison must be made for the "same" atmospheric conditions. This means that the mean, variance, and spectral density for the simulated wind should match those of the real atmosphere during the field test period. The tools

for computing these statistical parameters are discussed in this section.

Subroutine MEANVAR estimates mean and variance of a time series. Since each of the turbulence velocity components is computed by low pass filtering of a uniformly distributed white noise time series, it is expected that the resulting turbulent velocity fluctuations will have nearly a Gaussian distribution (1). To estimate the actual distribution subroutine ROB constructs a frequency histogram which can be compared with the standard normal distribution.

Subroutine PSD generates spectral density estimates of the generated velocity signals. It uses a fast Fourier transform (FFT) algorithm to calculate discrete Fourier transforms (DFT) (2). A cosine tapered data window is used to smooth the data at each end of the record before it is analyzed (which has the effect of sharpening the spectral window). In order to improve the accuracy of the results, the signal is broken into a number of segments and the spectral estimates for each segment are computed and then averaged for all segments at each frequency. A more detailed discussion of the digital signal analysis is given in Appendix I.B.

In order to obtain accurate estimates of the spectral density, relatively long sequences of random velocities are needed. The length of each of the time series seg-

ments in the code is set by the parameter LSPECT, which has been arbitrarily set equal to 128 in a parameter statement. It can easily be changed but must always equal an integer power of 2 for the FFT algorithm to work properly. The user specifies the number of random velocities generated as the input parameter, NRVELOC. The user can choose any size up to 6500, the dimension size of the array. Note that if NRVELOC is not evenly divisible by the segment length, LSPECT, then an appropriate number of zeros will be added to each time series. This might make the length of the time series exceed the declared array size for the velocity components. To avoid this, NRVELOC should be kept smaller than the velocity time series array size minus LSPECT, (currently  $\text{NRVELOC} < 6500 - 128$ ). Because of larger array sizes it might not be feasible to run this program interactively on some computers. Therefore, modification may be required depending on the needs and resources available to the user.

Table I.3.1. List of Input Variables.

---

CONST	constant coefficient in the power residue algorithm (subroutine RANDOM) for generation of uniformly distributed random numbers
DELTAT	time step interval for generation of random velocity components (sec)
DIVIDER	module used in function (mod) (.) in the power residue algorithm (subroutine RANDOM)
SEED	initial random number used in the power residue algorithm (subroutine RANDOM)
NRVELOC	number of elements of random turbulence velocity component sequences
OMEGA	rotor speed (rpm)
OMEGAZ	initial angular orientation in the rotor disk plane (deg)
ROTR	rotor radius (feet)
RRATIO	ratio of radial position to blade radius
TI	turbulence intensity ( $\frac{\sigma}{V_w}$ in percent)
TL	turbulence integral scale (feet)
VRANGE	number of standard deviations displayed for the turbulent velocity probability density function (usually selected to be 3)
$V_w$	mean wind velocity (mph)

---

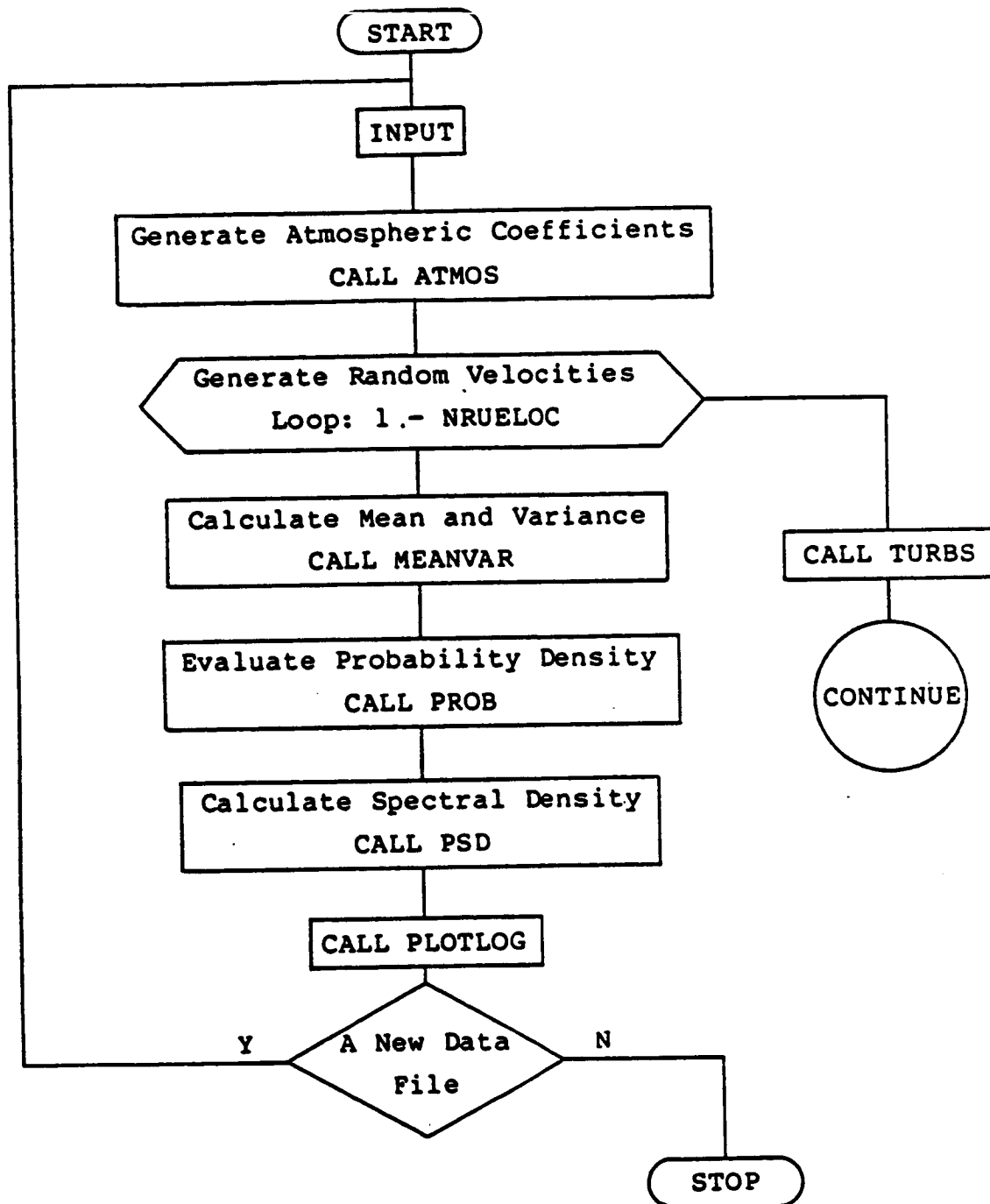
PROGRAM SIMULX

Figure I.3.1. Flow chart of the program SIMULX.



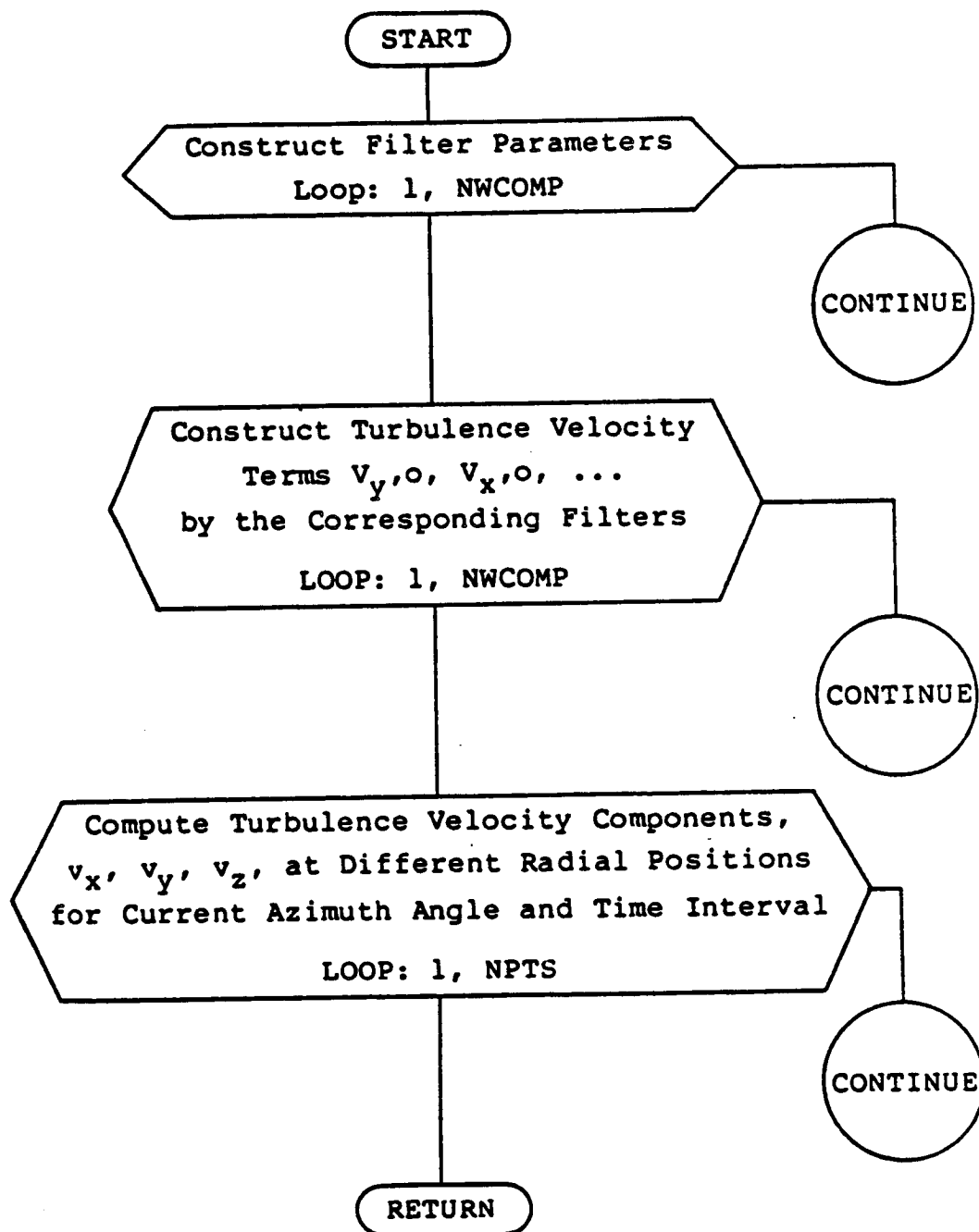
SUBROUTINE TURBS

Figure I.3.2. Flow chart of subroutine TURBS.

### I.3.5 References

1. Newland, D.E., An Introduction to Random Vibration and Spectral Analysis, Longman, 1975, pp. 80-81.
2. Ibid, Appendix 2.

## CHAPTER I.4 SIMULATION RESULTS

### I.4.1 Introduction

This chapter presents some typical results obtained using the computer code to simulate the turbulence inputs for wind turbines. Simulation results are presented for two wind turbine sizes. The first turbulence simulation is for the Mod-0A, 200 kW wind turbine, which has a rotor diameter of 125 ft. The spectral density of the simulated turbulence is compared with field test data taken from the vertical plane array experiments of George and Connell (1), for similar wind conditions. In addition, the results are compared with the theoretical Von Karman spectra for the atmospheric boundary layer. The second simulation is for a Mod-2, 300-ft diameter wind turbine. In this case, there is no appropriate test data which can be used for comparison, but a comparison is made with the Von Karman spectrum for the longitudinal velocity component.

### I.4.2 Comparison of Simulations

Figure 4.1 I. shows the simulation time series of the longitudinal velocity component,  $V_y$ , as observed from the tip of a rotating Mod-0A blade. In this simulation, the tip radius was taken as 62.5 ft and the rotor speed was 40 rpm. In addition, the parameters used for the turbulence simulation where  $V_w = 26.25$  ft/s,  $\sigma/V_w = 0.10$  and the turbulence integral scale,  $L$ , was 400 ft. In

Figure I.4.1, the mean wind speed has been removed. Figure I.4.2 presents the spectral density for the time series shown in Figure I.4.1. The simulated spectrum clearly shows the spikes at 1 and 2 cycles per rotor revolution that are the result of rotation of the blade through the wind turbulence field. However, the simulation results show no spikes higher than 2 cycles per revolution because the model only allowed for velocity fluctuation harmonics up to  $\sin 2\psi$  and  $\cos 2\psi$  as indicated by Eq. (1.28). The data taken from the vertical plane array is plotted showing harmonics up to 3 cycles per rotor revolution, but higher harmonics are present in the original presentation by George and Connell (1). The simulation results show considerably greater spectral energy in the frequency range of .1 to .3 hz than the VPA results. This is probably because the  $a^*$  and  $b^*$  coefficients used to generate the simulation were selected so that the Von Karman spectrum would be approximated in the low frequency range. As is shown in the figure, the comparison with the Von Karman spectrum in this frequency range is quite good. It would be possible to more closely approximate the vertical plane array data by adjusting the  $a^*$  and  $b^*$  coefficients for the  $V_{y,0}$  term of Eq. (1.28). In addition, it would be possible to add additional harmonics to the model in order to obtain the 3 and 4 cycles per revolution spectral spikes, but that would involve a signifi-

cant effort. It is hoped that some experience with the implementation of the existing model in a dynamics code could be obtained, before attempting to improve the simulation, and account for these additional effects.

Figure I.4.3 shows the probability density function for the time series of the  $V_y$  turbulent velocity fluctuations. As can be seen from the figure, the simulated velocity fluctuations closely approximate a Gaussian distribution.

Figure I.4.4 is a spectral density plot for the vertical velocity component,  $V_z$ , as provided by the simulation. The Von Karman spectrum for this turbulence component is also provided for comparison. The simulation is for the case where the turbulence is observed from the tip of a rotating Mod-0A blade. Whereas the Von Karman spectrum plotted is for a point fixed in space. The simulated spectrum shows a single spike at a frequency of 1 cycle per rotor revolution. Theoretically there should be many of these spikes each at a multiple of the rotor blade passage frequency. However, the simplified simulation model, Eq. (1.29), for the in-plane velocity components includes only the first harmonic. No field data is available for comparison of the in-plane velocity components. The simulation spectrum for the lateral velocity component was virtually identical to the results for the vertical component and therefore has not been presented.

Figure I.4.5 shows the probability density function for the time series of the  $V_z$  velocity fluctuations, and the figure shows the distribution to be approximately Gaussian.

Figure I.4.6 is the spectral density plot of the longitudinal velocity component,  $V_y$ , for a simulation run for a Mod-2 sized turbine. In this simulation, the mean wind speed was  $V_w = 32.15$  ft/s,  $\sigma/V_w = .061$  and the turbulence integral scale was taken as 500 ft. The velocity field was simulated at two radial locations along the rotor blade. One was at 30% span and the other was for the 70% span location. This illustrates one of the convenient features of this turbulence model. At each time step, the velocity fluctuations at all radial locations are obtained simultaneously, as can be seen by the form of Eq. (1.28). Figure I.4.6 includes the Von Karman spectrum for comparison. Figure I.4.7 shows a probability density plot for the velocity fluctuations at 70% span. Unfortunately, there is no appropriate test data with which to compare these simulation results at the Mod-2 sized turbine.

### I.4.3 Concluding Remarks

The authors offer the following conclusions and remarks on the basis of the work presented in this report:

1. The results presented here show that the turbulence simulation model does a reasonable job of representing many of the features of atmospheric turbulence.
2. The turbulence simulation model presented here does not model the spectral spikes in the wind input above 2 cycles per rotor revolution. If these spectral spikes at higher harmonics turn out to be important for cyclic load prediction then this model will be incomplete. It should be noted that this model does contain some spectral energy at the higher harmonics of rotor speed; it is the effect of rotating through the turbulence structure that is missing at the higher frequencies.
3. The great advantage of this model is its simple structure and fast computation speed. This simulation model will not significantly increase the complexity of a wind turbine dynamic model.

The authors hope that in the near future, this model will be used to generate inputs for a structural dynamic model,

so that its usefulness in predicting cyclic loads can be assessed. Ability to predict cyclic loads reasonably well for a small computational cost is the ultimate goal, and this simulation approach seems to offer promise of achieving that goal.



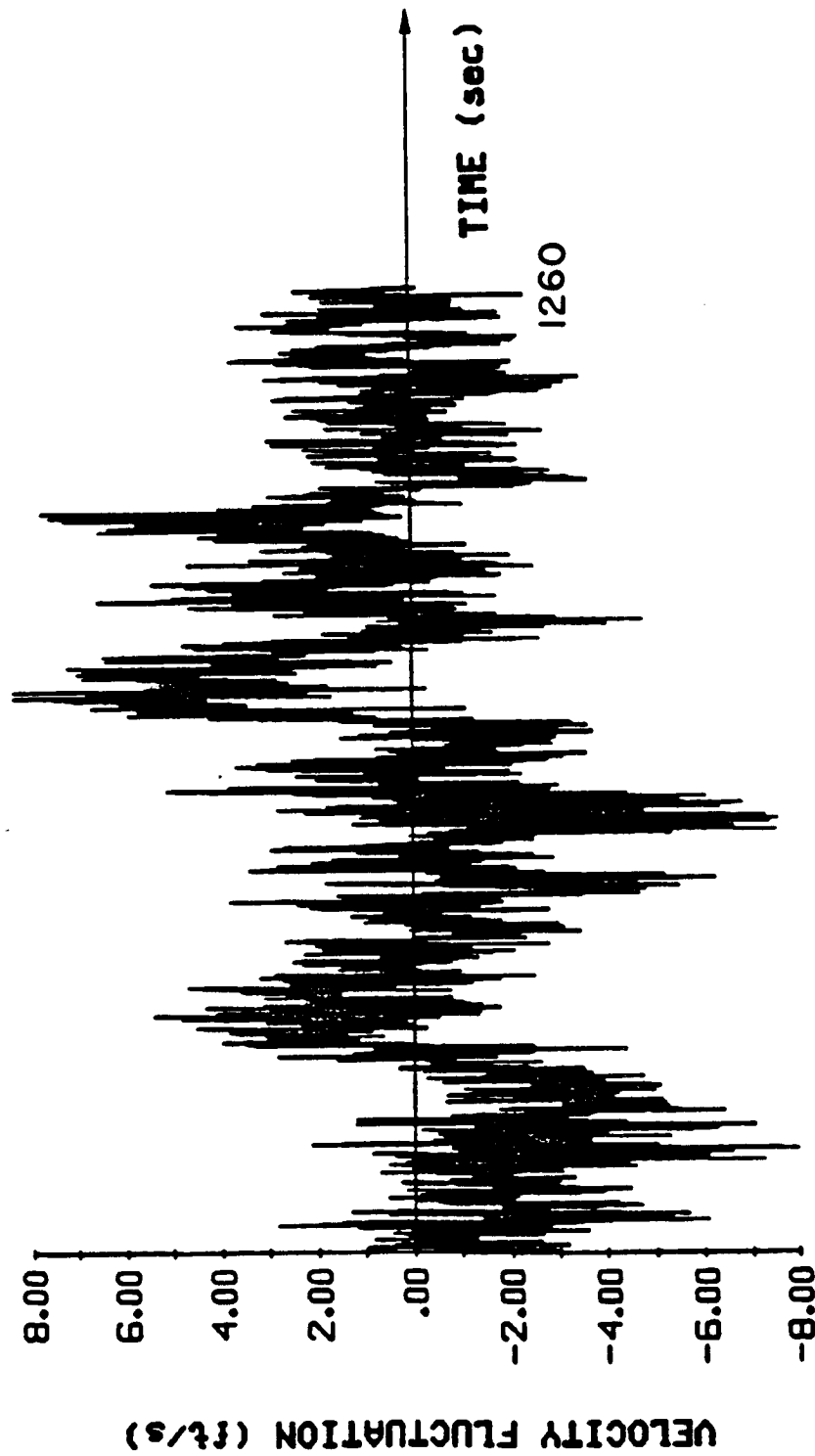


Figure I.4.1. Simulated time series for the longitudinal, velocity component,  $V_y'$ , as observed from the tip of a rotating Mod-0A blade with  $V_w = 26.25$  ft/s,  $\sigma/V_w = .10$ , and  $L = 400$  ft.

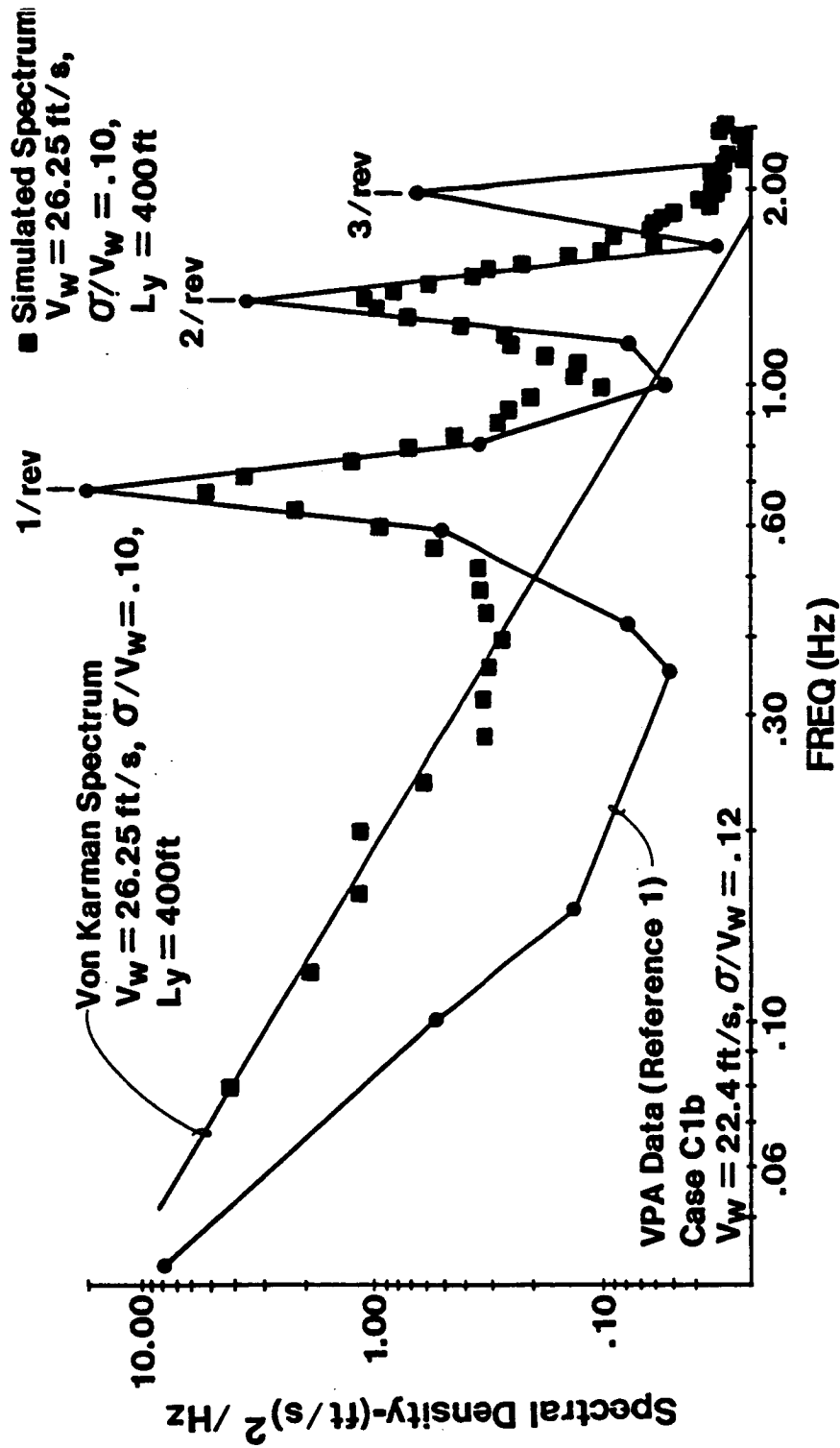


Figure I.4.2. Spectral density plot of the  $V_y$  simulated time series as observed from the tip of a Mod-0A wind turbine blade.

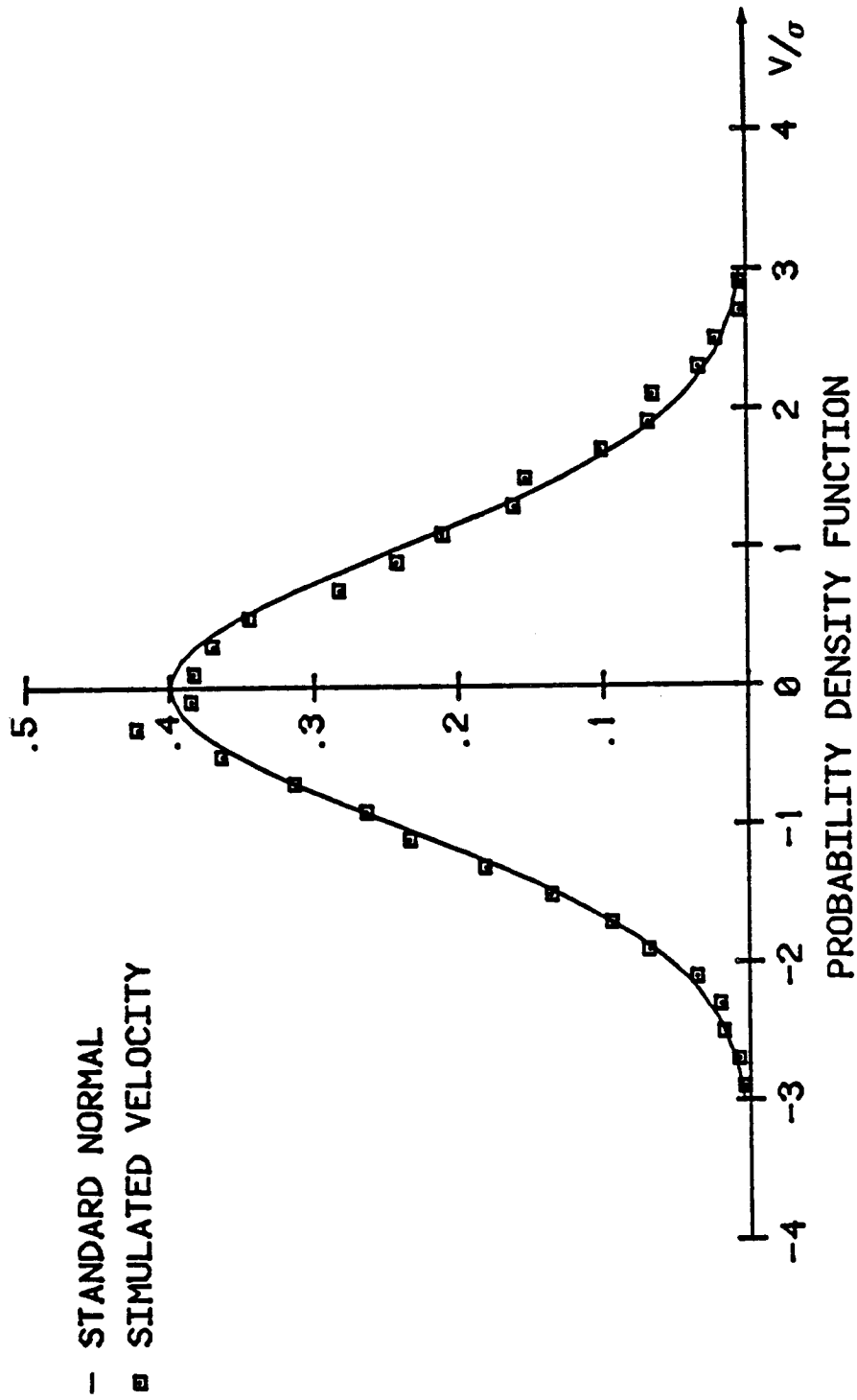


Figure I.4.3. Probability density for the Mod-0A turbine simulation,  $V_y$  component.

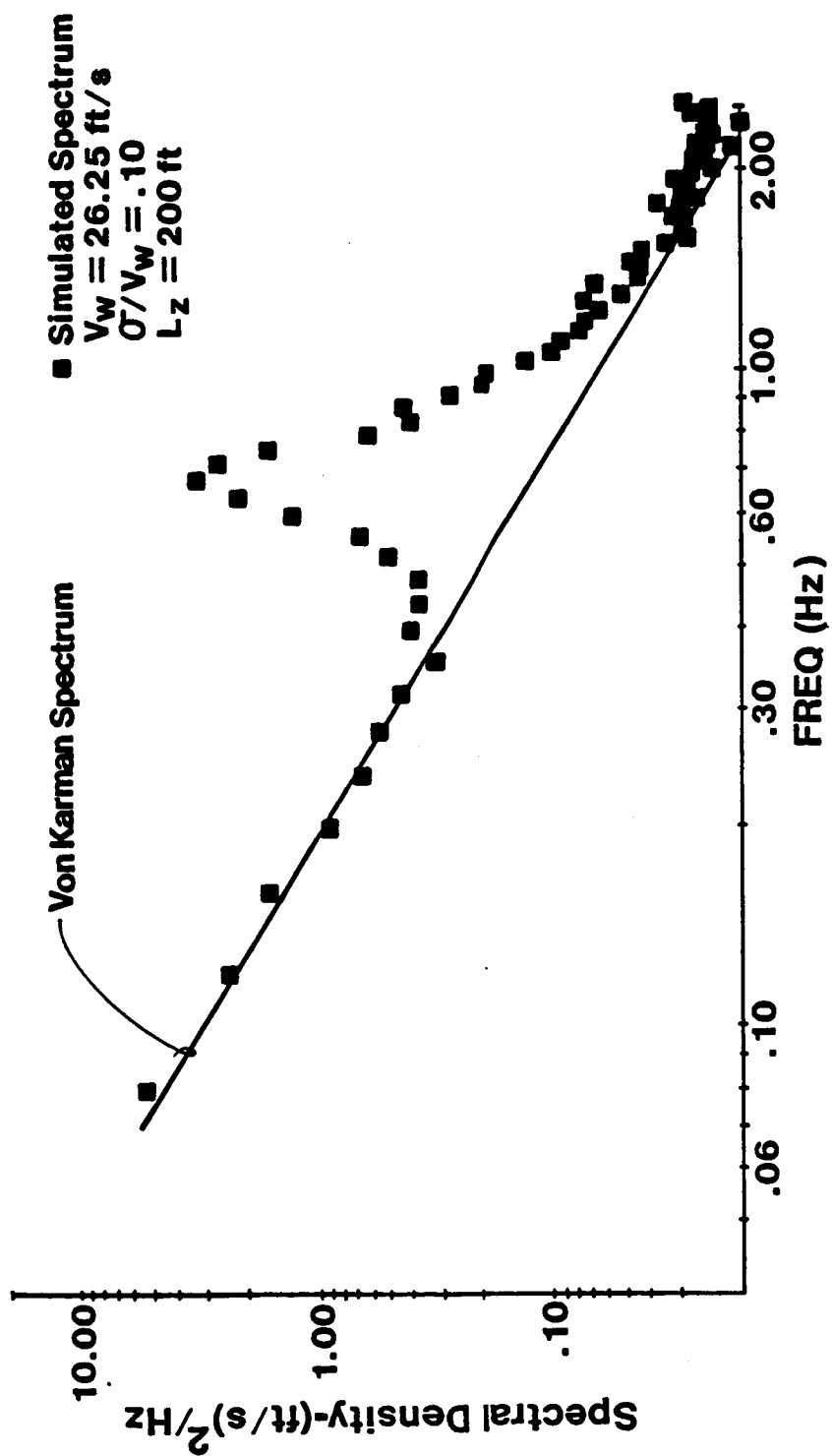


Figure I.4.4. Spectral density plot of the  $V_z$  simulated time series as observed from the tip of a Mod-0A wind turbine blade.

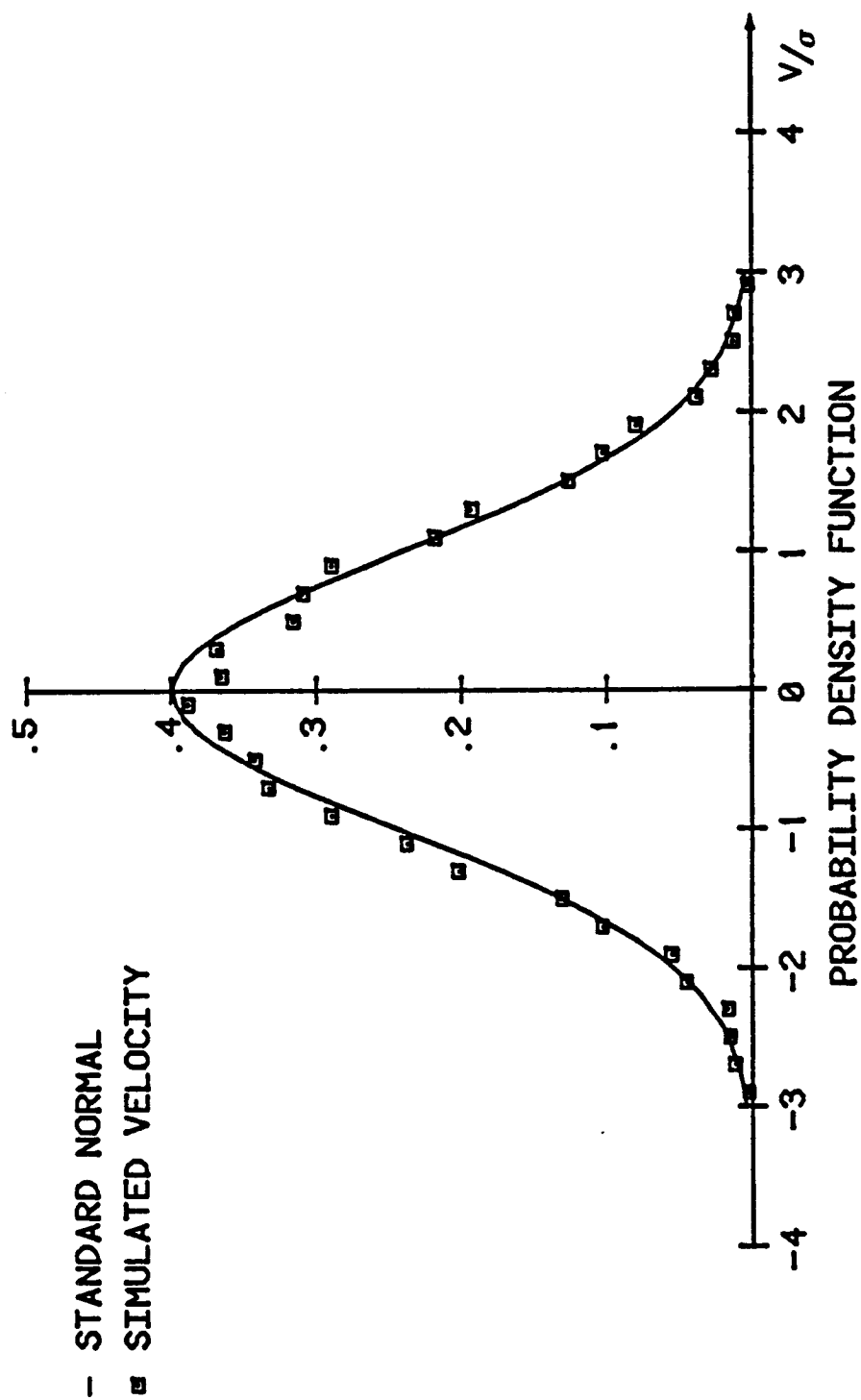


Figure I.4.5. Probability density for the Mod-0A turbulence stimulation,  $V_z$  component.

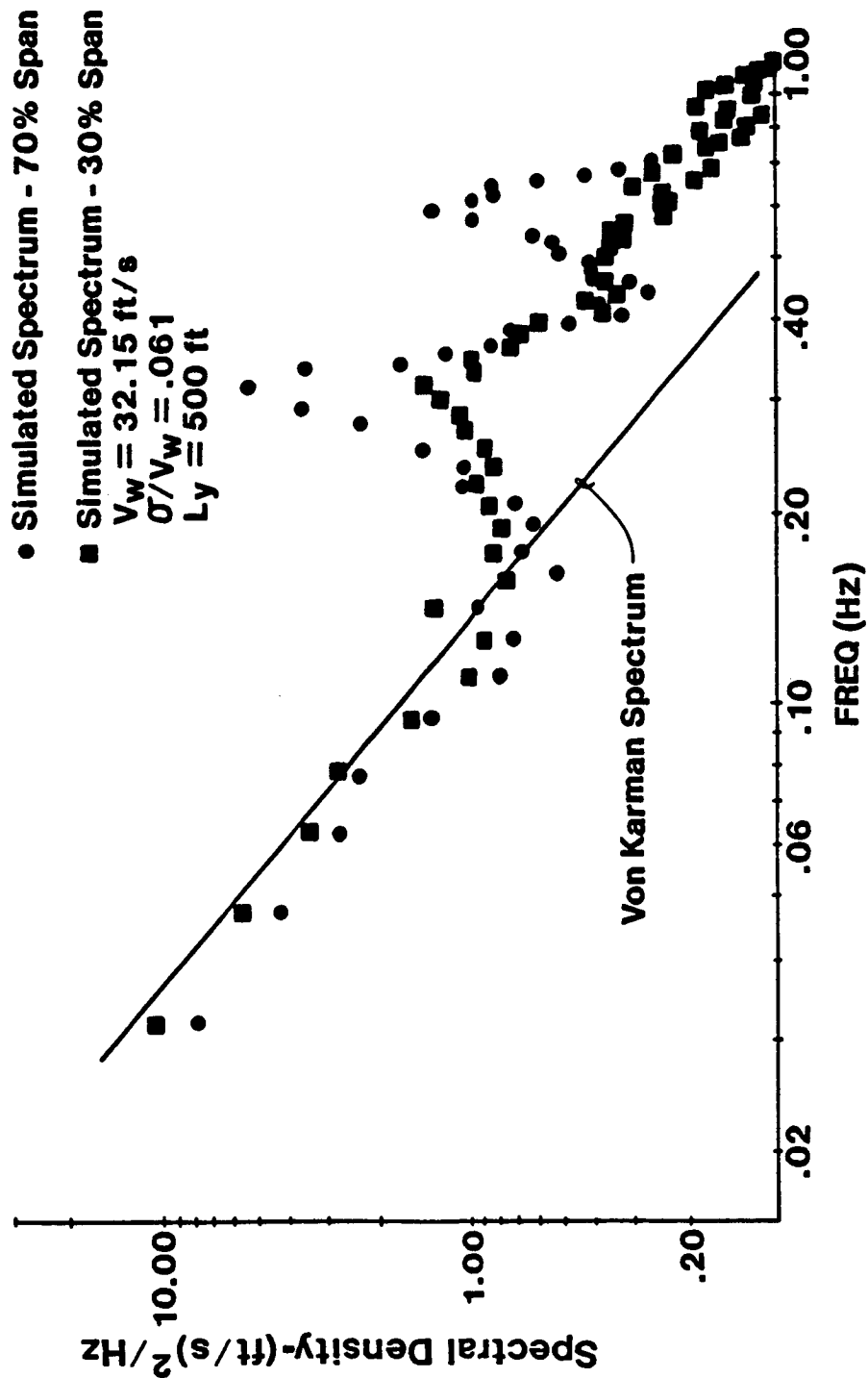


Figure I.4.6. Spectral density plot of the  $V_y$  turbulence component as observed from a Mod-2 rotor blade at different radial stations.

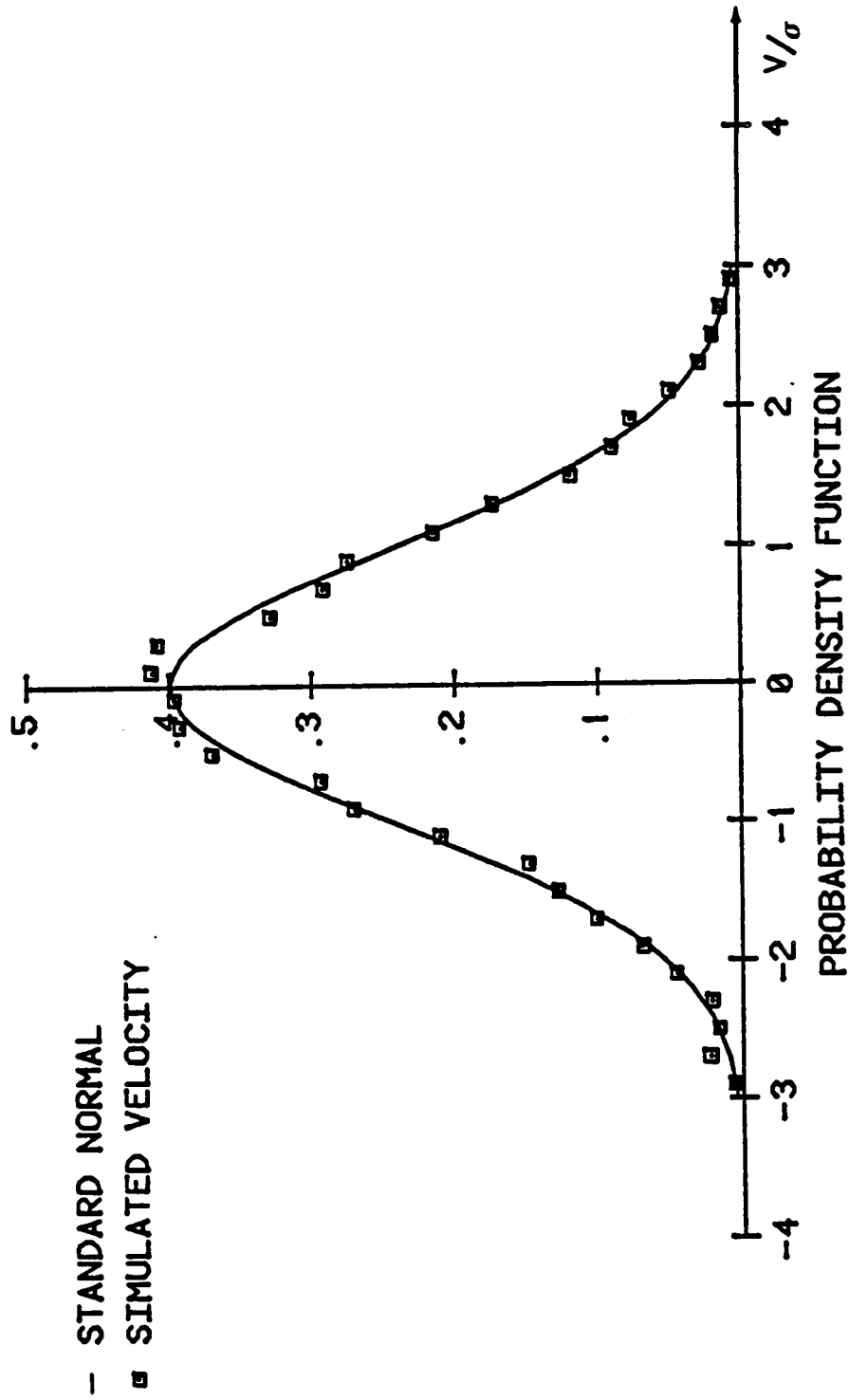


Figure I.4.7. Probability density for the  $V_y$  component of the Mod-2 simulation at 70% span.

#### I.4.4 Reference

1. George, R.L. and Connell, J.R., Rotationally Sampled Wind Characteristics and Correlations with MOD-0A Wind Turbine Response, Pacific Northwest Laboratory Report PNL-5238, September 1984.



## CHAPTER II.1. TURBINE MODEL

### II.1.1 Description of the Turbine Model

The turbine model and the computer code used in this work were originally developed in a previous project (1) at Oregon State University. The model is for the single-degree-of-freedom flapping response of an individual wind turbine blade. It accounts for the blade bending deformation about the smallest blade inertia axis. The rotor is assumed to rotate at a constant speed, and the hub is allowed to move in a prescribed yawing motion. Rotors that are tilted and yawed relative to the mean wind direction can be accommodated in a straightforward manner.

The model and the computer code are designed to operate with aerodynamic models of varying sophistication. The model includes the effects due to the mean wind, wind shear, tower shadow, and turbulent fluctuations.

Figure II.1.1 shows the orientation of the turbine blade under analysis with all the intermediate coordinates required to represent the blade motion. The capital  $X, Y, Z$  coordinates are the fixed reference system. The mean wind velocity at the hub,  $V_{hub}$ , and its fluctuating components,  $\delta V_X$ ,  $\delta V_Y$ , and  $\delta V_Z$  are given in this system. The rotor spin axis is allowed to tilt through a fixed angle  $\chi$  and also to have a prescribed time-dependent yawing motion given as  $\phi(t)$ , where  $\phi$  is the yaw angle. The yaw axis is

coincident with the  $Z$  coordinate axis. The hub, located at a distance " $a$ " from the yaw axis, is considered to be rigid and to have some radius  $h$ . The flexible portion of the blade begins at the outer hub radius,  $h$ . The airfoil shape may begin at  $h$  or at some position further out along the blade  $z$  axis. The blade is coned at some angle  $\beta_0$  as shown in the figure.

The  $x, y, z$  coordinates are located in the surface of revolution that a rigid blade would trace in space, with the  $y$  axis normal to this surface. The  $x_p, y_p, z_p$  are the blade principal bending coordinates, where the  $z_p$  axis is coincident with the elastic axis of the undeformed blade. Bending takes place about the  $x_p$  coordinate. It is further assumed that the blade principal axes of area inertia do not change along the  $z_p$  axis. The influence of blade twist on bending displacement is neglected. The orientation used to set the angle  $\theta_p$  for computations is the principal axis near the blade tip, because the deformation is largest there. The final coordinate system is the  $\eta, \zeta, \xi$  system which is on the principal axes of the deformed blade at some point along the elastic axis.

The rotor blade flapping motion is represented by a set of coordinate shape functions that are in the form of simple polynomials. Four functions are included in the computer code, but any number of the functions can be used, from only one up to a maximum of four. At present,

only cantilever blade attachment conditions have been implemented in the code. Thus, for the results presented in this report, the flapping motion is represented with only one coordinate function (i.e., one flap degree of freedom).

Application of the laws of Newtonian mechanics allows the development of the equations of motion for the rotor blade. Reference (1) presents the details of this development and further outlines a solution procedure called "Galerkin's method," which reduces the flap motion equations to a set of ordinary differential equations in terms of the blade tip modal displacement,  $s_k$ .

The model operates in the time domain, and the blade acceleration equation is integrated via a modified Euler trapezoidal predictor-corrector method. Results of the blade loads analysis are printed in tabulated forms for equidistant points along the blade length and equidistant azimuths around the rotor disk. They include the blade deflection, slope, and velocity, the flapwise shear and moment, edgewise shear and moment, and blade tension and structural torque at the root of the blade.

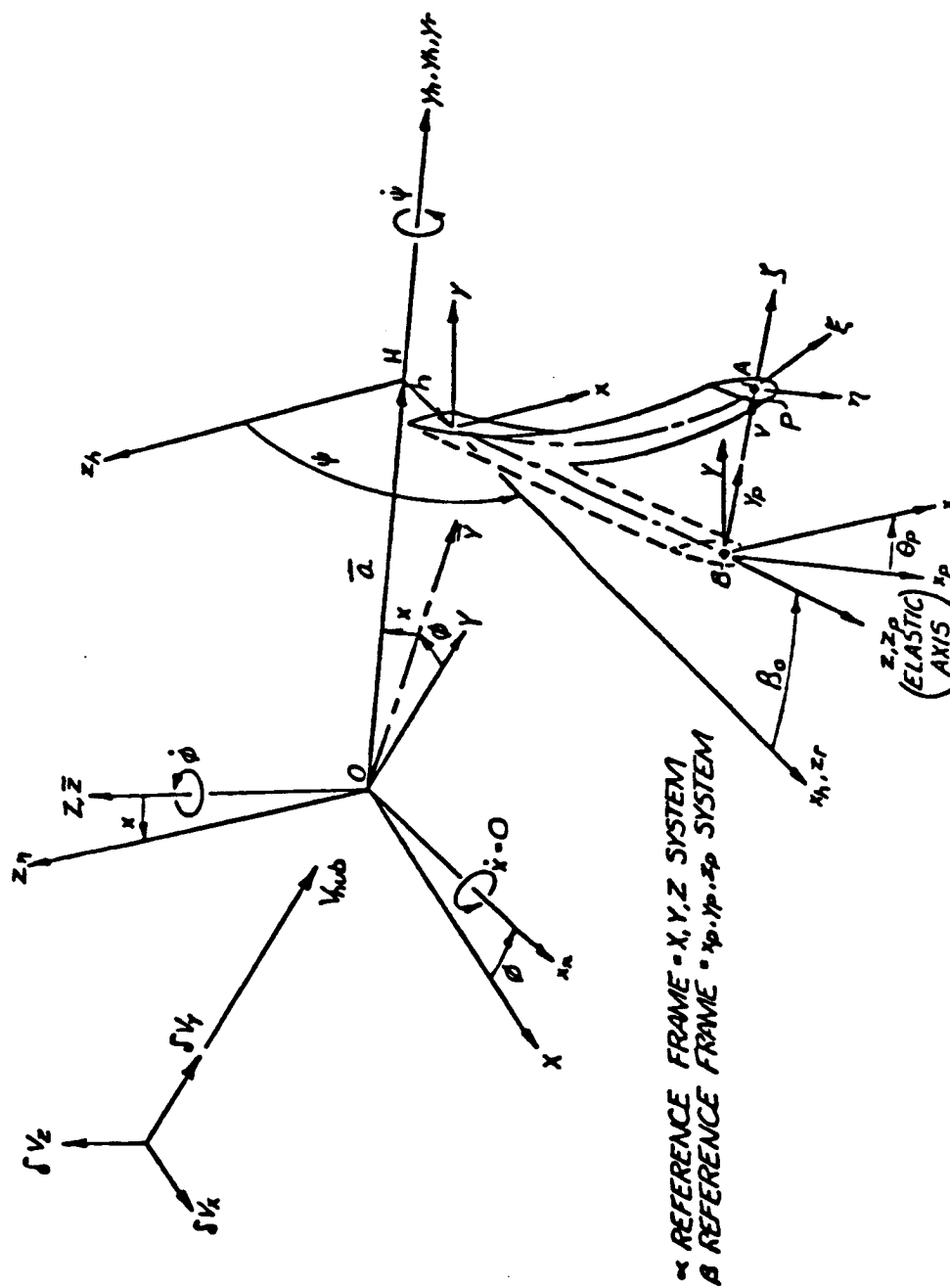


Figure II.1.1.1. Illustration of the rotor system coordinates.

### II.1.2 Reference

1. Thresher, R.W., Hershberg, E.L., Computer Analysis of Wind Turbine Blade Static and Dynamic Loads, Oregon State University, Dept. of Mechanical Engineering, Report RFP-76824, March 1984.

## CHAPTER II.2. CONTROL MODEL

### II.2.1 Introduction

The objective of the control model is to regulate the output torque by changing the pitch angle of the wind turbine blade. The blade pitch angle remains fixed in the computation of average torque values for each revolution which does not permit a continuous control action to be implemented. Therefore, a discrete control model with a time interval equal to the period of one rotor revolution is chosen. The control is only active after each revolution and is, therefore, relatively slow. Thus, a torque step response with a small overshoot which reaches steady state in a minimum number of steps is desirable. A control action which compensates for the flapping oscillation is also required. To achieve this goal, an integral control action is combined with a digital narrow band rejection filter. The integral control action eliminates the steady error in the resulting torque response.

### II.2.2 Development of the Transfer Function

For control purposes, the blade is modeled with one degree of freedom in the flap direction and its equation of motion is a nonlinear second order differential equation. The transfer function between the input blade pitch angle and the output torque is approximated by a general

second-order linear model. The blade torque response to a step change in the blade pitch angle in the absence of other inputs (gravity, turbulence, wind shear) is obtained using the simulation program and is compared with the approximate torque step response using the linear model. The parameters of the approximate response are adjusted so that it closely fits the blade torque response. Having determined the parameters of the approximated torque response, the transfer function between input pitch angle and output torque is determined for small perturbations from a nominal condition. The present analysis was done for a rotor speed of 72 RPM, wind speed of 18.5 mph, and blade pitch angle of 3 degrees. This nominal condition corresponds to a power of 9.72 kW for the three-bladed rotor. Figure II.2.1 shows the power curve for the turbine. The nominal point is at the beginning of power regulation. The turbine torque step response was obtained for step input changes of 0.5 and -0.5 degrees in nominal blade pitch angle. The response for each case showed similar frequency and damping but the magnitudes of their amplitude and phase were different. Figure II.2.2 shows the turbine and approximated torque step response for each case. The parameters of the estimated torque response for both cases were then averaged and an average estimated turbine transfer function was obtained as

$$\begin{aligned}
 T(s) &= TQ_o + \frac{b_1 s + b_2}{s^2 + 2\zeta\omega_n s + \omega_n^2} \\
 &= TQ_o + \frac{b_1 s + b_2}{((s + \sigma_d \pm i\omega_d))} \quad ((\cdot))
 \end{aligned}$$

where

$$\begin{aligned}
 TQ_o &= -1.311 \quad \text{ft-lb/deg} \\
 b_1 &= 75.854 \quad \text{ft-lb/deg}\cdot\text{sec} \\
 b_2 &= -3741.164 \quad \text{ft-lb/deg}\cdot\text{sec}^2 \\
 \zeta &= .0393 \\
 \omega_n &= 25.869 \quad \text{rad/sec} \\
 \sigma_d &= \zeta\omega_n = 1.017 \quad \text{rad/sec} \\
 \omega_d &= \omega_n \sqrt{1 - \zeta^2} = 25.849 \quad \text{rad/sec}
 \end{aligned}$$

and the notation  $((\cdot))$  denotes the product of two complex conjugate terms.

### II.2.3 Development of the Controller

Figure II.2.3a shows the block diagram of the turbine and control model. The system consists of the wind turbine and the averaging process. The transfer function of the wind turbine is given as

$$T_t(s) = TQ_o + \frac{b_1 s + b_2}{((s + \sigma_d \pm j\omega_d))} \quad ((\cdot))$$

The transfer function for the averaging process is developed in Appendix II.A and is



$$T_o(s) = \frac{12}{T^2 s^2 + 6Ts + 12}$$

where  $T$  is the period of one rotor revolution and it equals 5/16 sec. The turbine has a frequency bandwidth with limiting frequency corresponding to  $\sigma_d = 1.1017$  rad/sec and damped frequency of  $\omega_d = 25.849$  rad/sec compared to  $\sigma_d = \frac{3}{T} = 3.6$  rad/sec and  $\omega_d = \sqrt{3} = 2.078$  rad/sec for the averaging process. The averaging process thus has a higher frequency bandwidth (smaller time constant) and, therefore, will not be considered in the development of the control model.

The control is only active after each revolution and is, therefore, relatively slow. Thus, a torque step response with a small overshoot which reaches steady state in a minimum number of steps is desirable. To achieve this, a proportional feedback for fast response and an integral action to eliminate the steady state error are first tried.

The blade pitch angle remains fixed in the evaluation of average torque values for each revolution. Therefore, the control model is developed in the discrete time domain with a time interval equal to the period of one rotor revolution. Figure II.2.3b shows the system block diagram with a zero order hold and a sampler to perform the digital/analog conversion of the input and output signals to the turbine, respectively (1).

The method of root locus is used to design the control algorithm. The gain values are chosen such that the closed loop transfer function is stable and meets the desired performance criteria. The gain of the proportional feedback loop,  $k_1$ , is chosen first and then using this value, the gain in the integral control action,  $k_2$ , is selected. For stability and better performance the gains are chosen so that the poles of the closed loop transfer function are inside the unit circle and near the origin (2,3).

Figure II.2.3c shows the discrete block diagram for the system.  $G_t(z)$  is the z-transform for the turbine transfer function, zero order hold, and sampler, and is given as (Appendix II.B)

$$G_t(z) = \frac{C(z)}{D(z)} = \frac{C_2 z^2 + C_1 z + C_0}{z^2 + D_1 z + D_0}$$

where the coefficients in polynomials  $C(z)$  and  $D(z)$  are obtained as

$$C_2 = -1.300 \text{ ft-lb/deg}$$

$$D_1 = 0.782$$

$$C_1 = -8.251 \text{ ft-lb/deg}$$

$$D_0 = 0.184$$

$$C_0 = -4.014 \text{ ft-lb/deg}$$

Substituting for the coefficients in the transfer function, it can be written as

$$G_t(z) = (-1.30 \text{ ft-lb/deg}) \frac{(z + 0.531)(z + 5.815)}{((z + 0.391 + i0.176))}$$

Figure II.2.3d shows the location of poles and zeros of the turbine transfer function.

From Fig. II.2.3c, the transfer function for the inner feedback loop with proportional gain  $k_1$  between output torque,  $TQ(z)$ , and input control,  $U(z)$ , is obtained as

$$G_1(z) = \frac{TQ(z)}{U(z)} = \frac{G_t(z)}{1 + k_1 G_t(z)}$$

The root locus of  $G_1(z)$  for negative values of gain is shown in Fig. II.2.3e with  $k_1$  given as

$$\begin{aligned} k_1 &= (-1) \frac{D(z)}{C(z)} \\ &= (0.769 \text{ deg/ft-lb}) \frac{((z + 0.391 \pm i0.176))}{(z + 0.531)(z + 5.815)} \end{aligned}$$

The poles of the transfer function become unstable ( $|z| > 1$ ) for  $k_1 < -0.67 \text{ deg/ft-lb}$ .

The overall closed loop transfer function of the system shown in Fig. II.2.3c between output torque,  $TQ(z)$ , and reference torque,  $TQ_r$ , is given as

$$G(z) = \frac{TQ(z)}{TQ_r(z)} = \frac{k_2 z G_1(z)}{(z - 1) + k_2 z G_1(z)}$$

Figure II.2.3f shows the root locus of the system closed loop transfer function for gain  $k_1 = 0.0$  and  $-0.1 \text{ deg/ft-lb}$  with gain  $k_2$  given as

$$\begin{aligned} k_2 &= (-1) \frac{(z - 1) D(z)}{z C(z)} \\ &= (0.769 \text{ deg/ft-lb}) \frac{(z - 1)((z + 0.391 \pm i0.176))}{z (z + 0.531)(z + 5.815)} \end{aligned}$$

Figure II.2.3f shows that the poles of the closed loop transfer function can easily become unstable for small values of gain  $k_1$ . Also, since the poles are away from the origin, it will take many steps for the response to reach steady state which is not desirable.

An alternative to the proportional feedback is to trap the complex poles corresponding to flapping motion by introducing a pair of zeros with the same coordinate values in the  $z$ -plane. Figure II.2.4a shows the block diagram of this model.

The transfer function for the inner feedback loop with gain  $k_1$  between output torque and input control is given as

$$G_1(z) = \frac{TQ(z)}{U(z)} = \frac{G_t(z)}{1 + K_1 F(z) G_t(z)}$$

where

$$G_t(z) = \frac{C(z)}{D(z)} = \frac{C_2 z^2 + C_1 z + C_0}{z^2 + D_1 z + D_0}$$

and

$$F(z) = \frac{D(z)}{z^2} = \frac{z^2 + D_1 z + D_0}{z^2}$$

Figure II.2.4b shows the root locus for  $G_1(z)$  where gain  $k_1$  is given as

$$\begin{aligned} k_1 &= (-1) \frac{z^2 D(z)}{D(z) C(z)} \\ &= (0.769 \text{ deg/ft-lb}) \frac{z^2}{(z + 0.531)(z + 5.815)} \end{aligned}$$

From Figure II.2.4a the closed loop transfer function between output torque,  $TQ(z)$ , and input reference torque,  $TQ_r$ , is given as

$$G(z) = \frac{TQ(z)}{TQ_r} = \frac{k_2 z G_1(z)}{(z-1) + k_2 z G_1(z)}$$

Figure II.2.4c shows the root locus of the closed loop transfer function for gain  $k_1 = -0.1$  deg/ft-lb where  $k_2$  is given as

$$k_2 = (-1) \frac{(z-1) D(z) [z^2 + k_1 C(z)]}{z^3 C(z)}$$

$$= (0.769 \text{ deg/ft-lb})$$

$$\frac{(z-1)((z+0.391 \pm i0.176))((z+0.365 \pm i0.471))}{z^3(z+0.531)(z+5.815)}$$

In order to keep the system closed loop transfer function poles near the origin, the pole on the right half circle was chosen at  $z = 0.5$ . The corresponding value for gain  $k_2$  is  $-0.4275$  deg/ft-lb which makes the system unstable. Since the average transfer function was derived for one nominal condition, other operating conditions may not give the required pole and zero cancellation resulting in possible instability of the system.

As was shown, the poles of the closed loop transfer function can become unstable for small values of gain  $k_1$ . To make the system more stable and also keep the

poles of the system closed loop transfer function near the origin, gain  $k_1$  is set to zero and a new controller is introduced in the forward loop. It is a proportional plus integral control which filters out the effect of the poles of the turbine transfer function (notch filter). Figure II.2.5a shows the block diagram of the system and the controller. Pole  $z = p$  is selected such that the poles of the closed loop transfer function are located at the origin (dead-beat control). The system closed loop transfer function between output torque,  $TQ(z)$ , and input reference torque is given as

$$G(z) = \frac{TQ(z)}{TQ_r} = \frac{G_1(z)}{1 + G_1(z)}$$

where

$$G_1(z) = \frac{KD(z)}{(z - 1)(z - p)} G_t(z)$$

and

$$G_t(z) = \frac{C(z)}{D(z)}$$

Substituting and cancelling common terms  $G_1(z)$  becomes

$$G_1(z) = \frac{KC(z)}{(z - 1)(z - p)}$$

and

$$\begin{aligned} G(z) &= \frac{KC(z)}{(z - 1)(z - p) + KC(z)} \\ &= \frac{K[C_2 z^2 + C_1 z + z_0]}{(KC_2 + 1)z^2 + (KC_1 - p - 1)z + (KC_0 + p)} \end{aligned}$$

Poles of the closed loop transfer function are located the origin provided

$$KC_1 - p - 1 = 0$$

$$KC_0 + p = 0$$

or

$$p = \frac{-C_0}{C_0 + C_1} = -0.32727$$

$$K = \frac{1}{C_0 + C_1} = -0.08153$$

where  $C_0$  and  $C_1$  are the coefficients of the numerator of the turbine transfer function. Figure II.2.5b illustrates the root locus for the closed loop transfer function where  $K$  is given as

$$K = (0.769 \text{ deg/ft-lb}) \frac{(z - 1)(z + 0.32727)}{(z + 0.531)(z + 5.815)}$$

The closed loop transfer function of the system then becomes

$$G(z) = \frac{K (C_2 z^2 + C_1 z + C_0)}{(1 + KC_2) z^2}$$

Figure II.2.5c demonstrates the location of the poles and zeros of the resulting closed loop system transfer function.

To investigate the stability of the control system, the turbine transfer functions obtained for positive and negative step about the nominal condition are used instead

of the average transfer function. Figure II.2.5d shows the location of zeros and poles for each case. Both cases are stable and only the case for positive step demonstrates slightly oscillatory behavior. Figure II.2.6 shows the torque step response to a unit step change in reference torque for each case and the average model.



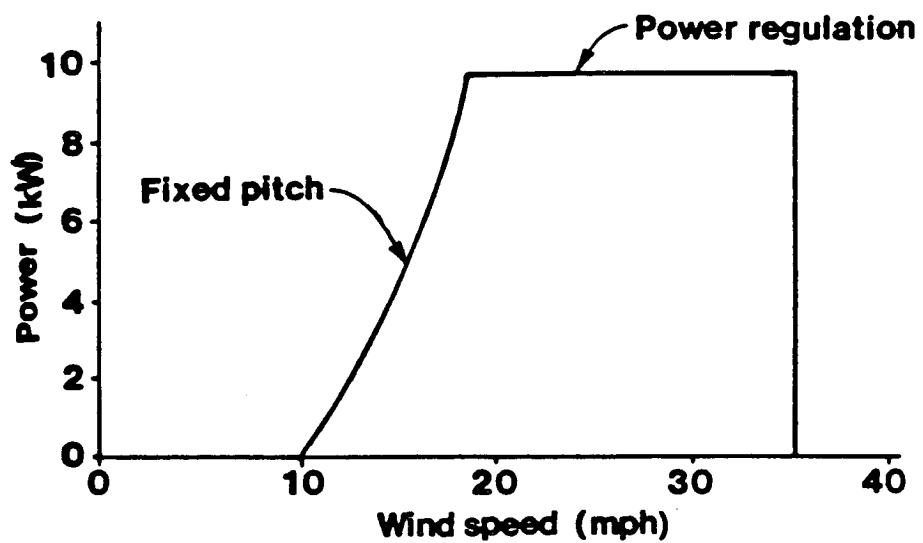
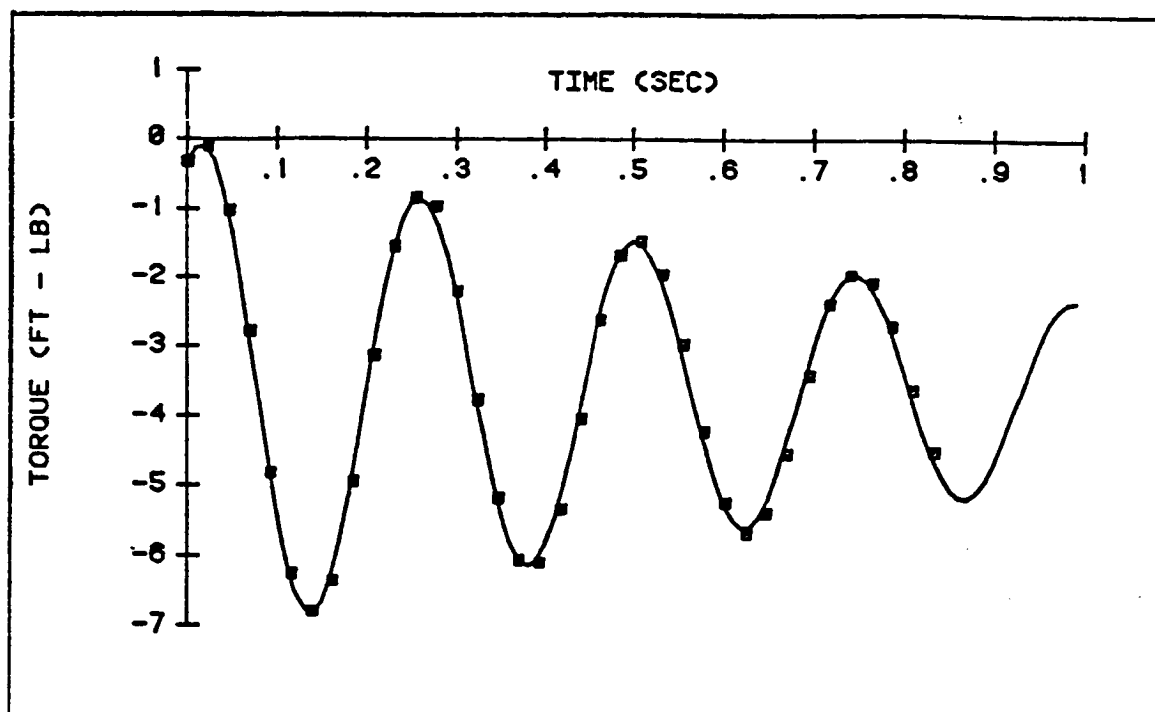
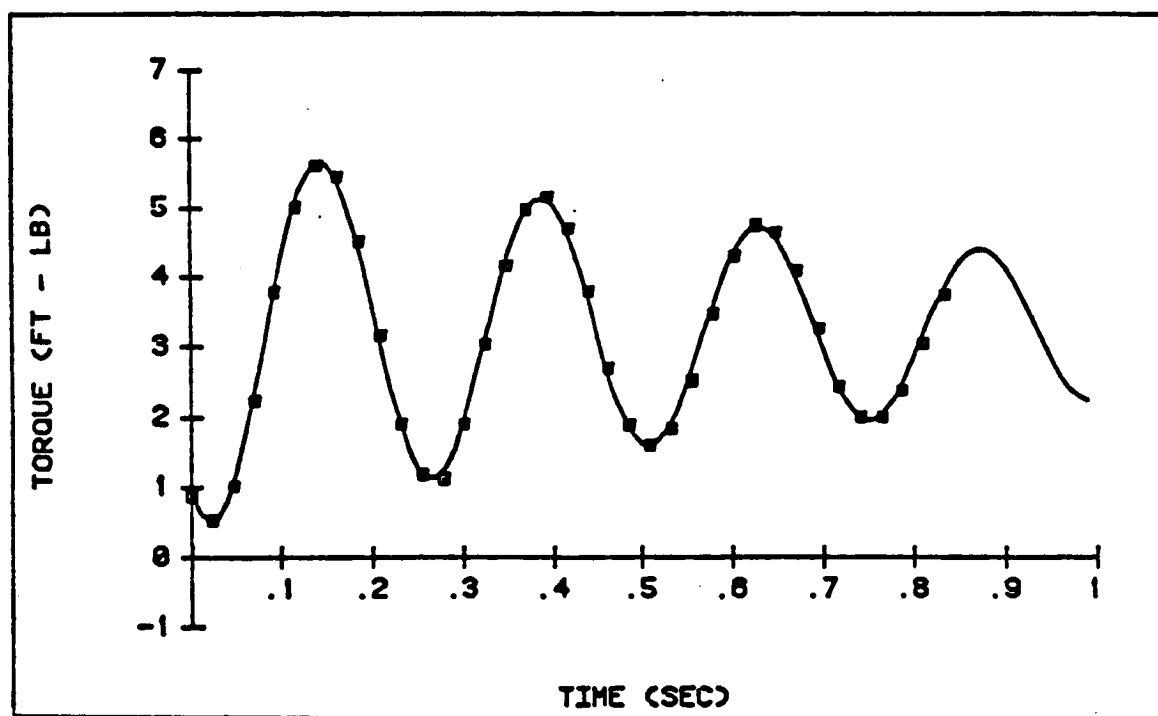


Figure II.2.1. Power regulation curve.



(a)



(b)

Figure II.2.2. Transient torque response to step change in pitch angle: a) -0.5 deg pitch change, b) +0.5 deg pitch change.

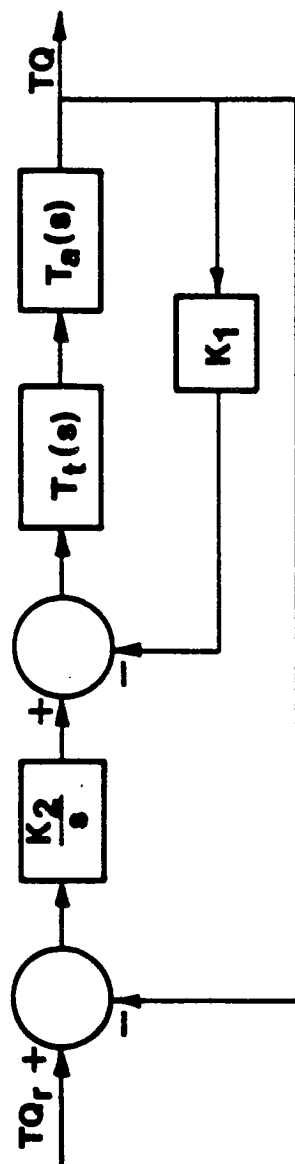


Figure II.2.3a. Block diagram of the wind turbine blade and proportional and integral feedback control model.

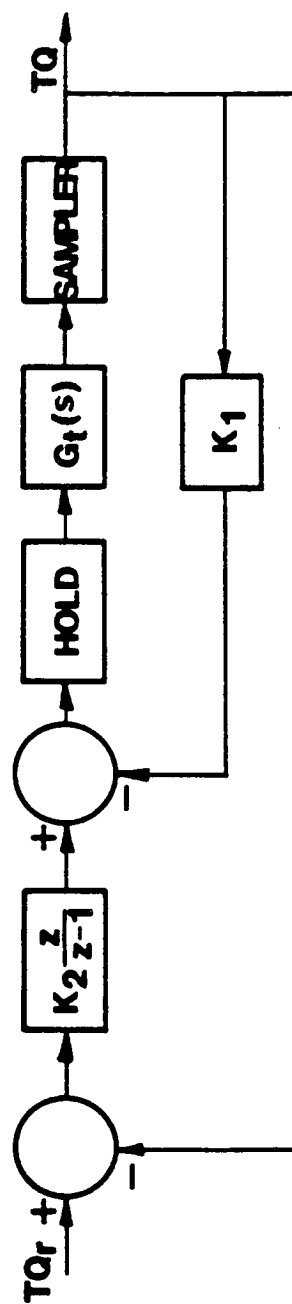


Figure II.2.3b. System block diagram with zero order hold and sampler.

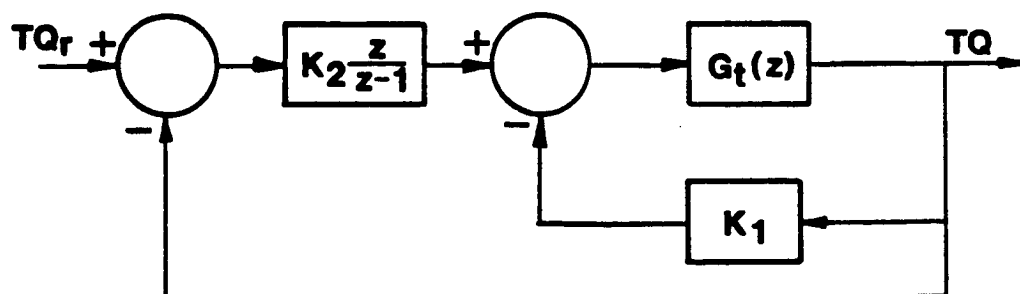


Figure II.2.3c. System discrete time block diagram.

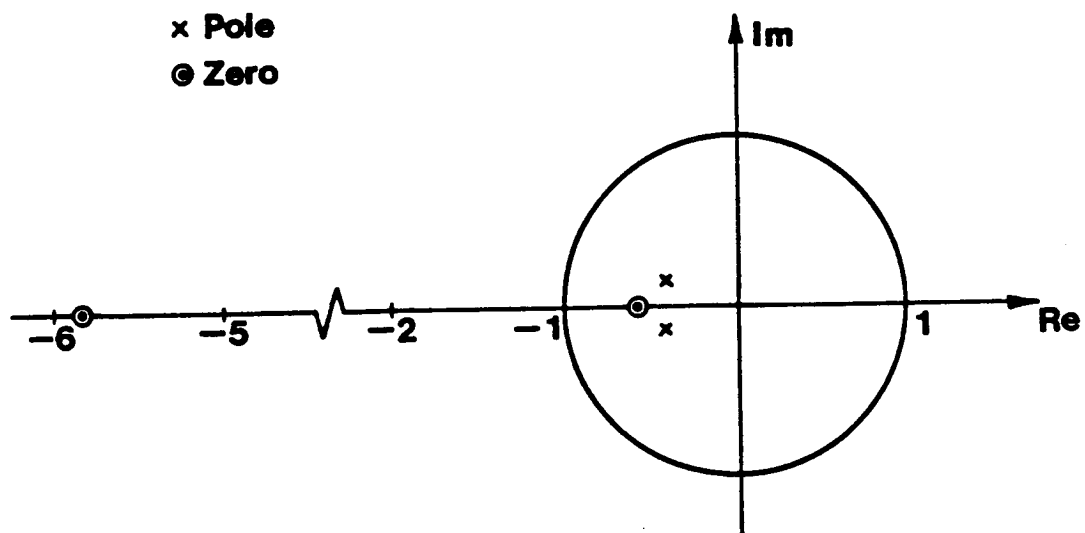


Figure II.2.3d. Location of poles and zeros of the wind turbine blade transfer function.

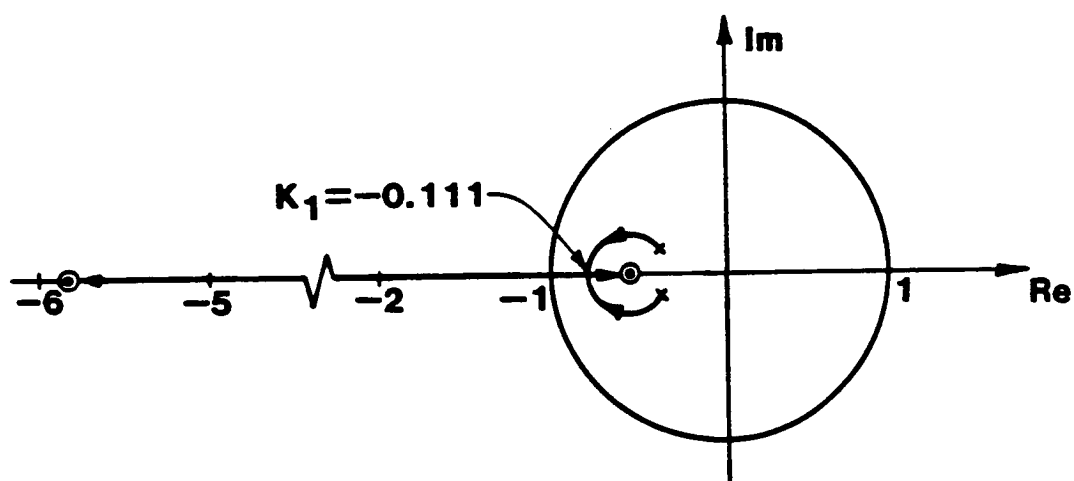
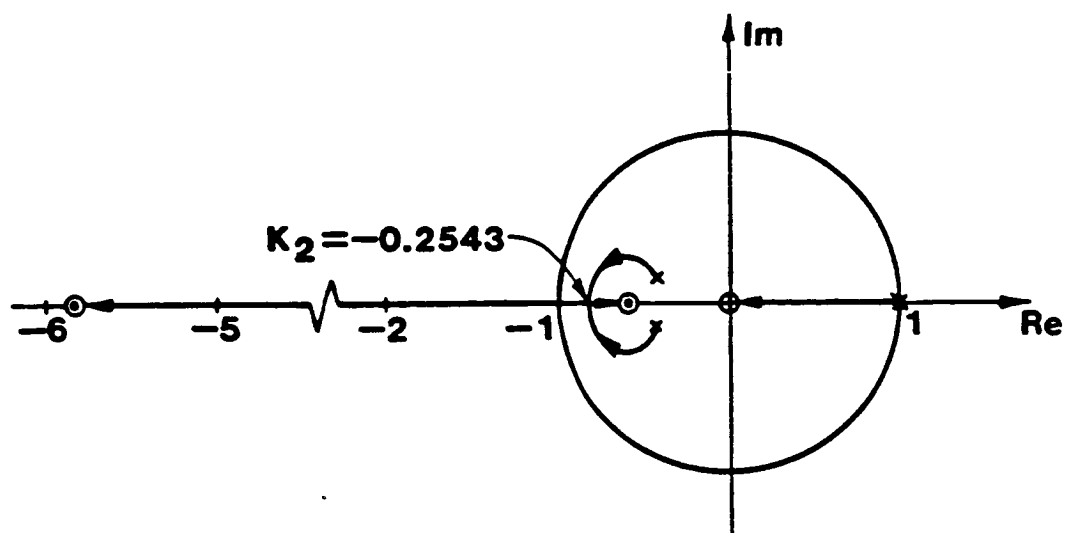
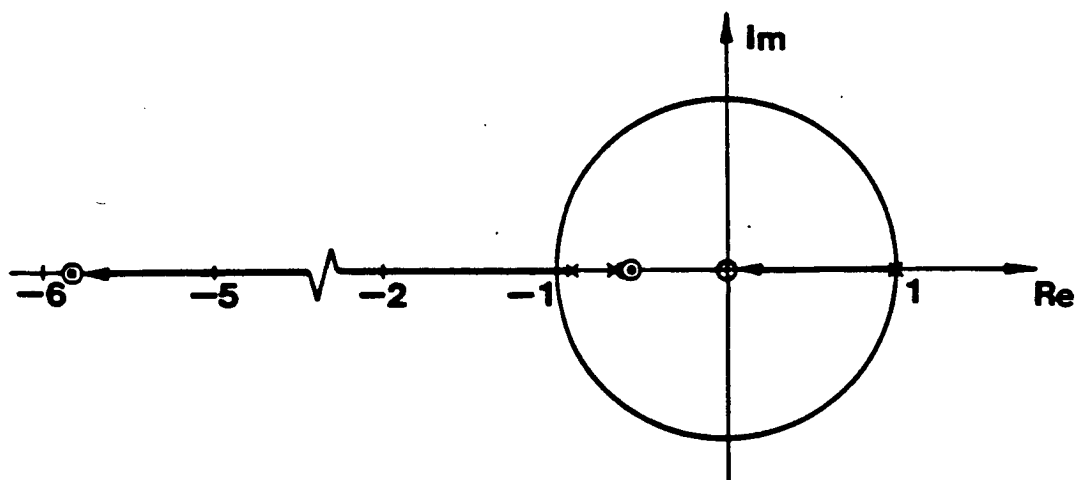


Figure II.2.3e. Root locus illustration of the system inner loop with proportional feedback controller.



(a)



(b)

Figure II.2.3f. Root locus illustration of the system closed loop transfer function for gain  
 a)  $k_1 = 0.0$ , b)  $k_1 = -0.1$  deg/ft-lb.

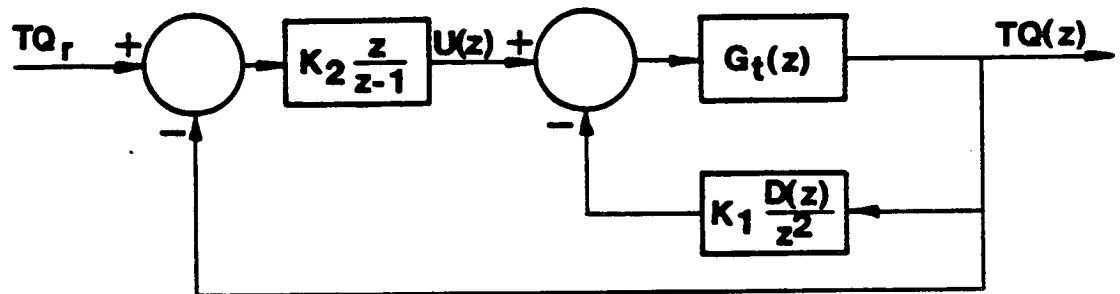


Figure II.2.4a. Discrete block diagram of the wind turbine blade and notch filter feedback controller.

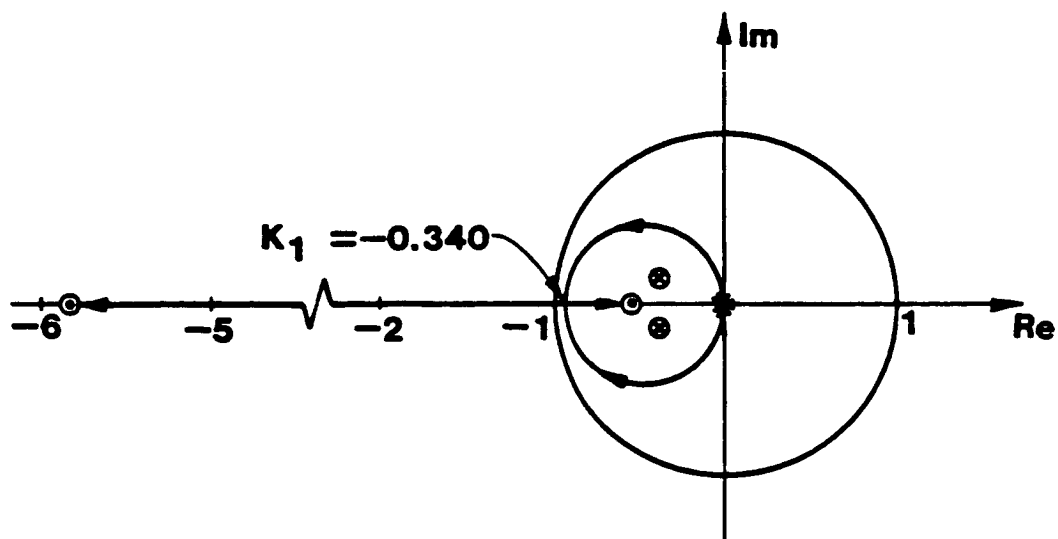


Figure II.2.4b. Root locus illustration of the system inner loop with notch filter feedback controller.

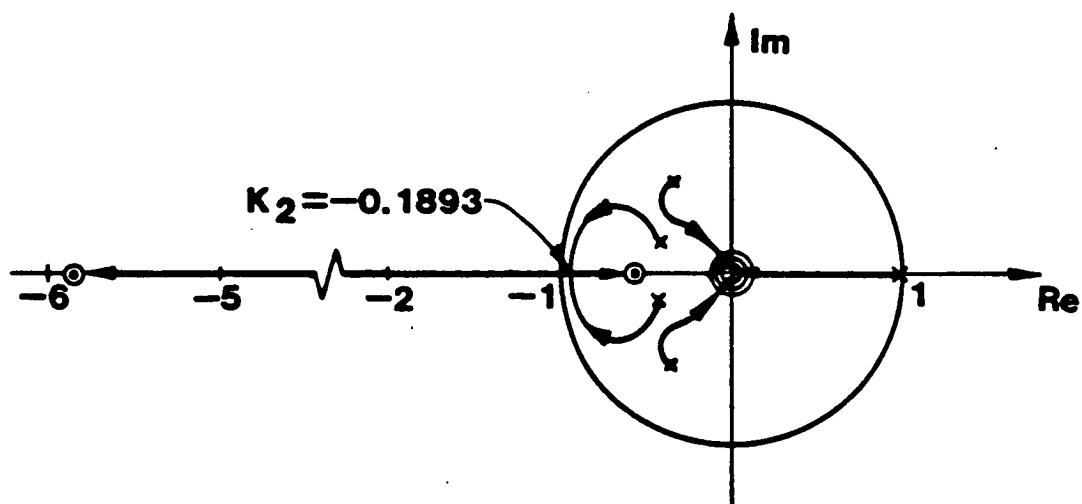


Figure II.2.4c. Root locus illustration of the system closed loop transfer function for gain  $k_1 = -0.1$  deg/ft-lb.



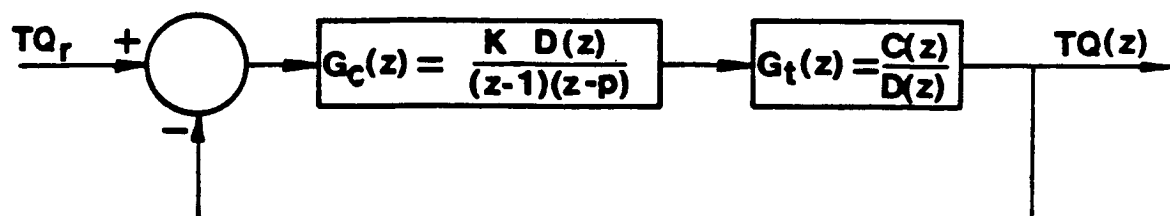


Figure II.2.5a. Discrete block diagram of the wind turbine blade and notch filter feedback controller with integral action.

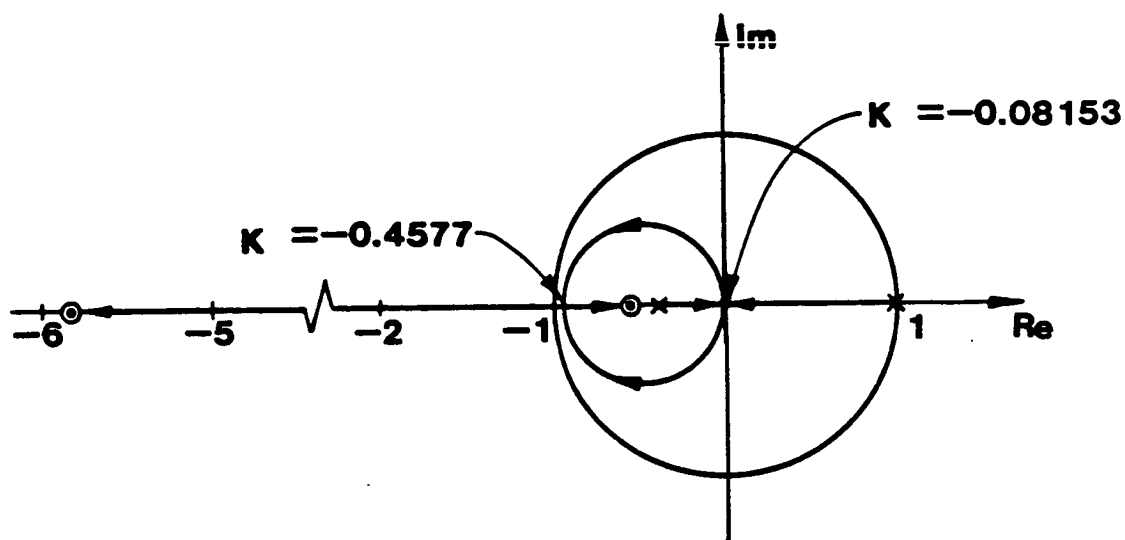


Figure II.2.5b. Root locus illustration of the system closed loop transfer function with notch filter and dead beat controller.

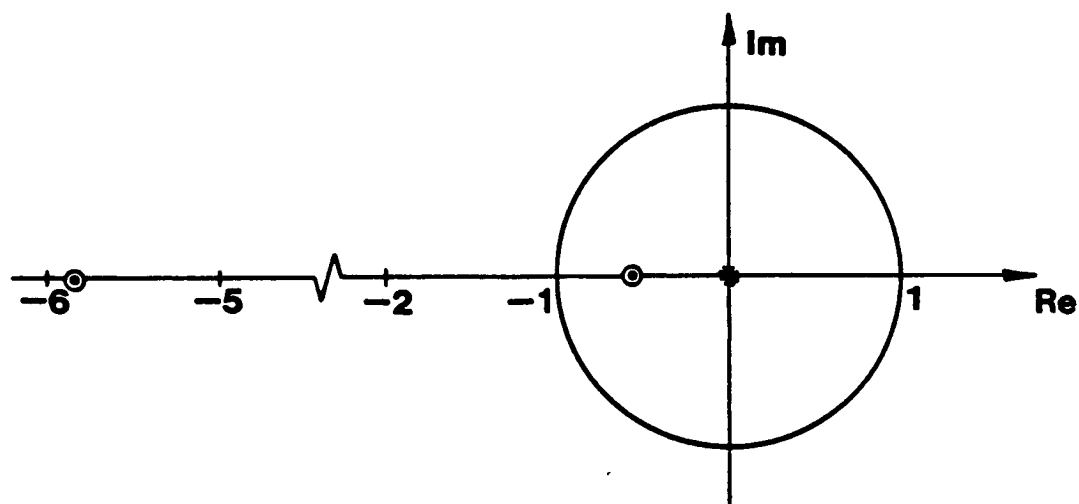
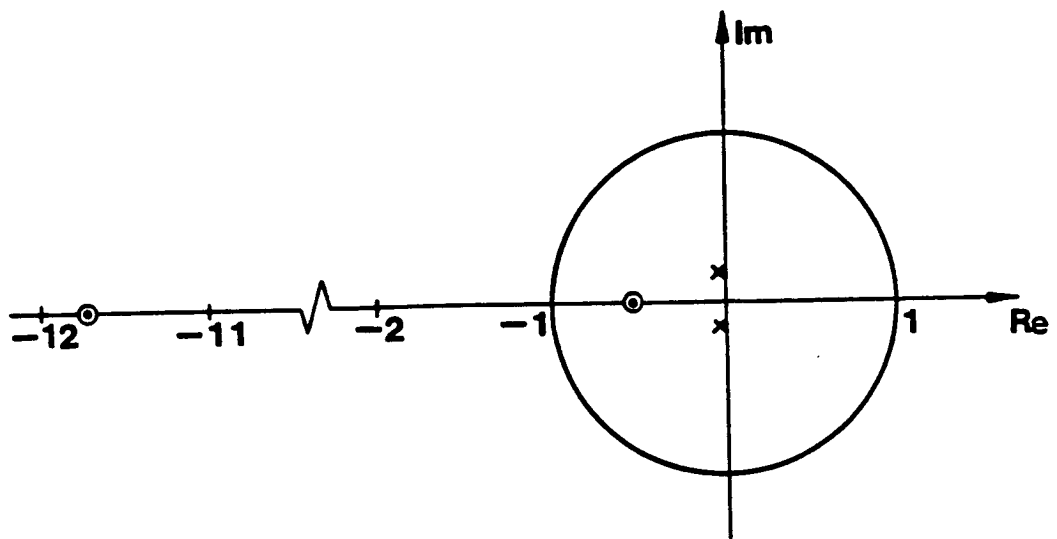
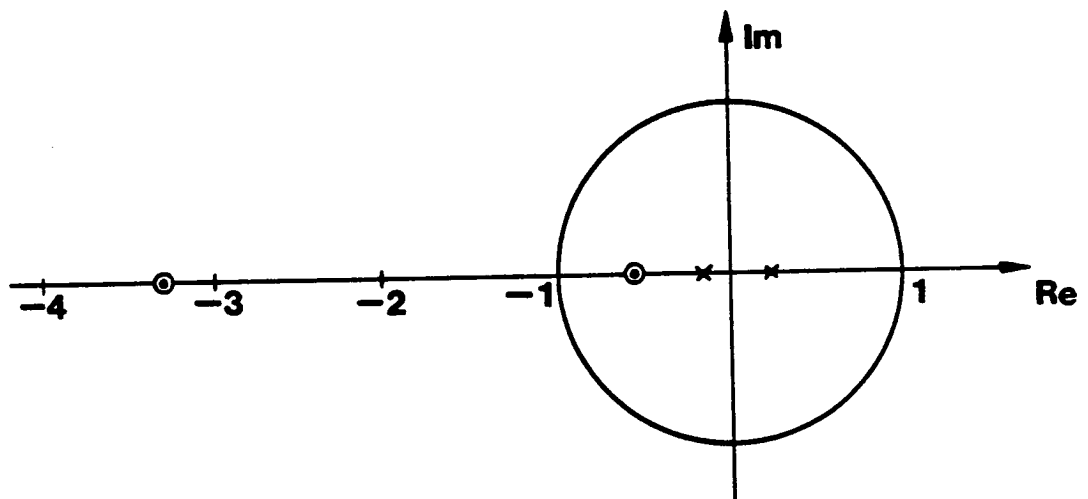


Figure II.2.5c. Location of poles and zeros of the system closed loop transfer function.



(a)



(b)

Figure II.2.5d. Location of poles and zeros of the system closed loop a) positive step transfer function, b) negative step transfer function.

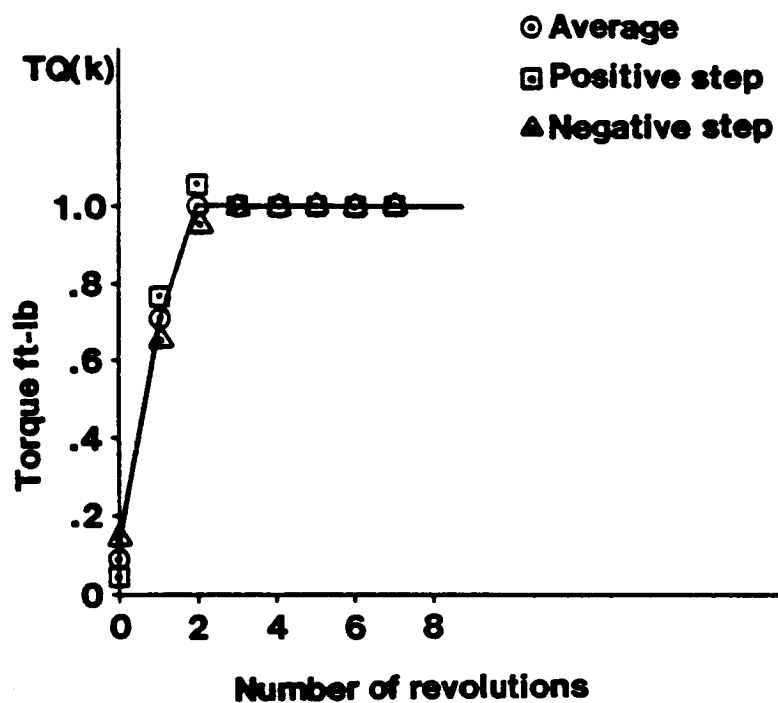


Figure II.2.6. Torque step response to a unit step change in reference torque.

#### II.2.4 References

1. Palm, W.J., Modeling, Analysis, and Control of Dynamic Systems, Wiley, 1983, pp. 213-264.
2. Kuo, B.C., Automated Control Systems, Prentice-Hall, 1982, pp. 383-460.
3. Cannon, R.H., Dynamics of Physical Systems, McGraw-Hill, 1967, pp. 644-682.

## CHAPTER II.3. IMPLEMENTATION OF THE CONTROL MODEL

## II.3.1 Controller Implementation

Figure II.2.12 shows the wind turbine discrete feed-back control model developed in Chapter II.2. The control action and wind turbine transfer functions are given as

$$G_t(z) = \frac{TQ(z)}{Q(z)} = \frac{C_2 z^2 + C_1 z + C_0}{z^2 + D_1 z + D_0}$$

$$G_c(z) = \frac{\theta(z)}{e(z)} = \frac{K[z^2 + D_1 z + D_0]}{(z - 1)(z - p)}$$

Applying the control action, the regulation algorithm is obtained as

$$\theta(i) = \theta(i - 1) + K\epsilon(i)$$

$$\epsilon(i) = p\epsilon(i - 1) + e(i) + D_1 e(i - 1) + D_0 e(i - 2)$$

where

$e(i)$ ,  $e(i - 1)$ , ... current and previous values of  
the output error

$\epsilon(i)$ ,  $\epsilon(i - 1)$ , ... filtered control error

$\theta(i)$ ,  $\theta(i - 1)$ , ... pitch angle command to actuator

$D_0$ ,  $D_1$ ,  $p$  constant control parameters

$K$  control gain

The wind turbine torque was evaluated by calculating the total moment of all loads acting on the turbine blade about the axis of rotation (1). Turbulence velocity in-

puts to the wind turbine simulation code were generated using the results developed in Section 1. Only uniform and gradient turbulence terms were considered.

Table II.3.1 demonstrates the control action logic implementation to control the output torque of the turbine. The control can be turned on or off and turbulence can be generated for different wind conditions. For this analysis a turbulence length scale,  $T_L$ , of 250 ft and an intensity ratio,  $T_I$ , of 15% are used.

In testing the control algorithm, it was determined that the static open loop gain of the wind turbine blade between the output torque and the input wind velocity varies substantially with wind speed. A static sensitivity analysis of the turbine at the nominal power output was conducted where changes in torque for a step change of 0.5 and -0.5 degrees in pitch angle from the pitch angle corresponding to the nominal torque were obtained for different wind speeds. Figure II.3.1 shows the results which demonstrates higher static gain at higher wind speed and, therefore, larger response which may cause instability of the system. The control action gain was then modified using a cubic polynomial fit of the static sensitivity data to maintain an overall constant gain at different wind speeds.

The modified regulation algorithm then becomes

$$\theta(i) = \theta(i - 1) + K * \epsilon(i)$$

$$\begin{aligned}\epsilon(i) = & -0.327 \epsilon(i - 1) + e(i) + 0.782 e(i - 1) \\ & - 0.184 e(i - 2)\end{aligned}$$

$$K^* = \frac{-0.08153 \text{ Deg/Ft-lb}}{9.80 \left(\frac{V}{V_N}\right)^3 - 47.02 \left(\frac{V}{V_N}\right)^2 + 83.87 \left(\frac{V}{V_N}\right) - 45.61}$$

$$V_N \triangleq V_{\text{NOMINAL}} = 18.5 \text{ MPH}$$



Table II.3.1. Control Algorithm Logic.

---

```
IF (OLD PITCH = FIXED VALUE) THEN
    IF (OUTPUT > REFERENCE)
        NEW PITCH = REGULATED VALUE
    ELSE
        NEW PITCH = FIXED VALUE
    ENDIF
ELSE
    NEW PITCH = REGULATED VALUE
    IF (NEW PITCH < FIXED VALUE) THEN
        NEW PITCH = FIXED VALUE
        RESET REGULATION
    ENDIF
ENDIF
```

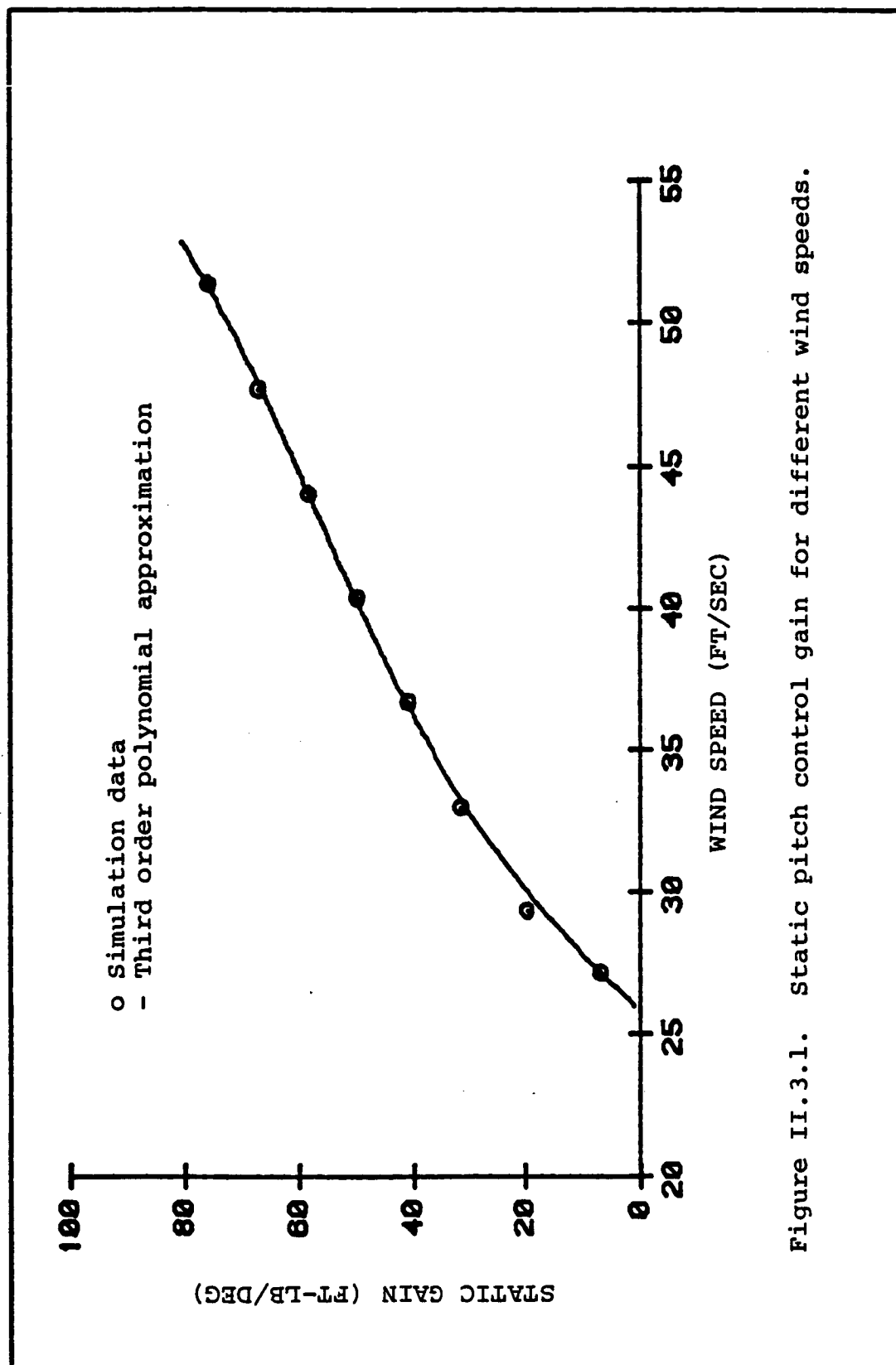


Figure II.3.1. Static pitch control gain for different wind speeds.

### II.3.2 Reference

1. Thresher, R.W., Hershberg, E.L., Computer Analysis of Wind Turbine Blade Static and Dynamic Loads, Oregon State University, Dept. of Mechanical Engineering, Report RFP-76824, March 1984.

## CHAPTER II.4. RESULTS AND CONCLUSIONS

The wind turbine response to step change in torque for two winds speeds without turbulence were obtained. Figure II.4.1 shows the torque response and corresponding blade pitch angle correction for 20% reduction in nominal torque at 20 mph wind speed. It is seen that the system reaches 99.5% of the steady state torque in eight revolutions (9.6 sec) with maximum overshoot of 2% which is well within the defined initial objectives for the controller. Similar results for 35 mph wind speed are shown in Fig. II.4.2 which demonstrates similar characteristics. The controller is shown to be stable at both ends of the operating range. Instantaneous single blade torque for fixed pitch (no control) and with active control for 20 mph wind speed are plotted in Figs. II.4.3 and II.4.4. Average single blade torque over each revolution for 12 revolutions for each case is shown in Fig. II.4.5. Similar results for 35 mph wind speed are demonstrated in Figs. II.4.6 to II.4.8. Table II.4.1 summarizes the statistical characteristics of the blade torque response in the turbulence for 20 mph and 35 mph wind speed. For the 20 mph wind speed, closer mean torque response to the reference torque of 324 ft-lb and smaller standard deviation are achieved with active control than with fixed pitch. The mean torque response is also maintained closer to the reference torque for the 35 mph wind speed. However, a

higher standard deviation resulted in this case which is directly related to the control action being implemented. Since the variance of the input turbulence in the model is large for 35 mph wind speed and turbulence intensity of 15%, a slow controller which is only active after each revolution could allow large deviations in instantaneous blade torque from the mean torque and, therefore, a large standard deviation. A faster controller which can correct the blade pitch angle more often than once every revolution will reduce extreme fluctuations of the blade torque. These statistics were compiled for 12 revolutions or 9.6 sec and a longer run stream is required to more precisely estimate these results. However, every run of the model costs about 200 cpu sec so this task is left as a future expansion of this work when more funding is available.

#### CONCLUSIONS

A discrete-time control algorithm is used to regulate the output torque of a wind turbine by changing the pitch angle of the turbine blade. The method is suitable for a wide class of pitch regulated turbines. The algorithm works well in conjunction with turbulence inputs. Torque response fluctuations for high wind speeds are excessive and a faster controller can help to reduce that. Also, further testing on a real machine is required to verify the present analysis.

Table II.4.1. Single Blade Torque Response in Turbulence.

Turbulence Intensity = 15%

Reference Torque = 324 ft-lb

Torque (ft-lb)	20 mph		35 mph	
	Fixed Pitch	Active Control	Fixed Pitch	Active Control
Average	330.0	324.1	337.8	330.5
St. Dev.	17.0	13.9	33.0	48.9

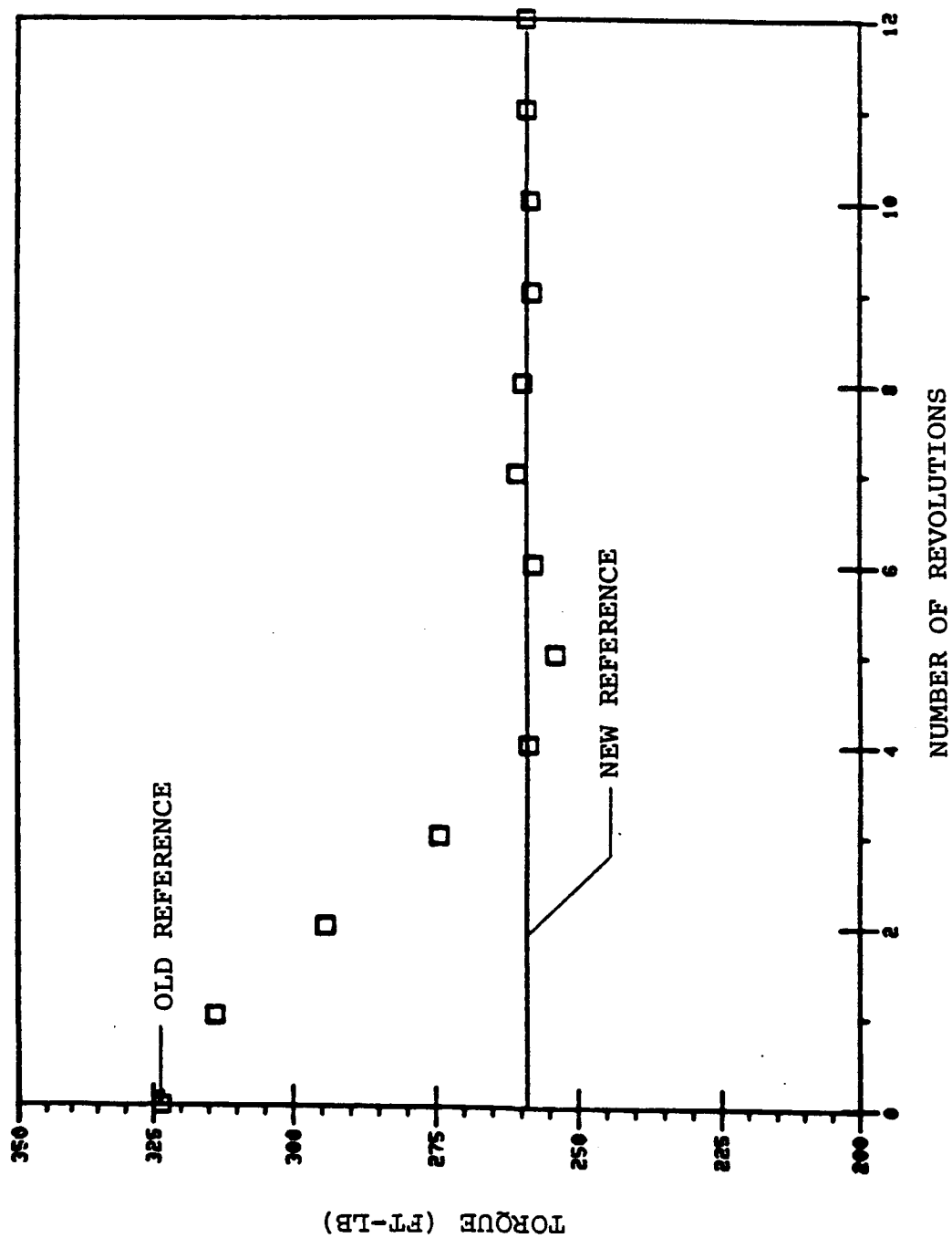


Figure II.4.1a. Average torque response for 20% step reduction in reference torque for wind speed = 20 mph

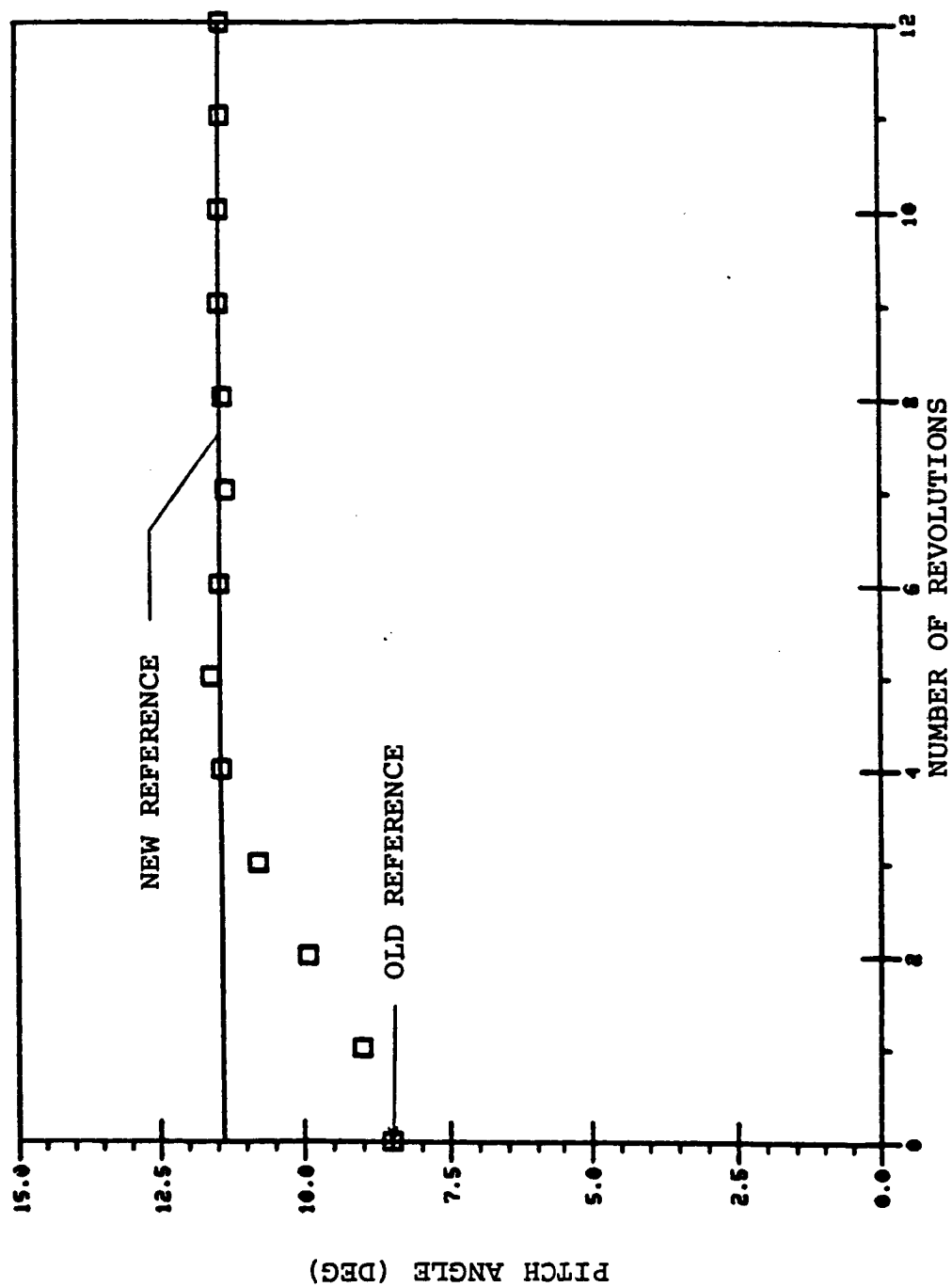


Figure II.4.1b. Blade pitch angle control for 20% step reduction in reference torque for wind speed = 20 mph



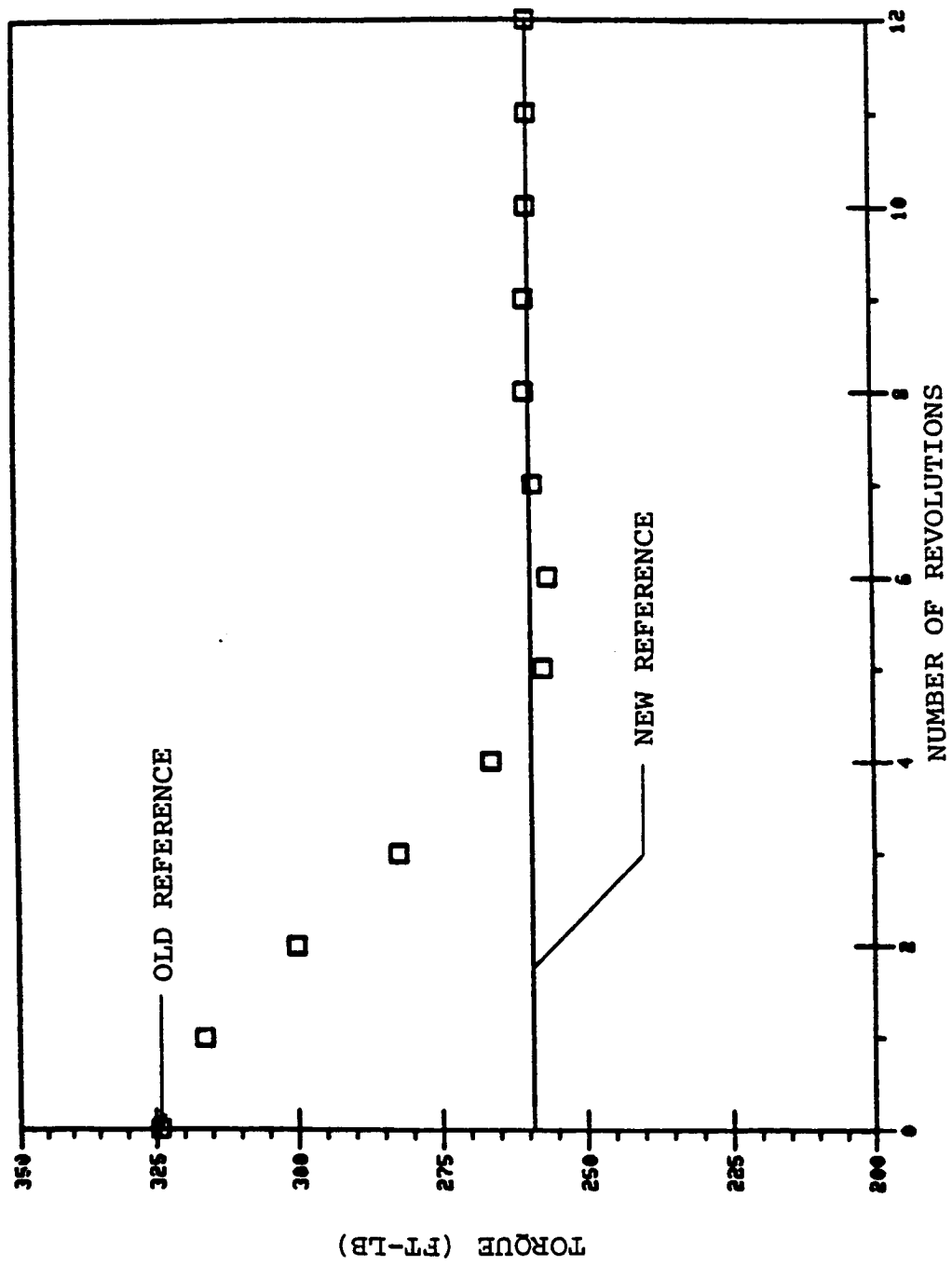


Figure II.4.2a. Average torque response for 20% step reduction in reference torque for wind speed = 35 mph.

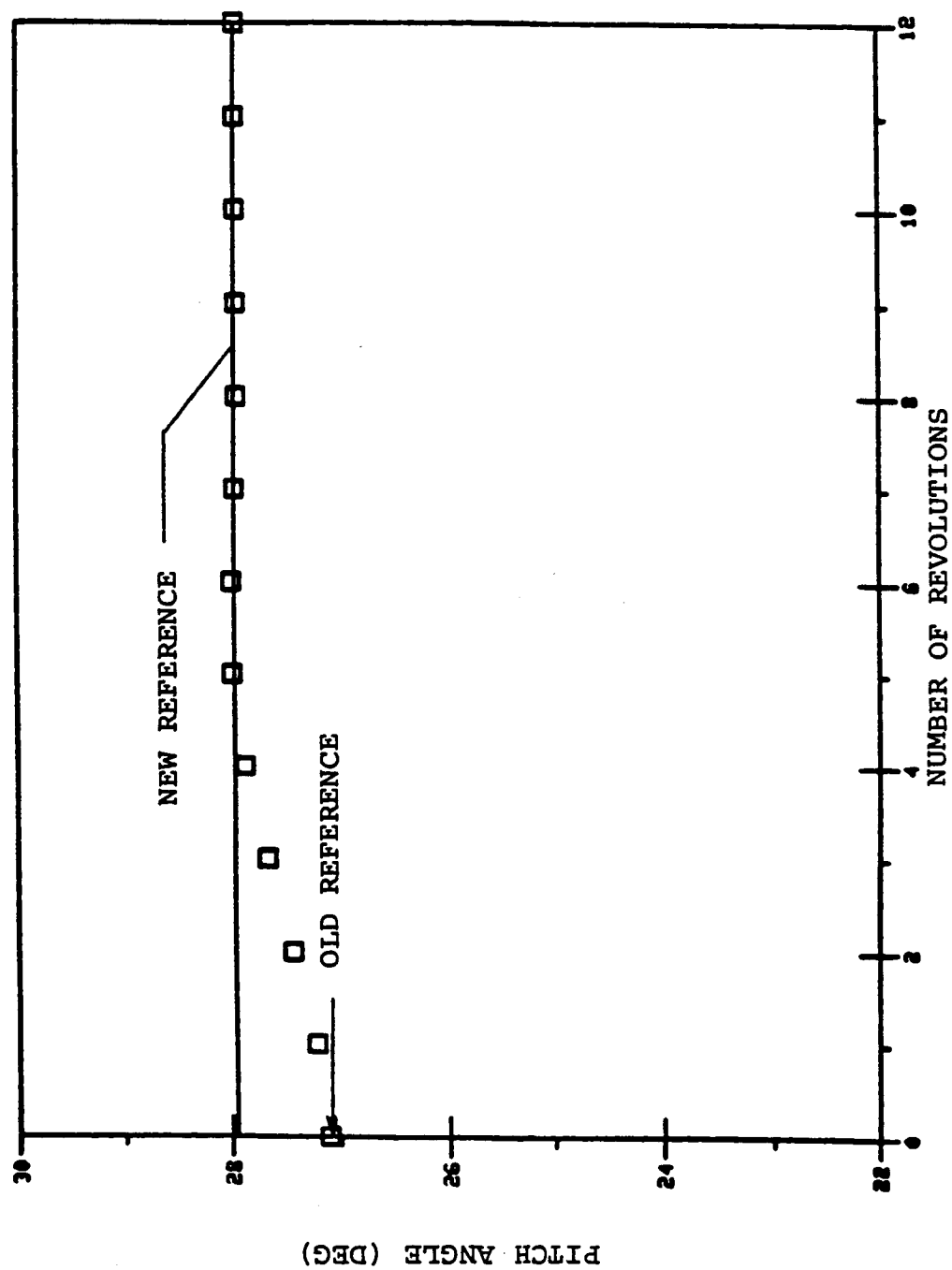


Figure II.4.2b. Blade pitch angle control for 20% step reduction in reference torque for wind speed = 35 mph.

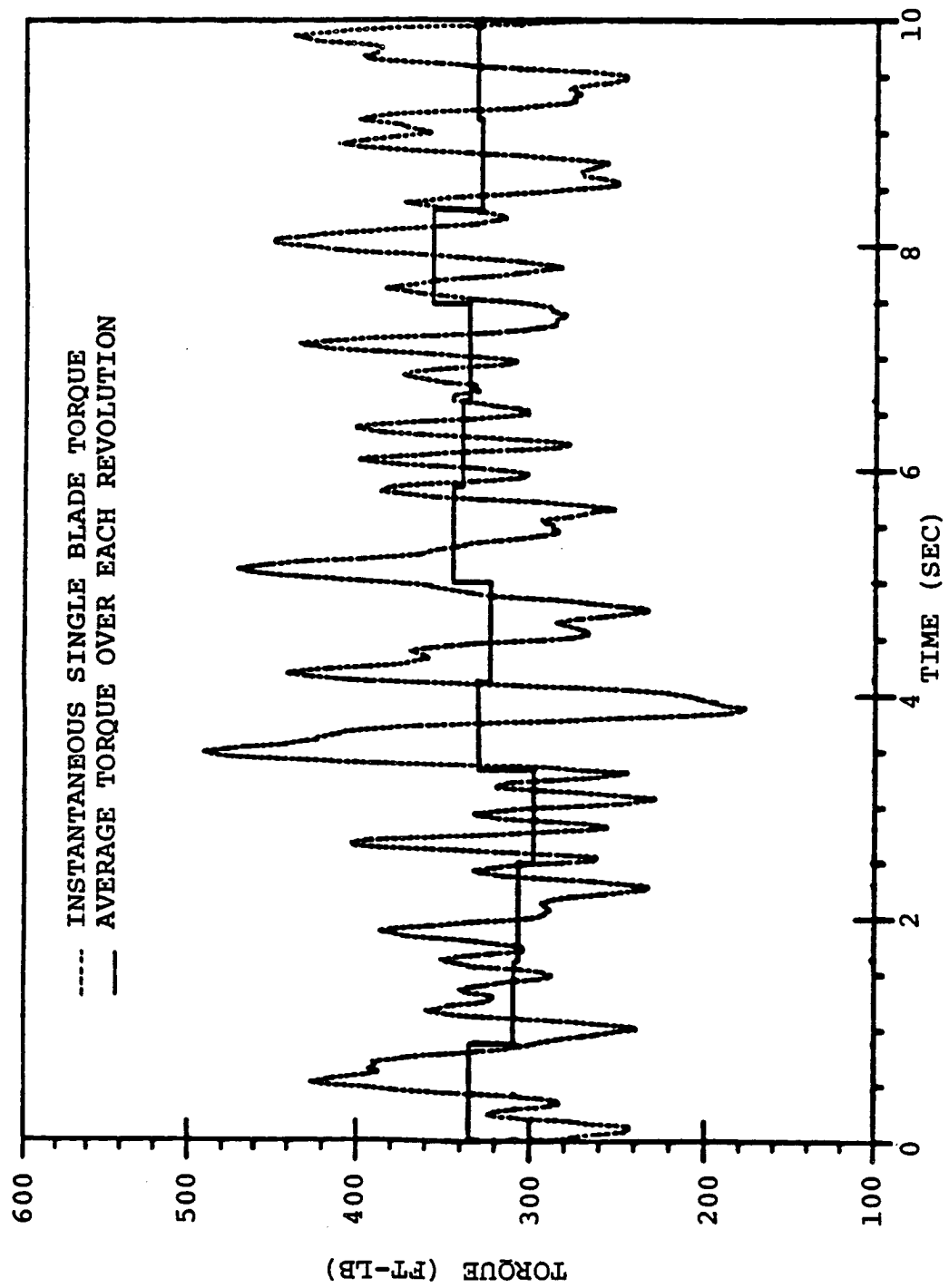


Figure II.4.3. Fixed pitch operation for wind speed = 20 mph.

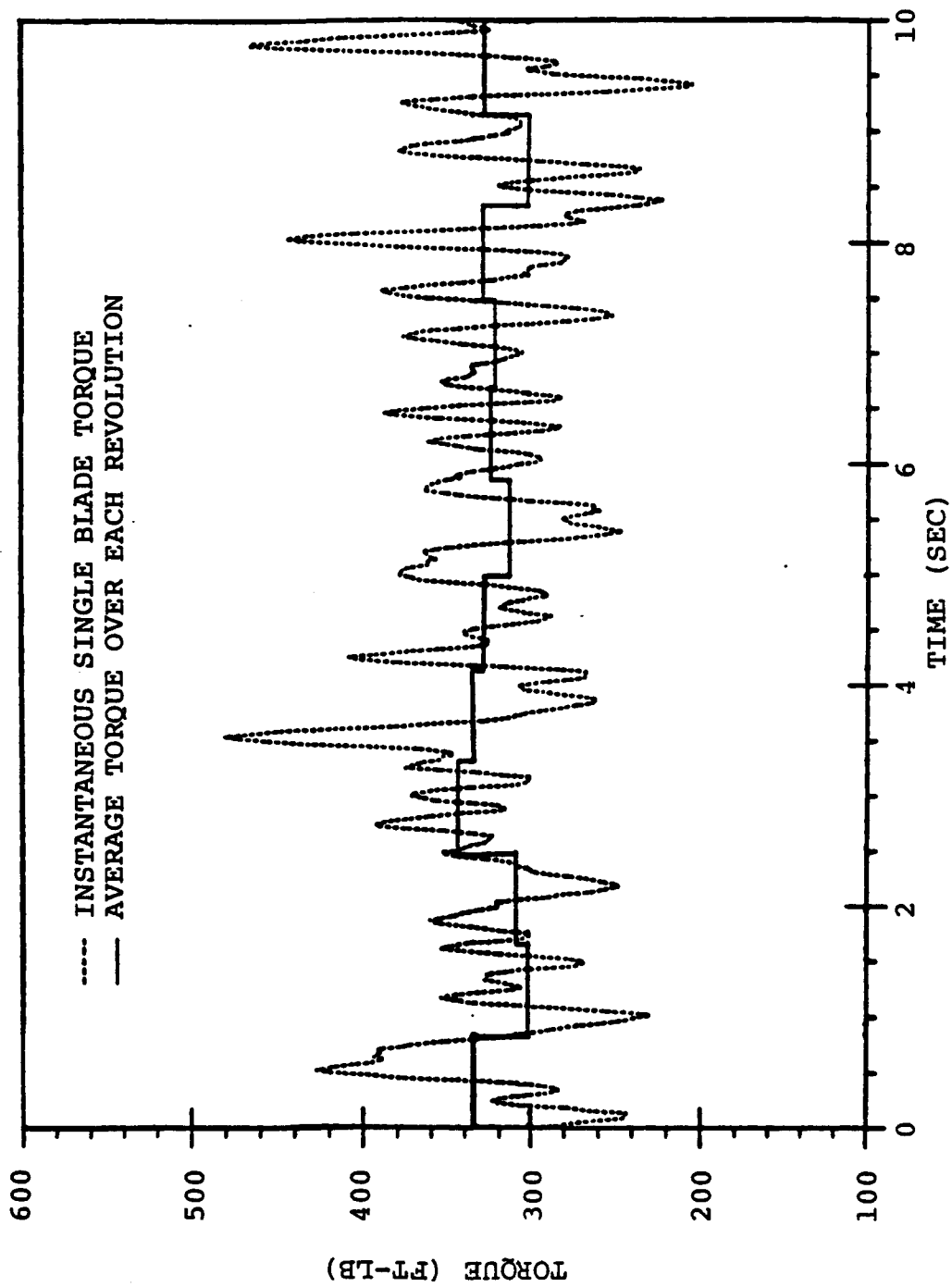


Figure II.4.4. Active pitch control operation for wind speed = 20 mph.

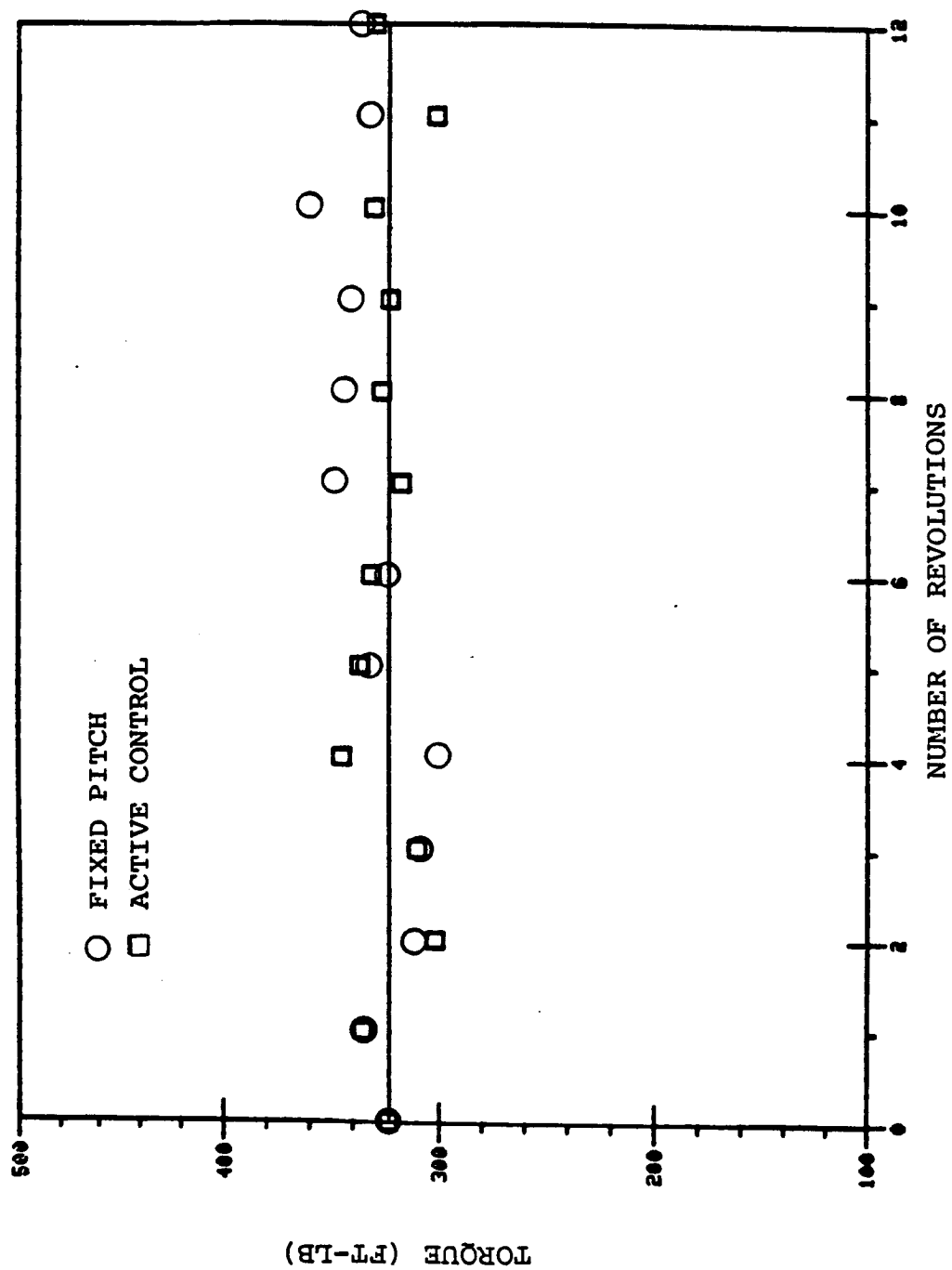


Figure II.4.5. Average single blade torque over each revolution for wind speed = 20 mph.

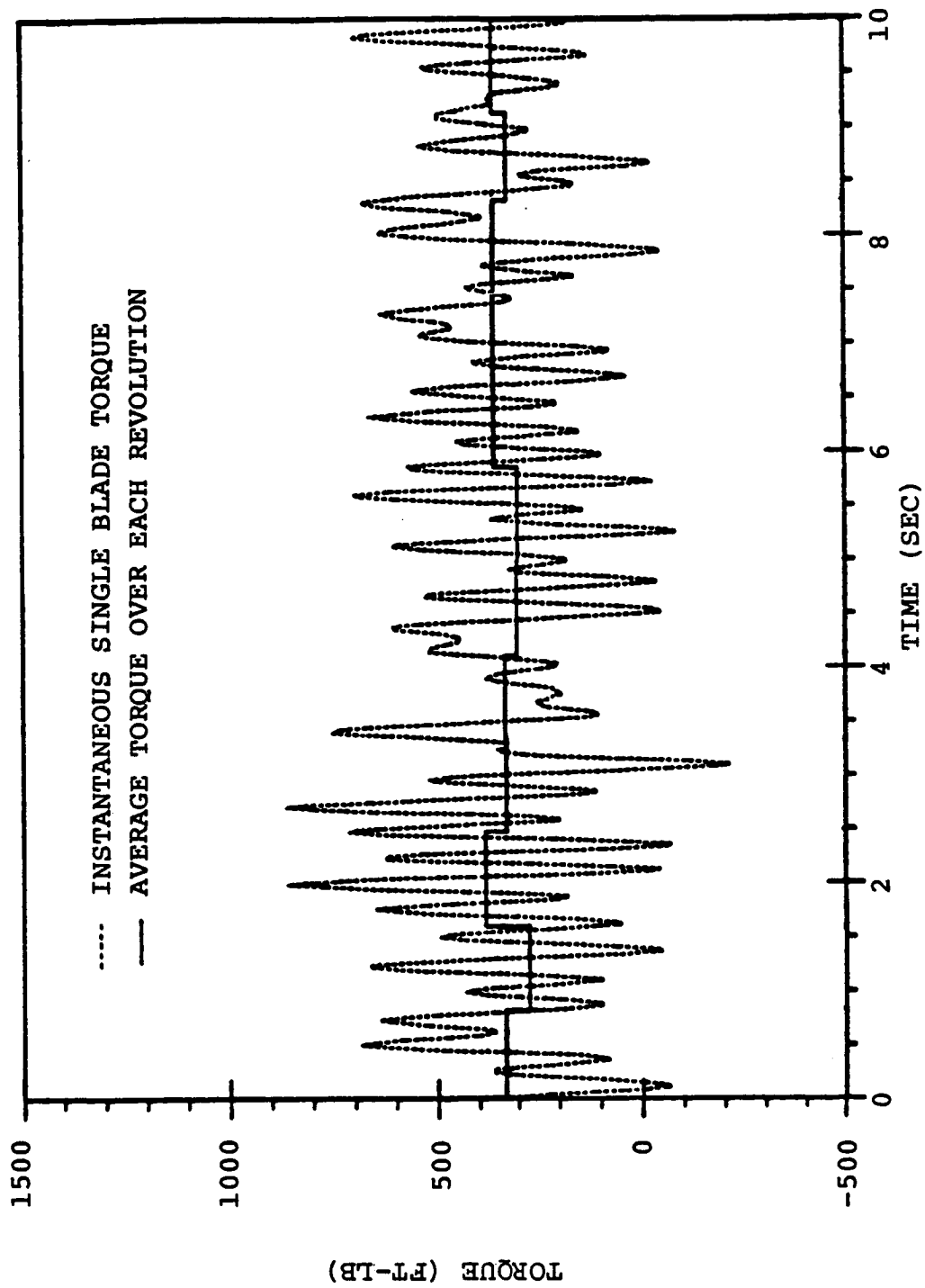


Figure II.4.6. Fixed pitch operation for wind speed = 35 mph.

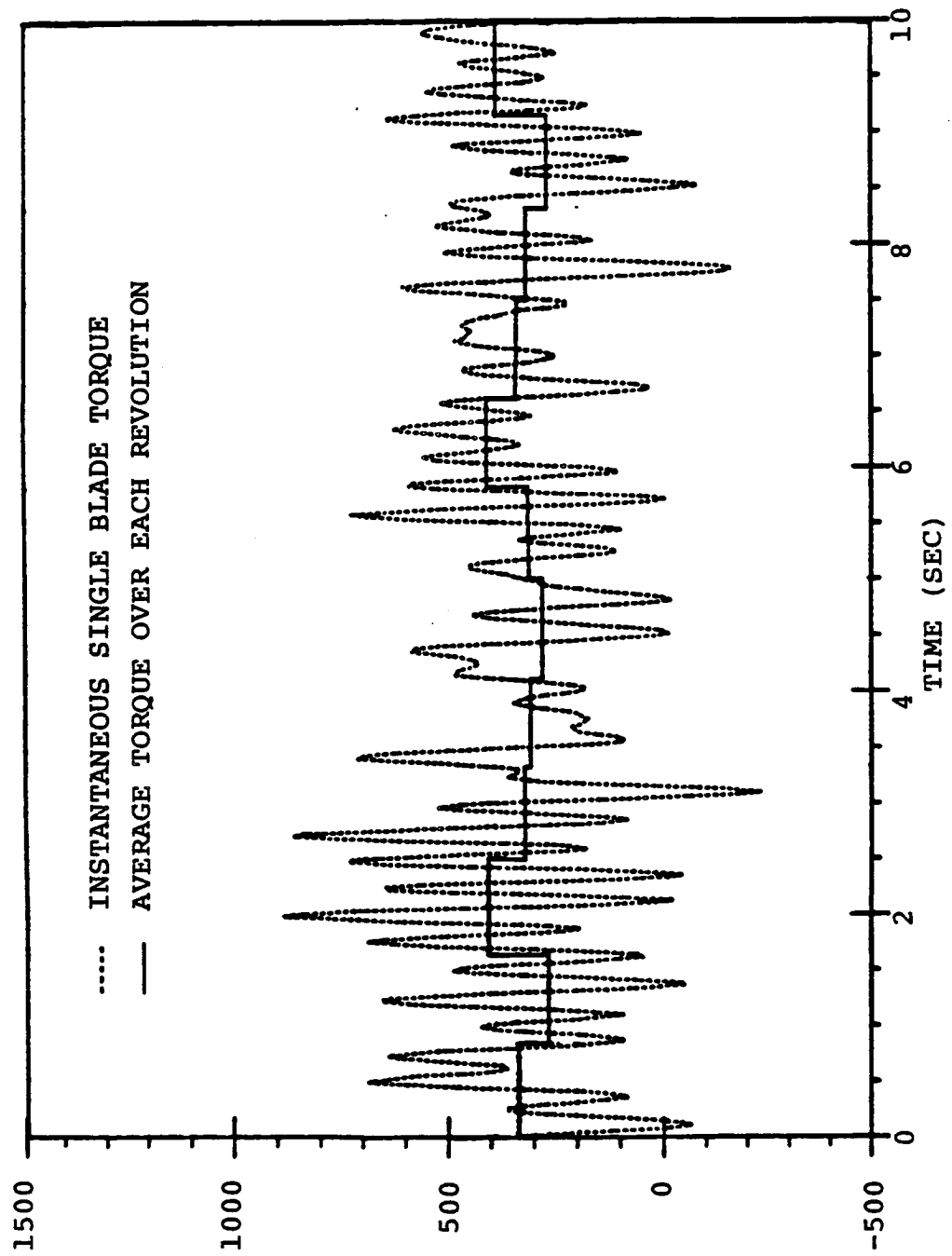


Figure II.4.7. Active pitch control operation for wind speed = 35 mph.

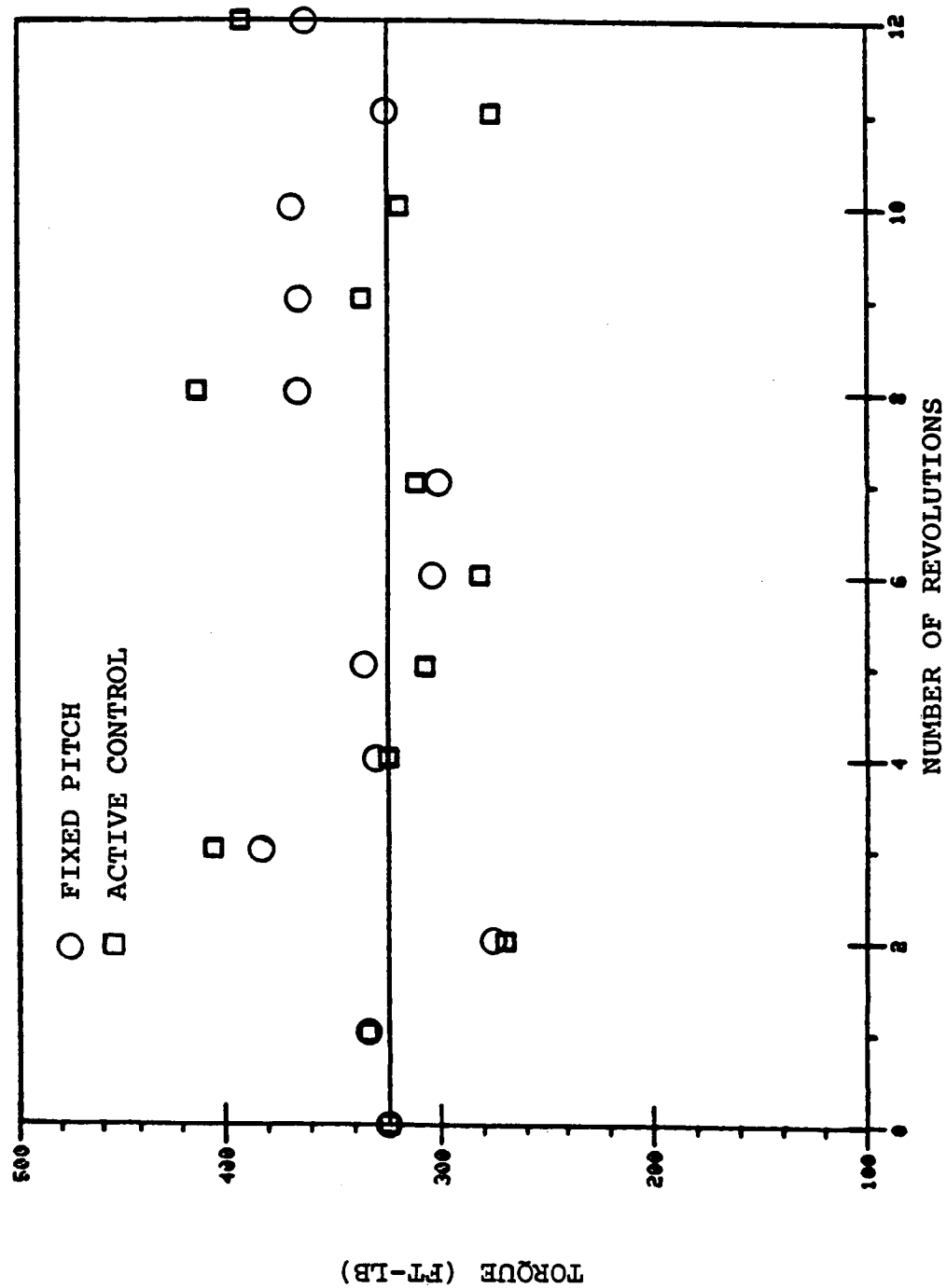


Figure II.4.8. Average single blade torque over each revolution for wind speed = 35 mph.



## BIBLIOGRAPHY

Abroamowitz, M.A. and Segun, I.A., Handbook of Mathematical Functions, U.S. Nat. Bureau Standards, 1964.

Brown, R.G., Random Signal Analysis and Kalman Filtering, John Wiley, 1983.

Cannon, R.H., Dynamics of Physical Systems, McGraw-Hill, 1967.

Connell, J.R., The Spectrum of Wind Speed Fluctuations Encountered by a Rotating Blade with a Wind Energy Conversion System: Observation and Theory, Battelle Pacific Northwest Laboratory, Report PNL 4083, 1981.

Cooley, J.W., Lewis, P.A., and Welch, P.D., The Application of the Fast Fourier Transform Algorithm to the Estimation of Spectra and Cross Spectra, IBM Research Paper, IBM Watson Research Center, Yorktown Heights, NY, 1967.

George, R.L. and Connell, J.R., Rotationally Sampled Wind Characteristics and Correlations with MOD-0A Wind Turbine Response, Pacific Northwest Laboratory Report PNL-5238, September 1984.

Hull, T.E. and Dobell, A.R., Random Number Generators, SIAM Rev. 4, 1962.

Isaacson, E. and Keller, H.B., Analysis of Numerical Methods, Wiley, 1966.

Kochenburger, R.J., Computer Simulation of Dynamic Systems, Prentice-Hall, 1972.

Kristensen, L. and Frandsen, Sten, "Model for Power Spectra Measured from the Moving Frame of Reference of the Blade of a Wind Turbine," Journal of Wind Engineering and Industrial Aerodynamics, V. 10, 1982.

Kuo, B.C., Automated Control Systems, Prentice-Hall, 1982.

Kwakernaak, H. and Sivan, R., Linear Optimal Control Systems, Wiley, 1972.

Mirham, G.A., Simulation, Statistical Foundations and Methodology, Academic Press, 1972.

Newland, D.E., An Introduction to Random Vibrations and Spectral Analysis, Longman, 1975.

Otnes, R.K. and Enochson, L., Digital Time Series Analysis, John Wiley, New York, 1972.

Palm, W.J., Modeling, Analysis, and Control of Dynamic Systems, Wiley, 1983.

Papoulis, A., Probability Random Variables and Stochastic Processes, McGraw-Hill, 1965.

Rosenbrock, H.H. Vibration and Stability Problems in Large Turbines Having Hinged Blades, ERA Technology Ltd., Surrey, England, Report C/T 133, 1955.

Thresher, R.W., et al., Modeling the Response of Wind Turbines to Atmospheric Turbulence, Oregon State University, Dept. of Mechanical Engineering, Report RLO/2227-81/2, August 1981.

Thresher, R.W. and Hershberg, E.L., Computer Analysis of Wind Turbine Blade Static and Dynamic Loads, Oregon State University, Dept. of Mechanical Engineering, Report RFP-76824, March 1984.

Thresher, R.W. and Holley, W.E., The Response Sensitivity of Wind Turbines to Atmospheric Turbulence, Oregon State University, Dept. of Mechanical Engineering, Report RLO/2227-81/1, May 1981.

Von Karman, T., "Sur la Theorie Statistique de la Turbulence," Comptes Rendus des Seances de l'Academie de Sciences, v. 226, 1948.

## APPENDIX I.A LINEAR LEAST-SQUARES REGRESSION (1)

For the general regression problem, the form of the relation

$$y = f(x, a) \quad (A.1)$$

where:  $x$  = independent variable

$a$  = vector of parameters

$y$  = dependent variable

is known and it is desired to determine the vector of parameters,  $a$ , when several data points  $(x_i, y_i)$  are given. In the case when the parameters appear linearly, i.e.,

$$y = a_1 f_1(x) + a_2 f_2(x) + \dots + a_n f_n(x) \quad (A.2)$$

the data parameters form a set of linear equations given by

$$\sum_{j=1}^n f_j(x_i) a_j = y_i \quad i = 1, \dots, m \quad (A.3)$$

When there are more data points than unknown parameters (i.e.,  $m > n$ ) the equations are overdetermined and it is unlikely that all equations can be satisfied exactly. When  $m < n$  the equations are underdetermined and many different sets of parameter values can be found which fit the data exactly. To determine a reasonable solution

to the problem, the parameters can be chosen to minimize the sum of the squares of the residuals, i.e.,

$$\text{Min}_a \sum_{i=1}^m (y_i - f(x_i, a))^2 \quad (\text{A.4})$$

It can be shown (2), in the case when the data are given exactly by

$$y_i = F(x, a_*) + e_i \quad (\text{A.5})$$

where  $a_*$  are the true parameters and  $e_i$  are mutually independent random errors which are normally distributed with zero mean, that the least-squares solution is equivalent to choosing the most probable values of  $a$ , given the data (assuming no prior knowledge of  $a$ ). In cases when there are more parameters than data (i.e.,  $m < n$ ) it is reasonable to set the last  $n-m$  parameters to zero then to determine the remaining  $m$  parameters which fit the data exactly.

In order to find the least squares solution, it is convenient to put the problem in matrix form

$$y - Fa = e \quad (\text{A.6})$$

where

$$F = \begin{matrix} & f_1(x_1) & f_2(x_1) & \cdots \\ & f_1(x_2) & \cdot & \\ & \cdot & & \cdot \\ & \cdot & & \\ y & y_1 & & \\ & \cdot & & \\ & \cdot & & \\ & y_m & & \end{matrix}$$

$e$  = residual vector (dimension  $m$ )

The necessary conditions for the minimum are easily found by differentiating to be

$$2\left(\frac{\partial e}{\partial a}\right)^T e = 0 \quad (\text{A.7})$$

or using Eq. (A.6) and the definition of  $F$

$$2(-F)^T(y - Fa) = 0$$

or, finally

$$(F^T F)a = F^T y \quad (\text{A.8})$$

The solution is unique when the matrix  $F^T F$  is nonsingular.

Instead of solving Eq. (A.8) directly for

$$a = (F^T F)^{-1} F^T y \quad (\text{A.9})$$

Golub (3) suggested using the Householder (4) decomposition of the matrix  $F$ , i.e.,

$$F = QR \quad (\text{A.10})$$

where  $Q$  is orthogonal and  $R$  has all elements below the diagonal equal to zero. Thus, Eq. (A.8) can be rewritten as

$$(QR)^T(QR)a = (QR)^T y \quad (A.11)$$

or since  $Q$  is orthogonal (i.e.,  $Q^{-1} = Q^T$ )

$$(R^T R)a = R^T Q^T y \quad (A.12)$$

for the case when  $m > n$ ,  $R$  is of the form

$$R = \begin{pmatrix} U \\ \dots \\ 0 \end{pmatrix}$$

where  $U$  is upper triangular, and the coefficient matrix for  $a$  becomes

$$R^T R = U^T U \quad (A.13)$$

Now, let the right hand side be partitioned so that

$$Q^T y = \begin{pmatrix} z_1 \\ \dots \\ z_2 \end{pmatrix} \quad (A.14)$$

Since  $U$  and  $F$  have the same rank =  $n$ , Eq. (A.14) becomes

$$Ua = z_1 \quad (A.15)$$

The solution to Eq. (A.15) involves only a simple back substitution since  $U$  is triangular.

This procedure has been implemented in a standard library subroutine supplied by the IMSL (5) and is utilized to compute the regression parameters in the turbulence model.

## I.A.1 References

1. Lawson, C.L. and Hanson, R.J., Solving Least Squares Problems, Prentice-Hall, 1974.
2. Goodwin, G.C. and Payne, R.L., Dynamic System Identification, Academic Press, 1977, pp. 29-41.
3. Golub, G., "Numerical Method for Solving Linear Least Squares Problems," Numerische Mathematik, V. 7, 1965, pp. 206-216.
4. Housholder, A.S., "Unitary Triangularization of a Nonsymmetric Matrix," J. Assn. Comput. Mach., V. 5, 1958, pp. 339-342.
5. Anon., Documentation for Routine LLSQF, The International Mathematical and Statistical Library, IMSL, Inc., Houston, TX.



## APPENDIX I.B DIGITAL SPECTRAL ANALYSIS

The power spectral density of a stationary random process  $x(t)$  is defined as

$$S_x(\omega) = \int_{-\infty}^{\infty} R_x(\tau) e^{-i\omega\tau} d\tau \quad (\text{B.1})$$

where  $R_x(\tau)$  is the autocorrelation function of  $x(t)$  given by

$$R_x(\tau) = E [x(t)x(t+\tau)] \quad (\text{B.2})$$

If the random process  $x(t)$  is sampled at intervals  $\Delta$  (constant) then the discrete value of  $x(t)$  at time  $t = r\Delta$  is written  $x_r$  and the sequence  $\{x_r\}$ ,  $r = 0, 1, 2, \dots$ , is called a discrete time series. The objective of time series analysis is to determine the statistical characteristics of the original function  $x(t)$  by manipulating the discrete time series  $\{x_r\}$ . The main interest is the frequency composition of  $x(t)$ . For this, the power spectral density of  $x(t)$  is estimated by analyzing the discrete time series obtained by sampling a finite segment of  $x(t)$ . Discrete Fourier transform (DFT) of a time series  $\{x_r\}$ ,  $r = 0, 1, 2, \dots, (N-1)$  is defined as follows:

$$X_k = \frac{1}{N} \sum_{r=0}^{N-1} x_r e^{-i\left(\frac{2\pi k}{N}\right)r} \quad k = 0, 1, 2, \dots, (N-1) \quad (\text{B.3})$$

and the inverse discrete Fourier transform (IDFT) is given by

$$x_r = \sum_{k=0}^{N-1} x_k e^{i\left(\frac{2\pi r}{N}\right)k} \quad r = 0, 1, 2, \dots, (N-1) \quad (\text{B.4})$$

where the range of the Fourier components  $x_k$  is limited to  $k = 0$  to  $(N-1)$  corresponding to harmonics of frequency  $\omega_k = \frac{2\pi k}{T} = \frac{2\pi k}{N\Delta}$  where  $T = N\Delta$  is the finite segment of the sampling function  $x(t)$  and  $\Delta$  is the sampling interval.

It can be shown (1) that the spectrum of  $x(t)$  can be estimated by  $\tilde{S}(\omega_k)$  as follows

$$\tilde{S}(\omega_k) \approx TS_k \quad (\text{B.5})$$

where  $S_k$  is the DFT of the discrete autocorrelation  $R_r$  which for two random processes  $x(t)$  and  $y(t)$  and their corresponding sampled time series  $\{x_r\}$  and  $\{y_r\}$  is given by

$$R_r = \frac{1}{N} \sum_{s=0}^{N-1} x_s y_{s+r} \quad r = 0, 1, 2, \dots, (N-1) \quad (\text{B.6})$$

Substituting for  $x_r$  and  $y_r$  from (B.4) it is possible to demonstrate that  $S_k$  can be obtained as

$$S_{xxk} = X_k^* X_k$$

$$S_{xyk} = X_k^* Y_k$$

(B.7)

$$S_{yxk} = Y_k^* X_k$$

$$S_{yyk} = Y_k^* Y_k$$

where the complex conjugate of X and Y are denoted as  $X^*$  and  $Y^*$ .

The fast Fourier transform subroutine listed in Reference (1) is used to evaluate the DFT's of the time series. The FFT works by partitioning the full sequence  $\{x_r\}$  into a number of shorter sequences. Instead of calculating DFT of the original sequence, only the DFT's of the shorter sequences are computed and then averaged to yield the full DFT of  $\{x_r\}$ . A cosine data taper function is used to smooth the data at each end of the data record before carrying out the DFT to improve the shape of the resulting spectral density (2,3).

## I.B.1 References

1. Newland, D.E., An Introduction to Random Vibrations and Spectral Analysis, Longman (1975).
2. Cooley, J.W., Lewis, P.A., and Welch, P.D. The Application of the Fast Fourier Transform Algorithm to the Estimation of Spectra and Cross Spectra. IBM Research Paper, IBM Watson Research Center, Yorktown Heights, NY, 1967.
3. Otnes, R.K. and Enochson, L., Digital Time Series Analysis, John Wiley, New York, 1972.

## APPENDIX C. COMPUTER CODE LISTING

Listing of the program SIMULX.

## PROGRAM SIMULX (INPUT,OUTPUT)

```

CCCCCCCCCCCCCCCCCCCCCCCCCCCCCCCCCCCCCCCCCCCCCCCCCCCCCCCCCCCC
C
C
C
C PROGRAM SIMULX GENERATES THE WIND TURBULANCE AT POINTS ALONG THE C
C BLADE IN THE ROTOR DISK AND FINDS THE FREQUENCY SPECTRUM OF EACH C
C VELOCITY COMPONENT. A UNIFORMLY DISTRIBUTED RANDOM NUMBER IS C
C GENERATED TO SIMULATE WHITE NOISE. EACH TURBULANCE VELOCITY TERM C
C MODELED AS A STATIONARY RANDOM PROCESS GIVEN BY AN EQUATION OF C
C THE FORM C
C
C           $D(U) / DT + A * U = B * W$  C
C
C WHERE W : NON-DIMENSIONAL ZERO MEAN WHITE NOISE WITH POWER C
C          SPECTRAL DENSITY SW. C
C          A; : ATMOSPHERIC PARAMETER CONSTANTS. C
C          B C
C SOLUTION TO THIS EQUATION FOR A DISCRETE TIME WHITE NOISE CAN BE C
C WRITTEN AS C
C
C           $U(K+1) = PHI(K,K+1) * U(K) + W(K)$  C
C
C WHERE U(K); : SOLUTIONS AT TIMES T(K); T(K+1) C
C          U(K+1) C
C          PHI(K),K+1) : TRANSITION FUNCTION FROM TIME T(K) C
C                      TO T(K+1) C
C          W(K) : DRIVEN RESPONSE AT T(K+1) DUE TO THE C
C                 PRESENCE OF WHITE NOISE INPUT DURING TIME C
C                 T(K), T(K+1) INTERVAL. NOTE THAT W(K) IS C
C                 A WHITE NOISE RANDOM SEQUENCE. C
C SUBROUTINE ATMOS GENERATES THE ATMOSPHERIC CONSTATNTS PARAMETERS C
C A'S AND B'S. SUBROUTINE RANDOM GENERATES A SEQUENCE OF UNIFORMLY C
C DISTRIBUTED RANDOM NUMBERS WHILE ROUTINE MEANVAR CALCULATES MEAN C
C AND VARIANCE OF TIME SERIES. C
C SUBROUTINE PSD IS USED TO GENERATE THE SPECTRUM OF THE GENERATED C
C SIGNALS. STANDARD PLOT OF RANDOM VELOCITY VS TIME IS OBTAINED C
C USING SUBROUTINE PLTSTND. SUBROUTINE PLTLOG PROVIDES LOG-LOG C
C PLOT FOR SPECUM VS FREQUENCY. C
C
C NOTE: IF THE NUMBER OF GENERATED RANDOM VELOCITY C
C COMPONENTS, NRVELOC, IS NOT EVENLY DIVISIBLE BY C
C LENGTH OF THE SPECTRUM, LSPECT, THEN NRVELOC C
C MUST BE SMALLER THAN THE DECLARED SIZE OF RANDOM C
C VELOCITY COMPONENT ARRAYS AT MOST BY LSPECT SO C
C AFTER PADDING THE TIME SERIES IT IS NOT OVER SIZED. C
C
C
C
C

```

```

C
C LIST OF ARGUMENTS:
C CONST : CONSTATNT COEFFICIENT IN THE POWER RESIDUE ALGORITHM
C         (SUBROUTINE RANDOM) FOR GENERATION OF UNIFORMLY
C         DISTRIBUTED RANDOM NUMBERS
C DIVIDER : MODULE USED IN FUNCTION MOD(.) IN SUBROUTINE RANDOM
C SEED : INITIAL RANDOM NUMBER USED IN THE POWER RESIDUE
C        ALGORITHM, SUBROUTINE RANDOM
C NWCOMP : NUMBER OF TURBULENT VELOCITY TERMS IN THE ATMOSPHERIC
C        MODEL
C NRVELOC : NUMBER OF ELEMENTS OF RANDOM TURBULENT VELOCITY
C           COMPONENTS SEQUENCE
C NPTS : NUMBER OF POINTS ALONG THE BLADE AT WHICH TURBULENT
C        VELOCITY IS EVALUATED
C NBINS : NUMBER OF SUBINTERVALS ON THE POSITIVE VELOCITY
C        AXIS FOR DETERMINING PROBABILITY DISTRIBUTION
C PROBDIS : ARRAY OF SIZE (2*NBINS) WHICH CONTAINS PROBABILITY
C           DISTRIBUTION OF THE TURBULENT VELOCITY COMPONENTS
C           IN EACH SUBINTERVAL(BIN)
C VRANGE : MAXIMUM VALUE OF TURBULENT VELOCITY AS AN INTEGER
C           MULTIPLE OF ITS VARIANCE, SUBROUTINE PROB
C
CCCCCCCCCCCCCCCCCCCCCCCCCCCCCCCCCCCCCCCCCCCCCCCCCCCCCCCCCCCC

```

```

INTEGER NWCOMP,NPTS,LSPECT,LP2,NRVELOC
INTEGER NBINS,NLABEL,CONST
PARAMETER (LSPECT=128,LP2=7)
PARAMETER (NWCOMP=12,NPTS=1,NLABEL=1,NBINS=16)
REAL R,ROTR,OMEGA,OMEGAZ,DELTAT,DIVIDER,VRANGE
REAL VX(6500),VY(6500),VZ(6500),Y(6500),X(200)
REAL PROBDIS(2*NBINS)
REAL XX(NPTS),YY(NPTS),ZZ(NPTS)
REAL A(NWCOMP),B(NWCOMP),CC(NWCOMP),DD(NWCOMP)
REAL PSY(LSPECT/2+1),F(LSPECT/2+1),SOUT(LSPECT/2+1)
COMPLEX ZY(LSPECT)
DOUBLE PRECISION SEED
CHARACTER *7 FILEIN, FILEOUT, LABEL(NLABEL)*40
CHARACTER *2 ANS1, ANS*1
COMMON /TURBINE/ OMEGA,OMEGAZ,ROTR
COMMON /WIND/ TL,TI,SW,VW
COMMON /ATMOS/ A,B
COMMON /RAND/ CONST, SEED, DIVIDER
NAMELIST /INDATA/ CONST,DELTAT,DIVIDER,SEED,NRVELOC,OMEGA,
& OMEGAZ,ROTR,RRATIO,TI,TL,VRANGE,VW

```

```

*
* .... CONVERSION FACTORS ....
*

```

```

PI      = ACOS(-1.)
CDEGRAD = PI/180.
CRPMRPS = 2.*PI/60.

```

```

      CMPHFPS = 5280./3600.
*
* .... INTERACTIVE : SELECT INPUT AND OUTPUT FILES,
*                      OPEN FILES, READ DATA FILE. USE NAMELIST.
881  PRINT *, ' '
      PRINT *, 'ENTER NAME OF THE NEW DATA FILE '
      READ '(A)', FILEIN
      OPEN (5,FILE=FILEIN)
      PRINT *, ' '
      PRINT *, 'ENTER THE NAME OF OUTPUT FILE '
      READ '(A)', FILEOUT
      OPEN (6,FILE=FILEOUT)
*
* .... INPUT ....
*
* .... READ THE PLOT LABELS ....
*
      DO 100 I=1,NLABEL
        READ (5,'(A)') LABEL(I)
100  CONTINUE
      READ (5,INDATA)
      REWIND (5)
      CLOSE (5)
*
* .... PRINT ECHO OF INPUT DATA ....
*
1    PRINT *, ' '
      PRINT 5, 'CONST    =', CONST
      PRINT 6, 'DELTAT   =', DELTAT , '(SEC) '
      PRINT 7, 'DIVIDER  =', DIVIDER
      PRINT 7, 'SEED     =', SEED
      PRINT 5, 'NRVELOC  =', NRVELOC
      PRINT 6, 'OMEGA    =', OMEGA , '(RPM) '
      PRINT 6, 'OMEGAZ   =', OMEGAZ , '(DEG) '
      PRINT 6, 'ROTR     =', ROTR , '(FEET) '
      PRINT 6, 'RRATIO   =', RRATIO
      PRINT 6, 'TI        =', TI , '(PERCENT) '
      PRINT 6, 'TL        =', TL , '(FEET) '
      PRINT 6, 'VRANGE   =', VRANGE
      PRINT 6, 'VW        =', VW , '(MILES/HR)'
5    FORMAT (1X,A15,I8)
6    FORMAT (1X,A15,F12.3,T35,A15)
7    FORMAT (1X,A15,E20.13)
*
* .... INTERACTIVE: CHANGE DATA VALUES & REPEAT ECHO CHECK OR CONTINUE ..
*
      PRINT *, ' '
      PRINT *, 'DO YOU WANT TO CHANGE ANY VALUES ? ENTER(Y OR N)'
      READ '(A)', ANS
      IF (ANS .EQ. 'Y') THEN
        PRINT *, ' '

```



```

      PRINT *, 'TO CHANGE VALUES, LEAVE COLUMN 1 BLANK AND TYPE'
      PRINT *, '$INDATA FOLLOWED BY VALUE ASSIGNMENTS IN THE FORM:'
      PRINT *, 'NAME = VALUE, NAME = VALUE ,..., $'
      PRINT *, 'NOTE : COLUMN 1 MUST BE BLANK; TERMINATE WITH $ '
      READ INDATA
      PRINT *, ' '
      GO TO 1
ENDIF

*
* ..... UNIT CONVERSIONS : (RPM) TO (RAD/SEC); (DEG) TO (RAD) ....
*                               (MPH) TO (FT/SEC)
*
      OMEGA = OMEGA * CRPMRPS
      OMEGAZ = OMEGAZ * CDEGRAD
      VW = VW * CMPHFPS
*
      WRITE (6,10) CONST,SEED,DIVIDER
10  FORMAT(//,5X,'POWER RESIDUE METHOD WITH THE FOLLOWING PARAMETERS'
&      ,/,5X,'IS USED TO GENERATE UNIFORMLY DISTRIBUTED RANDOM '
&      , 'NUMBERS',/,10X,'CONSTANT COEFF, CONST',T35,'= ',I8,/,10X
&      , 'SEED',T35,'= ',1X,E15.8,/,10X
&      , 'MODULE DIVIDER, DIVIDER',T35,'= ',1X,E20.13)
*
* .....
* ..... GENERATE ATMOSPHERIC COEFFICIENTS .....
* .....
      CALL ATMOS
* .....
* ..... PRINT ATMOSPHERIC COEFFS .....
      WRITE (6,15)
15  FORMAT(//,20X,'ACOEFF',12X,'BCOEFF')
      DO 140 I=1,NWCOMP
          WRITE (6,20) I,A(I),B(I)
20  FORMAT(/,5X,I5,5X,E13.6,5X,E13.6)
140  CONTINUE
* .....
* ..... GENERATE RANDOM VELOCITIES ...
* .....
      R = RRATIO * ROTR
      ANGSTEP = DELTAT * OMEGA
      IF (NPTS .EQ. 1) THEN
          BEGINR = R
          FINR = R
      ELSE
          NSEG=NPTS-1
          PRINT *, 'NO. OF SEGEMENTS ALONG THE BLADE, NSEG= ',NSEG
          PRINT *, 'NO. OF POINTS ALONG THE BLADE WHERE VELOCITY '
          PRINT *, 'COMPONENTS ARE CALCULATED, NPTS= ',NPTS
          PRINT *, 'ENTER THE BEGINNING AND FINAL RADIUS ALONG THE '
          PRINT *, 'BLADE, BEGINR, AND FINR.'
          READ *, BEGINR,FINR

```

```

ENDIF
DO 200 J=1,NRVELOC
  PSI=J*ANGSTEP+OMEGAZ
* ....
  CALL TURBS (XX,YY,ZZ,DELTAT,BEGINR,FINR,NPTS,PSI)
* ....
  VX(J)= XX(1)
  VY(J)= YY(1)
  VZ(J)= ZZ(1)
200 CONTINUE
* .... CALCULATE MEAN AND VARIANCE OF THE TIME SERIES
* ....
  CALL MEANVAR (VXMEAN,VXVAR,VX,NRVELOC)
  CALL MEANVAR (VYMEAN,VYVAR,VY,NRVELOC)
  CALL MEANVAR (VZMEAN,VZVAR,VZ,NRVELOC)
* ....
* ....
  WRITE (6,25) NRVELOC,DELTAT,R,OMEGA,OMEGAZ,VW,TL,TI,SW
  & ,VXMEAN,VXVAR,VYMEAN,VYVAR,VZMEAN,VZVAR
25  FORMAT(/,10X,'NUMBER OF RANDOM VELOCITIES GENERATED, NRVELOC'
  & ,T65,'= ',I5,/,10X,'TIME STEP TO GENERATE THE RANDOM '
  & , 'VELOCITY, DELTAT',T65,'= ',E12.5,/,10X,'RADIAL DISTANCE '
  & , 'TO SELECTED POINT ALONG THE ROTOR, R',T65,'= ',E12.5, /
  & ,10X,'ROTOR SPEED, OMGA',T44,'= ',E12.5,T64,'(RAD/SEC)', /
  & ,10X,'INITIAL ROTATION, OMEGA-ZERO',T44,'= ',E12.5,T64
  & , '(RAD)',/,10X,'WIND VELOCITY, VW',T44,'= ',E12.5,T64
  & , '(FEET/SEC)',/,10X,'TURBULENCE INTEGRAL SCALE, TL',T44
  & , '= ',E12.5,T64,'(FEET)',/,10X,'TURBULENCE INTENSITY, '
  & , 'TI',T44,'= ',E12.5,T64,'(PERCENT)',/,10X,'SPECTRUM OF THE '
  & , 'INPUT WHITE NOISE, SW =',T65,'= ',E12.5,5X,'(SEC)',/,10X
  & , 'MEAN VALUE OF VX =',E14.7,4X,'VARIANCE OF VX =',E14.7,/,10X
  & , 'MEAN VALUE OF VY =',E14.7,4X,'VARIANCE OF VY =',E14.7,/,10X
  & , 'MEAN VALUE OF VZ =',E14.7,4X,'VARIANCE OF VZ =',E14.7)

  DO 220 J=1,NRVELOC
    VX(J)=VX(J)-VXMEAN
    VY(J)=VY(J)-VYMEAN
    VZ(J)=VZ(J)-VZMEAN
220 CONTINUE
* ....
  PRINT *, 'TO GET LIST OF GENERATED RANDOM VELOCITIES VX, VY, VZ '
  PRINT *, 'ENTER (Y OR N)'
  READ '(A)', ANS
  IF (ANS.EQ. 'Y') THEN
    PRINT *, 'ENTER THE NO. OF RANDOM VELOCITIES TO PRINT '
    PRINT *, 'UP TO NRVELOC=',NRVELOC
    READ *, NOUT
* ....
    WRITE (6,27) NOUT,DELTAT
    DO 225 J=1,NOUT
      WRITE (6,29) J,VX(J),VY(J),VZ(J)

```

```

225     CONTINUE
      ENDIF
27     FORMAT (//,10X,'NUMBER OF RANDOM NUMBERS TO PRINT,NOUT=',I6,/,
      &         10X,'TIME STEP TO GENERATE THE RANDOM VELOCITIES '
      &         , 'VX, VY, VZ, DELTAT=',E10.3,/,T28
      &         , 'VX',T48,'VY',T68,'VZ', ' (MEANS ARE SUBTRACTED)')
29     FORMAT (10X,I4,T20,E14.7,T40,E14.7,T60,E14.7)
* ....
* .... PLOT RANDOM VELOCITY TIME SERIES VS TIME ....
      PRINT *, 'TO USE SUBROUTINE PLTSTND TO PLOT THE GENERATED RANDOM '
      PRINT *, 'VELOCITY VS TIME , ENTER (Y OR N) '
      READ '(A)', ANS
882   IF (ANS .EQ. 'Y' ) THEN
      PRINT *, 'SELECT THE RANDOM VELOCITY TIME SERIES.  ENTER '
      PRINT *, ' VX OR VY OR VZ. '
      READ '(A)', ANS1
      PRINT *, 'ENTER THE LENGTH OF RANDOM VELOCITY TIME SERIES '
      PRINT *, ',LVPLT FOR PLOTTING UP TO NRVELOC =',NRVELOC
      READ *, LVPLT
      IF ( ANS1 .EQ. 'VX' ) THEN
        DO 230 I=1,LVPLT
          Y(I)=VX(I)
230      CONTINUE
      ELSEIF ( ANS1 .EQ. 'VY' ) THEN
        DO 232 I=1,LVPLT
          Y(I)=VY(I)
232      CONTINUE
      ELSEIF ( ANS1 .EQ. 'VZ' ) THEN
        DO 234 I=1,LVPLT
          Y(I)=VZ(I)
234      CONTINUE
      ENDIF
* ....
      CALL PLTSTND (Y,LVPLT,DELTAT,ANS1)
* ....
      PRINT *
      PRINT *
      PRINT *, 'DO YOU WANT TO PLOT ANY OTHER RANDOM VELOCITY '
      PRINT *, 'TIME SERIES ? ENTER (Y OR N)'
      READ '(A)', ANS
      GO TO 882
    ENDIF
* .... EVALUATE PROBABILITY DISRIBUTION OF RANDOM VELOCITY ....
      PRINT *, 'DO YOU WANT TO EVALUATE PROBABILITY DISTRIBUTIONS OF'
      PRINT *, 'THE GENERATED RANDOM VELOCITIES ? ENTER (Y OR N)'
      READ '(A)', ANS
      IF (ANS .EQ. 'Y') THEN
        DO 250 KPROB =1,3
          IF (KPROB .EQ. 1) THEN
            DO 240 I=1,NRVELOC
              Y(I)=VX(I)

```

```

240      CONTINUE
          VARIANC=VXVAR
          ANS1 = 'VX'
      ELSEIF (KPROB .EQ. 2) THEN
          DO 242 I=1,NRVELOC
              Y(I)=VY(I)
242      CONTINUE
          VARIANC=VYVAR
          ANS1 = 'VY'
      ELSEIF (KPROB .EQ. 3) THEN
          DO 244 I=1,NRVELOC
              Y(I)=VZ(I)
244      CONTINUE
          VARIANC=VZVAR
          ANS1 = 'VZ'
      ENDIF
* ..... GENERATE UNITY VARIANCE RANDOM VELOCITY TIME SERIES .....
      DO 245 I=1,NRVELOC
          Y(I)=Y(I)/SQRT(VARIANC)
245      CONTINUE
* ....
* .... CALL PROB (Y,NRVELOC,NBINS,VRANGE,PROBDIS)
* ....
          NBX2=2*NBINS
          NBX2M1=NBX2-1
          DELTAV=VRANGE/(NBINS-1)
          DO 246 I=1,NBX2M1
              X(I)=-VRANGE+(I-1)*DELTAV
246      CONTINUE
          WRITE (6,30) ANS1,NRVELOC,ANS1
          DO 248 I=1,NBX2
              IF (I .EQ. 1) THEN
                  WRITE (6,32) X(I),PROBDIS(I)
              ELSEIF (I .EQ. NBX2) THEN
                  IM1=I-1
                  WRITE (6,34) X(IM1),PROBDIS(I)
              ELSE
                  IM1=I-1
                  PROB DEN = PROBDIS(I)/DELTAV
                  XAVE = (X(I)+X(IM1))/2.
                  STNDEN = EXP(-0.5*XAVE**2)/SQRT(2.*PI)
                  WRITE (6,36) X(IM1),X(I),PROBDIS(I),XAVE,PROB DEN
                      & ,STNDEN
              ENDIF
248      CONTINUE
250      CONTINUE
      ENDIF
30  FORMAT (//,10X,'PROBABILITY DISTRIBUTION OF RANDOM VELOCITY '
& , 'TIME SERIES',A4,' OF LENGTH = ',15,/,10X
& , 'PROBABILITY OF VARIATES',15X,'MID-INTERVAL',5X
& , 'PROBABILITY DENSITY',5X,'STANDARD NORMAL',/,10X

```

```

&      , 'IN THE INTERVAL', T66, 'ORDINATES OF ', A4, T93
&      , 'ORDINATES', /)
32  FORMAT (10X, 'LESS THAN ', 3X, '(', F6.2, ') = ', E11.4)
34  FORMAT (10X, 'GREATER THAN ', '(', F6.2, ') = ', E11.4)
36  FORMAT (15X, '(', F6.2, ' ', F6.2, ') = ', E11.4, T52, F6.2
&      , T68, E12.6, T90, E12.6)
* ....
* .... GENERATE FREQUENCY SPECTUM OF THE GENERATED RANDOM VELOCITY ....
* ....
PRINT *, 'DO YOU WANT TO GENERATE THE FREQUENCY SPECTRUM OF '
PRINT *, 'THE TIME SERIES ? ENTER (Y OR N)'
READ '(A)', ANS
884 IF (ANS .EQ. 'Y') THEN
    PRINT *, 'INPUT ONE TIME SERIES TO GENERATE SPECTRUM. '
    PRINT *, 'ENTER VX OR VY OR VZ '
    READ '(A)', ANS1
    IF (ANS1 .EQ. 'VX' )      THEN
        DO 252 I=1, NRVELOC
            Y(I)=VX(I)
252    CONTINUE
    ELSEIF (ANS1 .EQ. 'VY' ) THEN
        DO 254 I=1, NRVELOC
            Y(I)=VY(I)
254    CONTINUE
    ELSEIF (ANS1 .EQ. 'VZ' ) THEN
        DO 256 I=1, NRVELOC
            Y(I)=VZ(I)
256    CONTINUE
    ENDIF

* .... LENGTH OF THE TIME SERIES HAS TO BE EVENLY DIVISIBLE .....
* .... BY L, LENGTH OF EACH SUBSEGMENT. IF THIS CONDITION .....
* .... DOES NOT MEET PAD BOTH TIME SERIES WITH ZEROES AT .....
* .... RIGHT END. ....
* .... NOTE: IF THE NUMBER OF GENERATED RANDOM VELOCITY .....
* .... COMPONENTS, NRVELOC, IS NOT EVENLY DIVISIBLE BY .....
* .... LENGTH OF THE SPECTRUM, LSPECT, THEN NRVELOC .....
* .... MUST BE SMALLER THAN THE DECLARED SIZE OF RANDOM .....
* .... VELOCITY COMPONENT ARRAYS AT MOST BY LSPECT. ....
* ....
LD2=LSPECT/2
LD2P1=LD2+1
NSEG=INT(NRVELOC/LSPECT)
RNSEG=REAL(NRVELOC)/REAL(LSPECT)
DIFF=RNSEG-NSEG
IF(DIFF .NE. 0.0) THEN
    LTS=(NSEG+1)*LSPECT
    IPAD=NRVELOC+1
    DO 300 J=IPAD, LTS
        Y(J)=0.0
300    CONTINUE

```

```

ENDIF
* ....
CALL PSD (Y,LTS,LSPECT,LP2,DELTAT,PSY,ZY)
* ....
* .... FORM THE FREQUENCY VECTOR ....
* ....
DO 325 I=1,LD2P1
    II=I-1
    F(I)=II/(LSPECT*DELTAT)
325 CONTINUE
* ....
* .... PRINT POWER SPECTRUM ....
WRITE (6,40) ANS1
DO 340 I=1,LD2P1
    WRITE (6,42) F(I),PSY(I)
340 CONTINUE
* .... PRINT SUM OF THE POWER SPECTRA ....
SUMY=0.0
DO 345 K=1,LD2P1
    SUMY=SUMY+PSY(K)
345 CONTINUE
WRITE (6,44) ANS1 , SUMY
40 FORMAT(//,5X,'FREQUENCY',T20,'POWER SPECTRUM',/,T24,A4)
42 FORMAT(4X,F10.4,T20,E14.7)
44 FORMAT(//,10X,'SUM OF THE PSD OF(',A4,')S=',E14.7)
* ....
* .... ELIMINATE ZERO FREQUENCY FOR LOG-LOG PLOTTING ....
* ....
DO 370 I=2,LD2P1
    J=I-1
    F(J)=F(I)
370 CONTINUE
* ....
* .... PLOT LOG-LOG SPECTRAL DENSITY OF RANDOM VELOCITY VS FREQUENCY ....
PRINT *, 'TO USE PLTLOG TO PLOT THE SPECTRUM ENTER (Y OR N)'
READ '(A)', ANS
IF (ANS.EQ. 'Y') THEN
* .... GENERATE SPECTRUM VECTORS ....
DO 380 I=2,LD2P1
    J=I-1
    SOUT(J)=PSY(I)
380 CONTINUE
* ....
* .... PLOT POWER SPECTRUM ....
* ....
CALL PLTLOG (SOUT,F,LD2,LABEL,ANS1)
* ....
PRINT *
ENDIF

PRINT *, 'DO YOU WANT SPECTRUM FOR OTHER TIME SERIES? '

```

```
      PRINT *, 'ENTER (Y OR N)'  
      READ '(A)', ANS  
      GO TO 884  
ENDIF
```

\*

```
PRINT *, 'DO YOU WANT TO PROCESS ANOTHER DATA FILE ? '  
PRINT *, 'ENTER (Y OR N)'  
READ '(A)', ANS  
IF (ANS .EQ. 'Y') GO TO 881  
STOP  
END
```

SUBROUTINE TURBS (XX,YY,ZZ,DELTAT,BEGINR,FINR,NPTS,PSI)

```

CCCCCCCCCCCCCCCCCCCCCCCCCCCCCCCCCCCCCCCCCCCCCCCCCCCCCCCCCCCC
C
C
C   SUBROUTINE TURBS CONSTRUTS TURBULENCE VELOCITY COMPONENTS
C   ALONG THE BLADE FOR EACH AZIMUTH ANGLE AT EACH TIME STEP.
C   THE NUMBER OF POINTS ALONG THE BLADE AT WHICH TURBULENCE
C   VELOCITY IS EVALUATED IS GIVEN AS A PARAMETER , NPTS IN
C   PROGRAM SIMULX, AND CAN EASILY BE CHANGED. THE TURBULENCE
C   VELOCITY COMPONENTS ARE COMPUTED AT EQUALLY DISTANCED
C   POINTS ALONG THE BLADE FROM AN INITIAL RADIUS TO A FINAL
C   RADIUS WHICH USER CAN DETERMINE.
C   IN THE PRESENT ANALYSIS ONLY ONE RADIAL POSITION AT THE
C   TIP WAS CONSIDERED (NPTS = 1).
C
C
CCCCCCCCCCCCCCCCCCCCCCCCCCCCCCCCCCCCCCCCCCCCCCCCCCCCCCCCCCCC

```

```

      INTEGER CONST,NPTS,NWCOMP
      REAL BEGINR,FINR,DELTAT,PSI,DIVIDER
      PARAMETER ( NWCOMP=12 )
      REAL XX(NPTS),YY(NPTS),ZZ(NPTS),U(NWCOMP),W(NWCOMP)
      REAL A(NWCOMP),B(NWCOMP),CC(NWCOMP),DD(NWCOMP)
      DOUBLE PRECISION SEED
      COMMON /TURBINE/ OMEGA,OMEGAZ,ROTR
      COMMON /WIND/ TL,TI,SW,VW
      COMMON /ATMOS/ A,B
      COMMON /RAND/ CONST, SEED, DIVIDER
      SAVE W
      DATA W /NWCOMP * 0.0/
      * .... GENERATE COEFFICIENTS FOR FILTERS .....
      DO 10 I=1,NWCOMP
        AT=DELTAT*A(I)
        CC(I)=EXP(-AT)
        DD(I)=B(I)*SQRT((6.*SW/A(I))*(1.-EXP(-2.*AT)))
10    CONTINUE
      * .... GENERATE NWCOMP RANDOM NUMBERS .....
      * ....
      CALL RANDOM (U,NWCOMP)
      * ....
      * .... GENERATE WIND VELOCITY COMPONENTS ....
      DO 20 I=1,NWCOMP
        U(I)=U(I)-0.5
        W(I)=CC(I)*W(I)+DD(I)*U(I)
20    CONTINUE
      IF (NPTS .EQ. 1) THEN
        RSTEP=0.0

```



```

ELSE
  RSTEP=(FINR-BEGR)/(NPTS-1)
ENDIF
R=BEGINR
PSIX2=2*PSI
ROTRSQ=ROTR*ROTR
DO 30 I=1,NPTS
  R=R+(I-1)*RSTEP
  RSQ=R*R
  XX(I)=W(1)-(W(6)-W(7))*R*COS(PSI)
&      -(W(8)-W(9))*R*SIN(PSI)
  YY(I)=W(2)+W(5)*R*COS(PSI)+W(4)*R*SIN(PSI)
&      +W(10)*(RSQ-ROTRSQ/2.)
&      +W(11)*RSQ*COS(PSIX2)+W(12)*RSQ*SIN(PSIX2)
  ZZ(I)=W(3)+(W(6)+W(7))*R*SIN(PSI)
&      +(W(8)+W(9))*R*COS(PSI)
30 CONTINUE
RETURN
END

```

## SUBROUTINE ATMOS

```

CCCCCCCCCCCCCCCCCCCCCCCCCCCCCCCCCCCCCCCCCCCCCCCCCCCCCCCCCCCC
C
C
C SUBROUTINE ATMOS COMPUTES THE TURBULENCE MODEL PARAMETERS A, B,
C AND SW, WHERE A(I) AND B(I) ARE THE DIAGONAL ELEMENTS FOR
C THE MATRICES IN THE WIND STATE EQUATION
C  $DX/DT = -A * X + B * W$  AND W IS WHITE NOISE WITH PSD=SW.
C THE EQUATIONS WERE DETERMINED BY LEAST SQUARE REGRESSION TO
C DATA PRODUCED BY NUMERICAL COMPUTATION. (SEE REPORT)
C
C
CCCCCCCCCCCCCCCCCCCCCCCCCCCCCCCCCCCCCCCCCCCCCCCCCCCCCCCCCCCC

```

```

INTEGER NWCOMP
PARAMETER (NWCOMP=12)
REAL ROTR, TI, TL, SW, VW
REAL A(NWCOMP), B(NWCOMP)
COMMON /TURBINE/ OMEGA, OMEGAZ, ROTR
COMMON /WIND/ TL, TI, SW, VW
COMMON /ATMOS/ A, B

```

\* .... CALCULATE THE POWER SPECTRUM FOR THE NOISE INPUT ....

```

SW=TL*(TI*TI)/VW/10000.
RR=ROTR/TL
VWSQ=VW*VW
ROTRSQ=ROTR**2
DIMCOA= VW/TL
DIMCOBZ=VWSQ/TL
DIMCOB1=VWSQ/(ROTR*TL)
DIMCOB2=VWSQ/(ROTRSQ*TL)
A(1)= (2.-2.894*RR*(1.-.1383*RR))/(1.+2.049*RR) *DIMCOA
B(1)= (2.-3.290*RR*(1.+0.0270*RR))/(1.+2.054*RR) *DIMCOBZ
A(2)= (1.-1.713*RR*(1.-.0791*RR))/(1.+2.048*RR) *DIMCOA
B(2)= (SQRT(2.)-2.713*RR*(1.+0.0159*RR))/(1.+2.051*RR)
+ *DIMCOBZ
A(3)= A(1)
B(3)= B(1)
A(4)= (.327/RR + .595 - .114*RR) * DIMCOA
B(4)= (.281/RR**25 + .645 - .150*RR) *DIMCOB1
A(5)= A(4)
B(5)= B(4)
A(6)= (.434/RR + .917 - .153*RR) *DIMCOA
B(6)= (.258/RR**25 + .647 - .1093*RR) *DIMCOB1
A(7)= (.5342/RR + 1.276 -.2147*RR) *DIMCOA
B(7)= (.1167/RR**25 + .7733 -.1284*RR) *DIMCOB1

```

```
A(8)= A(7)
B(8)= B(7)
A(9)= (1.654/RR + 1.069 + 2.154*RR) *DIMCOA
B(9)= (.3546/RR**.25 + .3951 + .2593*RR) *DIMCOB1
A(10)= (1.091/RR + .0276 + .0686*RR) *DIMCOA
B(10)= (.5508/RR**.25 + .6473 -.1365*RR) *DIMCOB2
A(11)= (1.081/RR + .0279 + .0685*RR) *DIMCOA
B(11)= (.3896/RR**.25 + .4567 -.0948*RR) *DIMCOB2
A(12)= A(11)
B(12)= B(11)
RETURN
END
```

## SUBROUTINE RANDOM (S,N)

```

CCCCCCCCCCCCCCCCCCCCCCCCCCCCCCCCCCCCCCCCCCCCCCCCCCCCCCCCCCCC
C                                                                 C
C                                                                 C
C   SUBROUTINE RANDOM GENERATES UNIFORMLY DITRIBUTED RANDOM   C
C   NUMBERS BETWEEN ZERO AND ONE USING POWER RESIDUE METHOD.   C
C                                                                 C
C                                                                 C
CCCCCCCCCCCCCCCCCCCCCCCCCCCCCCCCCCCCCCCCCCCCCCCCCCCCCCCCCCCC

```

```

      INTEGER CONST,N
      REAL DIVIDER,S(N)
      DOUBLE PRECISION SEED,INTPROD
      COMMON /RAND/ CONST, SEED, DIVIDER
      DO 10 I=1,N
        INTPROD=CONST*SEED
        IF (INTPROD .LT. DIVIDER) THEN
          S(I)=INTPROD
        ELSE
          S(I)=INTPROD-INT(INTPROD/DIVIDER)*DIVIDER
        ENDIF
        SEED=S(I)
        S(I)=S(I)/DIVIDER
10    CONTINUE
      RETURN
      END

```

SUBROUTINE MEANVAR (MEAN,VAR,S,N)

```

CCCCCCCCCCCCCCCCCCCCCCCCCCCCCCCCCCCCCCCCCCCCCCCCCCCCCCCCCCCC
C                                                                 C
C                                                                 C
C  SUBROUTINE MEANVAR COMPUTES MEAN AND VARIANCE                C
C  OF TIME SERIES.                                              C
C                                                                 C
CCCCCCCCCCCCCCCCCCCCCCCCCCCCCCCCCCCCCCCCCCCCCCCCCCCCCCCCCCCC

```

```

      INTEGER N
      REAL  MEAN,VAR,S(N)
      SUM=0.
      DO 20 I=1,N
        SUM=SUM+S(I)
20    CONTINUE
      MEAN=SUM/FLOAT(N)
      DIFF=0.
      DO 30 I=1,N
        DIFF=DIFF+(S(I)-MEAN)**2
30    CONTINUE
      VAR=DIFF/FLOAT(N)
      RETURN
      END

```

SUBROUTINE PROB (VTS,LVTS,NBINS,VRANGE,PROBDIS)

```

CCCCCCCCCCCCCCCCCCCCCCCCCCCCCCCCCCCCCCCCCCCCCCCCCCCCCCCCCCCC
C                                                                 C
C                                                                 C
C   SUBROUTINE PROB COMPUTES PROBABILITY DISTRIBUTION           C
C   OF TIME SERIES.                                           C
C                                                                 C
C                                                                 C
CCCCCCCCCCCCCCCCCCCCCCCCCCCCCCCCCCCCCCCCCCCCCCCCCCCCCCCCCCCC

```

```

      INTEGER LVTS,NBINS,BINNUM
      REAL DELTAV,VRANGE
      REAL VTS(LVTS),PROBDIS(2*NBINS)
      NBX2=2*NBINS
      DO 20 I=1,NBX2
        PROBDIS(I)=0.0
20    CONTINUE
      DELTAV=VRANGE/(NBINS-1)
      DO 30 I=1,LVTS
        IF ( VTS(I) .LT. 0.0 ) THEN
          IF ( VTS(I) .GE. -VRANGE ) THEN
            BINNUM=NBINS+INT(VTS(I)/DELTAV)
          ELSE
            BINNUM=1
          ENDIF
          PROBDIS(BINNUM)=PROBDIS(BINNUM)+1./LVTS
        ELSEIF ( VTS(I) .GE. 0.0 ) THEN
          IF ( VTS(I) .LE. VRANGE ) THEN
            BINNUM=NBINS+INT(VTS(I)/DELTAV)+1
          ELSE
            BINNUM=2*NBINS
          ENDIF
          PROBDIS(BINNUM)=PROBDIS(BINNUM)+1./LVTS
        ENDIF
30    CONTINUE
      RETURN
      END

```

## SUBROUTINE PSD (Y,N,L,LP2,DT,PSY,ZY)

```

CCCCCCCCCCCCCCCCCCCCCCCCCCCCCCCCCCCCCCCCCCCCCCCCCCCCCCCCCCCC
C
C  SUBROUTINE PSD USES FFT TO ESTIMATE THE FREQUENCY SPECTRUM OF  C
C  TIME SERIES                                                    C
C
C  ARGUMENTS                                                    C
C      Y      -INPUT VECTOR OF LENGTH N CONTAINING              C
C              THE TIME SERIES.                                C
C      N      -INPUT LENGTH OF THE TIME SERIES.                 C
C      L      -LENGTH OF THE TIME SERIES IN EACH SEGMENT.      C
C              L MUST BE A POWER OF 2.                          C
C      LP2    -L=2**LP2 (L AS POWER OF TWO)                     C
C      LD2P1  -SPECTRAL COMPUTATIONS ARE AT                     C
C              LD2P1= (L/2)+1 FREQUENCIES.                     C
C      DT     -SAMPLING INTERVAL (SEC)                          C
C      PSY    -OUTPUT VECTOR OF LENGTH LD2P1 CONTAINING         C
C              THE SPECTRAL ESTIMATES OF Y                     C
C              NOTE THAT THE SPECTRAL ESTIMATES ARE             C
C              TAKEN AT FREQUENCIES (I-1)/(L*DT) (HERTZ)        C
C              FOR I=1,2, ...,LD2P1                             C
C      ZY     -COMPLEX WORK VECTOR OF LENGTH L                  C
C
C  REMARKS :                                                    C
C      1) THE SPECTRAL DENSITY FUNCTION IS DEFINED              C
C          ACCORDING TO EQ. 2.3 FROM CHAPTER TWO.               C
C      2) PRIOR TO CALLING PSD, THE MEAN OF TIME                C
C          SERIES Y SHOULD BE REMOVED FROM EACH                 C
C          ELEMENT OF THE TIME SERIES.                          C
C      3) THE OUTPUT IS RETURNED IN UNITS WHICH ARE            C
C          THE (SQUARE OF THE DATA)/FREQUENCY                 C
C
C  SEGMENT AVERAGING IS USED TO OBTAIN THE SMOOTH ESTIMATES    C
C  THE TOTAL SAMPLE SIZE N = NSEG*L = NSEG*(2**LP2)           C
C  WHERE NSEG = NUMBER OF SEGMENTS                             C
CCCCCCCCCCCCCCCCCCCCCCCCCCCCCCCCCCCCCCCCCCCCCCCCCCCCCCCCCCCC

```

```

REAL Y(N),PSY(L/2+1)
COMPLEX ZY(L)

```

```

LD2P1 = L/2 + 1
NSEG  = INT(N/L)
PI    = ACOS(-1.0)

```

C SCALE FACTOR 0.875 IS DUE TO THE COSINE TAPPERING  
 C TO ADJUST THE POWER SPECTRAL ESTIMATE RESULTS

FACTOR=(DT\*REAL(L))/(0.875)

C INITIALIZE THE PSY

DO 5 J=1,LD2P1

PSY(J)=0.0

5 CONTINUE

DO 50 I=1,NSEG

ND=(I-1)\*L

DO 10 J=1,L

JPND=J+ND

ZY(J)=CMPLX(Y(JPND),0.0)

10 CONTINUE

\* .....

\* ..... TAPERING THE DATA SEQUENCE USING .....

\* ..... THE COSINE TAPER DATA WINDOW .....

\* .....

CALL TAPER(ZY,L,DT)

\* .....

\* ..... COMPUTE DFT .....

\* .....

CALL FFT(ZY,LP2,L)

\* .....

DO 30 J=1,LD2P1

PSY(J)=PSY(J)+FACTOR\*ABS(ZY(J))\*ABS(ZY(J))

30 CONTINUE

50 CONTINUE

\* ..... AVERAGE THE RESULTS FROM NSEG SEPARATE SEGMENTS .....

DO 60 I=1,LD2P1

PSY(I)=PSY(I)/REAL(NSEG)

60 CONTINUE

RETURN

END



```
K=ME/2
W=CMPLX(COS(PI/K),-SIN(PI/K))
DO 6 J=i,k̄
  DO 5 L=J,N,ME
    LPK=L+K
    T=A(LPK)*U
    A(LPK)=A(L)-T
    A(L)=A(L)+T
  U=U*W
5
6
RETURN
END
```

## SUBROUTINE FFT(A,NP,N)

```

CCCCCCCCCCCCCCCCCCCCCCCCCCCCCCCCCCCCCCCCCCCCCCCCCCCCCCCCCCCC
C
C
C   SUBROUTINE FFT FROM NEWLAND (PG 220), REFERENCE 1
C   APPENDIX B, CALCULATES THE DFT OF A SEQUENCE A(1),
C   A(2), ...,A(N), WHERE N = 2**NP, BY THE FFT METHOD.
C
C   ARGUMENTS
C       A  -INPUT COMPLEX VECTOR OF LENGTH N
C           CONTAINING THE DISCRETE TIME SERIES
C       -OUTPUT COMPLEX VECTOR OF LENGTH N
C           CONTAINING THE REQUIRED DFT
C       NP -N=2**NP
C       N  -INPUT LENGTH OF THE TIME SERIES
C
CCCCCCCCCCCCCCCCCCCCCCCCCCCCCCCCCCCCCCCCCCCCCCCCCCCCCCCCCCCC

```

COMPLEX A(N),U,W,T

PI=ACOS(-1.0)

C     DIVIDE ALL ELEMENTS BY N

```

      DO 1 J=1,N
        A(J)=A(J)/N
1      CONTINUE
      ND2=N/2
      NM1=N-1
      J=1
      DO 4 L=1,NM1
        IF (L .GE. J) GO TO 2
        T=A(J)
        A(J)=A(L)
        A(L)=T
2      K=ND2
3      IF (K .GE. J) GO TO 4
        J=J-K
        K=K/2
        GO TO 3
4      J=J+K
      DO 6 M=1,NP
        U=(1.0,0.0)
        ME=2**M

```

SUBROUTINE TAPER(ZY,L,DT)

```

CCCCCCCCCCCCCCCCCCCCCCCCCCCCCCCCCCCCCCCCCCCCCCCCCCCCCCCCCCCC
C
C
C   A SMOOTH FILTER SHAPE FOR FFT ESTIMATES TO
C   REDUCE LEAKAGE CAN BE OBTAINED BY TAPERING
C   THE ORIGINAL RANDOM TIME SERIES AT EACH END.
C   SUBROUTINE TAPER USES A COSINE TAPER DATA
C   WINDOW TO SMOOTH THE DATA AT 1/10 OF EACH
C   END OF THE RECORD (SEE FIG 11.8, PG 146, NEWLAND,
C   REFERENCE 1 IN APPENDIX B).
C
C   ARGUMENTS
C       ZY  -INPUT COMPLEX VECTOR OF LENNGTH
C            L CONTAINING THE ORIGINAL DISCRETE
C            TIME SERIES
C            -OUTPUT COMPLEX VECTOR OF LENGTH
C            L CONTAINING THE TAPERED DATA
C       L   -INPUT LENGTH OF THE TIME SERIES
C       DT  -SAMPLING INTERVAL
C
CCCCCCCCCCCCCCCCCCCCCCCCCCCCCCCCCCCCCCCCCCCCCCCCCCCCCCCCCCCC

```

COMPLEX ZY(L)

```

PI=ACOS(-1.0)
T=DT*REAL(L)
TD10=T/10.0
C1=9.0*TD10
CONST=PI/TD10
DO 20 I=1,L
    TIME=DT*REAL(I-1)
    IF (TIME .LE. TD10) THEN
        WT = 0.5 - 0.5 * COS(CONST * TIME)
        ZY(I) = ZY(I)*WT
    ELSEIF (TIME .GE. C1) THEN
        WT = 0.5 + 0.5 * COS(CONST * (TIME-C1))
        ZY(I) = ZY(I) * WT
    END IF
20 CONTINUE
RETURN
END

```

```

SUBROUTINE PLTSTND (VTS,LVPLT,DELTAT,ANS1)
INTEGER MARK,ICODE,IRATE,MODEL
PARAMETER (MARK=0)
REAL DELTAT,WIDTH,HEIGHT,VBIAS,TBIAS
REAL VTS(LVPLT)
CHARACTER *40 TIMELBL, VELCLBL, ANS1*2
DATA ICODE/ 1 /,IRATE/ 2400 /,MODEL/ 4014 /
DATA WIDTH/ 9.0 /,HEIGHT/ 7.0 /
DATA TORIG/ 0.0 /, VORIG/ 0.0 /, TBIAS/ 3. /, VBIAS/ 1. /
TIMELBL = 'TIME (SEC)'
VELCLBL = 'RANDOM TURBULENCE VELOCITY '//ANS1
* .... FORM MIN & MAX ON THE TIME AXIS ....
      TMIN=0.0
      TMAX=LVPLT*DELTAT
      TFACT=WIDTH/(TMAX-TMIN)
* .... FIND MIN & MAX OF RANDOM VELOCITY VECTOR, VTS ....
      CALL CHECK (VTS,LVPLT,VMIN,VMAX)
      VFACT=HEIGHT/(VMAX-VMIN)
* ....
      CALL PLOTTYPE (ICODE)
      CALL TKTYPE (MODEL)
      CALL BAUD (IRATE)
      CALL SIZE (WIDTH+6. , HEIGHT+3.)
      CALL TEKPAUS
* ....
      CALL SCALE (TFACT,VFACT,TBIAS,VBIAS,TMIN,VMIN)
      CALL AXISL (TMIN,TMAX,TORIG,VMIN,VMAX,VORIG,0.0,1.0,
&              0 , 0 , -1 , 2 , 1. , 1. ,0.2, 0 )
* ..... PRINT HEADINGS .....
      XPOS=TMAX+.1/TFACT
      YPOS=-0.2/VFACT
      CALL SYMBOL (XPOS,YPOS,0.0,0.2,40,TIMELBL)
      XPOS=TMIN+1./TFACT
      YPOS=VMAX+0.4/VFACT
      CALL SYMBOL (XPOS,YPOS,0.0,0.2,40,VELCLBL)
* .... PLOT RANDOM VELOCITY ....
      CALL VECTORS
      IP=0
      DO 10 I=1,LVPLT
        IJ=I-1
        XT=IJ*DELTAT
        YV=VTS(I)
        CALL PLOT (XT,YV,IP,MARK)
        IP=1
10      CONTINUE
      CALL PLOTEND
      RETURN
      END

```

```

SUBROUTINE PLTLOG (SPECT,FREQ,LHALF,LABEL,ANSPLT)
INTEGER MARK,NLABEL,ICODE,IRATE,MODEL
PARAMETER (NLABEL=1,MARK=26)
REAL WIDTH,HEIGHT,FBIAS,SBIAS
REAL SPECT(LHALF),FREQ(LHALF)
CHARACTER *40 LABEL(NLABEL), FREQLBL, PSDLBL*60, ANSPLT*2
DATA ICODE/1/ IRATE/2400/ MODEL/4014/ WIDTH/9./ HEIGHT/7./
DATA FBIAS/1./ SBIAS/1./
FREQLBL = 'FREQ (HZ) '
PSDLBL = 'PSD OF '//ANSPLT//' '//LABEL(NLABEL)
* .... FIND MIN AND MAX OF THE FREQUENCY VECTOR ....
      CALL CHECK (FREQ,LHALF,FMINC,FMAXC)
      FMIN=ALOG10(FMINC)
      FMAX=ALOG10(FMAXC)
      FFACT=WIDTH/(FMAX-FMIN)
* .... FIND MIN & MAX OF THE SPECTRUM VECTOR ....
      CALL CHECK (SPECT,LHALF,SMINC,SMAXC)
      CALL RANGEL (SMINC,SMAXC,SMINR,SMAXR)
      SMIN=ALOG10(SMINR)
      SMAX=ALOG10(SMAXR)
      SFACT=HEIGHT/(SMAX-SMIN)
* ....
      CALL PLOTTYPE(ICODE)
      CALL TKTYPE(MODEL)
      CALL BAUD(IRATE)
      CALL SIZE(WIDTH+2.5,HEIGHT+2.5)
      CALL TEKPAUS
* ....
      CALL SCALE (FFACT,SFACT,FBIAS,SBIAS,FMIN,SMIN)
      CALL AXISL (FMINC,FMAXC,FMINC,SMINC,SMAXC,SMINC,1.,1.
&          ,0,0,1,1,1,1.,0.1,3)
* ....
* .... PRINT HEADINGS ....
* ....
      XPOS=FMIN+3.5/FFACT
      YPOS=SMIN-0.25/SFACT
      CALL SYMBOL (XPOS,YPOS,0.,0.2,40,FREQLBL)
      XPOS=FMIN+1./FFACT
      YPOS=SMAX+0.2/SFACT
      CALL SYMBOL (XPOS,YPOS,0.,0.2,60,PSDLBL)
* ....
* .... PLOT POWER SPECTRUM ....
* ....
      CALL POINTS
      IP=0
      DO 100 I=1,LHALF
        XF=ALOG10(FREQ(I))
        YS=ALOG10(SPECT(I))
        CALL PLOT (XF,YS,IP,MARK)
        IP=1

```

100           CONTINUE  
          CALL PLOTEND  
          RETURN  
          END

## APPENDIX D. INPUT DATA FILE

The following sample input data file is for Mod-0A turbine.





APPENDIX E. PROCEDURAL EXAMPLE OF THE PROGRAM SIMULX  
INTERACTIVE RUN

DO YOU WANT SPECTRUM FOR OTHER TIME SERIES?  
 ENTER (Y OR N)  
 ? Y  
 INPUT ONE TIME SERIES TO GENERATE SPECTRUM.  
 ENTER UX OR UY OR UZ  
 ? UZ  
 TO USE PLTLOG TO PLOT THE SPECTRUM ENTER (Y OR N)  
 ? N  
 DO YOU WANT SPECTRUM FOR OTHER TIME SERIES?  
 ENTER (Y OR N)  
 ? N  
 DO YOU WANT TO PROCESS ANOTHER DATA FILE ?  
 ENTER (Y OR N)  
 ? N 42.224 CP SECONDS EXECUTION TIME.

ENTER NAME OF THE NEW DATA FILE  
 ? DATNZAR

ENTER THE NAME OF OUTPUT FILE  
 ? OUTNZAR

CONST	-	16807		(SEC)
DELTAT	-	.200		
DIVIDER	-	.2147483647000E+10		
SEED	-	.1234570000000E+06		
NRVELOC	-	6300		
OMEGA	-	40.000		(RPM)
OMEGAZ	-	90.000		(DEG)
ROTR	-	62.500		(FEET)
RATIO	-	1.000		
TI	-	10.000		(PERCENT)
TL	-	400.000		(FEET)
URANGE	-	3.000		
UU	-	17.900		(MILES/HR)

DO YOU WANT TO CHANGE ANY VALUES ? ENTER(Y OR N)  
 ? N  
 TO GET LIST OF GENERATED RANDOM VELOCITIES UX, UY, UZ  
 ENTER (Y OR N)  
 ? N  
 TO USE SUBROUTINE PLTSTND TO PLOT THE GENERATED RANDOM  
 VELOCITY VS TIME , ENTER (Y OR N)  
 ? N  
 DO YOU WANT TO EVALUATE PROBABILITY DISTRIBUTIONS OF  
 THE GENERATED RANDOM VELOCITIES ? ENTER (Y OR N)  
 ? Y  
 DO YOU WANT TO GENERATE THE FREQUENCY SPECTRUM OF  
 THE TIME SERIES ? ENTER (Y OR N)  
 ? Y  
 INPUT ONE TIME SERIES TO GENERATE SPECTRUM.  
 ENTER UX OR UY OR UZ  
 ? UX  
 TO USE PLTLOG TO PLOT THE SPECTRUM ENTER (Y OR N)  
 ? N  
 DO YOU WANT SPECTRUM FOR OTHER TIME SERIES?  
 ENTER (Y OR N)  
 ? Y  
 INPUT ONE TIME SERIES TO GENERATE SPECTRUM.  
 ENTER UX OR UY OR UZ  
 ? UY  
 TO USE PLTLOG TO PLOT THE SPECTRUM ENTER (Y OR N)  
 ? N

## APPENDIX F. RESULTS OF THE SAMPLE RUN FOR Mod-0A TURBINE

The simulated results are as observed from the tip of a Mod-0A wind turbine blade.

POWER RESIDUE METHOD WITH THE FOLLOWING PARAMETERS  
IS USED TO GENERATE UNIFORMLY DISTRIBUTED RANDOM NUMBERS

CONSTANT COEFF, CONST : 16897  
SEED : .12345789E+06  
MODULE DIVIDER, DIVIDER : .2147483647660E+10

	ACOEFF	BCOEFF
1	.109271E+00	.277278E+01
2	.524894E-01	.182229E+01
3	.109271E+00	.277279E+01
4	.175240E+00	.294581E-01
5	.175240E+00	.294581E-01
6	.240920E+00	.286800E-01
7	.305939E+00	.258837E-01
8	.305939E+00	.258837E-01
9	.787020E+00	.275591E-01
10	.460793E+00	.662569E-03
11	.456611E+00	.468268E-03
12	.456611E+00	.468268E-03

NUMBER OF RANDOM VELOCITIES GENERATED, NRVELOC : 6300  
TIME STEP TO GENERATE THE RANDOM VELOCITY, DELTAT : .20000E+00  
RADIAL DISTANCE TO SELECTED POINT ALONG THE ROTOR, R : .62500E+02  
ROTOR SPEED, OMEGA : .41888E+01 (RAD/SEC)  
INITIAL ROTATION, OMEGA-ZERO : .15708E+01 (RAD/SEC)  
WIND VELOCITY, UH : .26253E+02 (FEET/SEC)  
TURBULENCE INTEGRAL SCALE, TL : .40000E+03 (FEET)  
TURBULENCE INTENSITY, TI : .10000E+02 (PERCENT)  
SPECTRUM OF THE INPUT WHITE NOISE, SU : .15236E+00 (SEC)  
MEAN VALUE OF UX : .278735E+00 VARIANCE OF UX : .691818E+01  
MEAN VALUE OF UY : .468214E+00 VARIANCE OF UY : .784657E+01  
MEAN VALUE OF VZ : -.242526E-01 VARIANCE OF VZ : .586834E+01

PROBABILITY DISTRIBUTION OF RANDOM VELOCITY TIME SERIES UX OF LENGTH = 6300

PROBABILITY OF UNBIASED IN THE INTERVAL	MID-INTERVAL	PROBABILITY DENSITY ORDINATES OF UX	STANDARD NORMAL ORDINATES
--	--------------	--	------------------------------

PROBABILITY DISTRIBUTION OF RANDOM VELOCITY TIME SERIES				UV OF LENGTH = 6300	
PROBABILITY OF VARIATES IN THE INTERVAL		MID-INTERVAL		PROBABILITY DENSITY ORDINATES OF UV	
LESS THAN	( -3.00 )	( -3.00 )	( -3.00 )	( -3.00 )	( -3.00 )
( -3.00 )	.1587E-03	-2.90	.555556E-02	.595253E-02	.595253E-02
( -2.80 )	.1111E-02	-2.70	.103175E-01	.104209E-01	.104209E-01
( -2.60 )	.2063E-02	-2.50	.222222E-01	.175283E-01	.175283E-01
( -2.40 )	.4444E-02	-2.30	.259841E-01	.283270E-01	.283270E-01
( -2.20 )	.5397E-02	-2.10	.531746E-01	.439836E-01	.439836E-01
( -2.00 )	.1063E-01	-1.90	.738055E-01	.556158E-01	.556158E-01
( -1.80 )	.1478E-01	-1.70	.968317E-01	.940491E-01	.940491E-01
( -1.60 )	.1921E-01	-1.50	.132540E+00	.129518E+00	.129518E+00
( -1.40 )	.2651E-01	-1.30	.200000E+00	.171369E+00	.171369E+00
( -1.20 )	.4000E-01	-1.10	.238808E+00	.217852E+00	.217852E+00
( -1.00 )	.4778E-01	-.90	.245238E+00	.266085E+00	.266085E+00
( -.80 )	.4965E-01	-.70	.244444E+00	.312254E+00	.312254E+00
( -.60 )	.5889E-01	-.50	.311905E+00	.352065E+00	.352065E+00
( -.40 )	.6230E-01	-.30	.358730E+00	.381388E+00	.381388E+00
( -.20 )	.7175E-01	-.10	.35667E+00	.396953E+00	.396953E+00
( .00 )	.7333E-01	.10	.379365E+00	.386953E+00	.386953E+00
( .20 )	.7587E-01	.30	.363482E+00	.381388E+00	.381388E+00
( .40 )	.7270E-01	.50	.385714E+00	.352065E+00	.352065E+00
( .60 )	.6714E-01	.70	.35714E+00	.312254E+00	.312254E+00
( .80 )	.6222E-01	.90	.31111E+00	.266085E+00	.266085E+00
( 1.00 )	.4873E-01	1.10	.243651E+00	.217852E+00	.217852E+00
( 1.20 )	.3825E-01	1.30	.191270E+00	.171369E+00	.171369E+00
( 1.40 )	.2317E-01	1.50	.115873E+00	.139518E+00	.139518E+00
( 1.60 )	.1810E-01	1.70	.904762E-01	.940491E-01	.940491E-01
( 1.80 )	.7619E-02	1.90	.380952E-01	.556158E-01	.556158E-01
( 2.00 )	.6825E-02	2.10	.341270E-01	.439836E-01	.439836E-01
( 2.20 )	.5555E-02	2.30	.277778E-01	.283270E-01	.283270E-01
( 2.40 )	.3492E-02	2.50	.174603E-01	.175283E-01	.175283E-01
( 2.60 )	.3968E-02	2.70	.108413E-01	.104209E-01	.104209E-01
( 2.80 )	.3968E-02	2.90	.555556E-02	.595253E-02	.595253E-02
( 3.00 )	.1111E-02				
GREATER THAN ( 3.00 )	.6349E-03				

PROBABILITY DISTRIBUTION OF RANDOM VELOCITY TIME SERIES				UV OF LENGTH = 6300	
PROBABILITY OF VARIATES IN THE INTERVAL		MID-INTERVAL		PROBABILITY DENSITY ORDINATES OF UV	
LESS THAN	( -3.00 )	( -3.00 )	( -3.00 )	( -3.00 )	( -3.00 )
( -3.00 )	.1111E-02	-2.90	.396825E-02	.595253E-02	.595253E-02
( -2.80 )	.7937E-03	-2.70	.793651E-02	.104209E-01	.104209E-01
( -2.60 )	.1587E-02	-2.50	.174603E-01	.175283E-01	.175283E-01
( -2.40 )	.3492E-02	-2.30	.198413E-01	.283270E-01	.283270E-01
( -2.20 )	.3968E-02	-2.10	.355079E-01	.439836E-01	.439836E-01
( -2.00 )	.7302E-02	-1.90	.600476E-01	.556158E-01	.556158E-01
( -1.80 )	.1381E-01	-1.70	.944444E-01	.940491E-01	.940491E-01
( -1.60 )	.1889E-01	-1.50	.136508E+00	.129518E+00	.129518E+00
( -1.40 )	.2730E-01	-1.30	.181746E+00	.171369E+00	.171369E+00
( -1.20 )	.3635E-01	-1.10	.24127E+00	.217852E+00	.217852E+00
( -1.00 )	.4683E-01	-.90	.284286E+00	.266085E+00	.266085E+00
( -.80 )	.5286E-01	-.70	.312698E+00	.312254E+00	.312254E+00
( -.60 )	.6254E-01	-.50	.363492E+00	.352065E+00	.352065E+00
( -.40 )	.7270E-01	-.30	.422222E+00	.381388E+00	.381388E+00
( -.20 )	.8444E-01	-.10	.384127E+00	.396953E+00	.396953E+00
( .00 )	.7683E-01	.10	.382540E+00	.386953E+00	.386953E+00
( .20 )	.7651E-01				

PROBABILITY DISTRIBUTION OF RANDOM VELOCITY TIME SERIES UZ OF LENGTH - 6300			
PROBABILITY OF VARIATES IN THE INTERVAL	MID-INTERVAL	PROBABILITY DENSITY ORDINATES OF UZ	STANDARD NORMAL ORDINATES
LESS THAN (-3.00) -	-2.00	.238095E-02	.595253E-02
(-2.80) -	-2.70	.119948E-01	.104209E-01
(-2.60) -	-2.50	.150794E-01	.175283E-01
(-2.40) -	-2.30	.16667E-01	.28270E-01
(-2.20) -	-2.10	.452381E-01	.439836E-01
(-2.00) -	-1.90	.555556E-01	.656158E-01
(-1.80) -	-1.70	.102381E-00	.940491E-01
(-1.60) -	-1.50	.130952E+00	.125518E+00
(-1.40) -	-1.30	.201587E+00	.171369E+00
(-1.20) -	-1.10	.237302E+00	.217852E+00
(-1.00) -	-1.00	.288889E+00	.265885E+00
(-.80) -	-.90	.32540E+00	.312254E+00
(-.60) -	-.70	.342063E+00	.352065E+00
(-.40) -	-.50	.362698E+00	.381388E+00
(-.20) -	-.30	.388095E+00	.396953E+00
(.00) -	-.10	.365079E+00	.366953E+00
(.20) -	.00	.315079E+00	.312254E+00
(.40) -	.30	.308730E+00	.266085E+00
(.60) -	.70	.288889E+00	.217852E+00
(.80) -	.90	.217460E+00	.171369E+00
(1.00) -	1.00	.192857E+00	.125518E+00
(1.20) -	1.10	.125190E+00	.940491E-01
(1.40) -	1.30	.102381E+00	.656158E-01
(1.60) -	1.50	.793651E-01	.439836E-01
(1.80) -	1.70	.389952E-01	.28270E-01
(2.00) -	2.00	.277778E-01	.175283E-01
(2.20) -	2.30	.126084E-01	.104209E-01
(2.40) -	2.50	.119048E-01	.595253E-02
(2.60) -	2.70	.317460E-02	
(2.80) -	2.90		
(3.00) -			
GREATER THAN (			

## PROBABILITY DISTRIBUTION OF RANDOM VELOCITY TIME SERIES UZ OF LENGTH - 6300

PROBABILITY OF VARIATES IN THE INTERVAL	MID-INTERVAL	PROBABILITY DENSITY ORDINATES OF UZ	STANDARD NORMAL ORDINATES
LESS THAN (-3.00) -	-2.00	.238095E-02	.595253E-02
(-2.80) -	-2.70	.119948E-01	.104209E-01
(-2.60) -	-2.50	.150794E-01	.175283E-01
(-2.40) -	-2.30	.16667E-01	.28270E-01
(-2.20) -	-2.10	.452381E-01	.439836E-01
(-2.00) -	-1.90	.555556E-01	.656158E-01
(-1.80) -	-1.70	.102381E-00	.940491E-01
(-1.60) -	-1.50	.130952E+00	.125518E+00
(-1.40) -	-1.30	.201587E+00	.171369E+00
(-1.20) -	-1.10	.237302E+00	.217852E+00
(-1.00) -	-1.00	.288889E+00	.265885E+00
(-.80) -	-.90	.32540E+00	.312254E+00
(-.60) -	-.70	.342063E+00	.352065E+00
(-.40) -	-.50	.362698E+00	.381388E+00
(-.20) -	-.30	.388095E+00	.396953E+00
(.00) -	-.10	.365079E+00	.366953E+00
(.20) -	.00	.315079E+00	.312254E+00
(.40) -	.30	.308730E+00	.266085E+00
(.60) -	.70	.288889E+00	.217852E+00
(.80) -	.90	.217460E+00	.171369E+00
(1.00) -	1.00	.192857E+00	.125518E+00
(1.20) -	1.10	.125190E+00	.940491E-01
(1.40) -	1.30	.102381E+00	.656158E-01
(1.60) -	1.50	.793651E-01	.439836E-01
(1.80) -	1.70	.389952E-01	.28270E-01
(2.00) -	2.00	.277778E-01	.175283E-01
(2.20) -	2.30	.126084E-01	.104209E-01
(2.40) -	2.50	.119048E-01	.595253E-02
(2.60) -	2.70	.317460E-02	
(2.80) -	2.90		
(3.00) -			
GREATER THAN (			

FREQUENCY	POWER SPECTRUM UX	FREQUENCY	POWER SPECTRUM UY
.0000	.6049776E+02	.0000	.8989386E+02
.0391	.9142553E+01	.0391	.1706530E+02
.0781	.4392374E+01	.0781	.4204839E+01
.1172	.1679976E+01	.1172	.1871292E+01
.1563	.1372716E+01	.1563	.1153121E+01
.1953	.6355281E+00	.1953	.1167095E+01
.2344	.4387497E+00	.2344	.6118766E+00
.2734	.4920447E+00	.2734	.3259570E+00
.3125	.3293057E+00	.3125	.3297577E+00
.3516	.4551208E+00	.3516	.3092288E+00
.3906	.3742490E+00	.3906	.2687522E+00
.4297	.3363930E+00	.4297	.3199178E+00
.4688	.4426219E+00	.4688	.3419386E+00
.5078	.8901370E+00	.5078	.3487520E+00
.5469	.1336677E+01	.5469	.5458201E+00
.5859	.8356935E+01	.5859	.9514736E+00
.6250	.3142170E+01	.6250	.2168570E+01
.7031	.2461201E+01	.6641	.5168488E+01
.7422	.9707069E+00	.7031	.3560563E+01
.7813	.9767400E+00	.7422	.1244913E+01
.8203	.4996871E+00	.7813	.7072755E+00
.8594	.2980353E+00	.8203	.448072E+00
.8984	.2608651E+00	.8594	.2789843E+00
.9375	.1700205E+00	.8984	.2527932E+00
.9766	.1378442E+00	.9375	.2019094E+00
1.0158	.1494149E+00	.9766	.1031491E+00
1.0547	.1313543E+00	1.0156	.1348067E+00
1.0938	.1022334E+00	1.0547	.1318198E+00
1.1328	.6868052E-01	1.0938	.1765182E+00
1.1719	.7944809E-01	1.1328	.2443295E+00
1.2109	.6845696E-01	1.1719	.2587490E+00
1.2500	.6064474E-01	1.2109	.4152425E+00
1.2891	.6818579E-01	1.2500	.7203783E+00
1.3281	.4364089E-01	1.2891	.0657761E+00
1.3672	.5203108E-01	1.3281	.1071430E+01
1.4063	.3601760E-01	1.3672	.824152E+00
1.4453	.4075913E-01	1.4063	.5735425E+00
1.4844	.3749977E-01	1.4453	.3685053E+00
1.5234	.3325957E-01	1.4844	.3094007E+00
1.5625	.3163256E-01	1.5234	.2187015E+00
1.6016	.3018275E-01	1.5625	.1403191E+00
1.6406	.2819096E-01		
1.6797	.3115463E-01		
1.7188	.2854833E-01		
1.7578	.2519400E-01		
1.7969	.2379286E-01		
1.8359	.2121934E-01		
1.8750	.3200871E-01		
1.9141	.2368969E-01		
1.9531	.2438889E-01		
1.9922	.2110549E-01		
2.0313	.2244003E-01		
2.0703	.3337690E-01		
2.1094	.1591815E-01		

SUM OF THE PSD OF( UX )S= .1152977E+03

1.5625	1.403191E+00	.9766	.186657E+00
1.6016	.101462E+00	1.0156	.127490E+00
1.6406	.603779E-01	1.0547	.1000470E+00
1.6797	.8760638E-01	1.0938	.9063876E-01
1.7188	.6238084E-01	1.1328	.761685E-01
1.7578	.6009705E-01	1.1719	.7246598E-01
1.7969	.5577859E-01	1.2109	.636310E-01
1.8359	.4889308E-01	1.2500	.7237054E-01
1.8750	.3500600E-01	1.2891	.5168605E-01
1.9141	.381924E-01	1.3281	.6642795E-01
1.9531	.324358E-01	1.3672	.437151E-01
1.9922	.3436401E-01	1.4063	.4236130E-01
2.0313	.3036546E-01	1.4453	.4652180E-01
2.0703	.3361854E-01	1.4844	.4171425E-01
2.1094	.316210E-01	1.5234	.3293463E-01
2.1484	.3414904E-01	1.5625	.2695288E-01
2.1875	.29925E-01	1.6016	.2829352E-01
2.2266	.2434398E-01	1.6406	.2749536E-01
2.2656	.2874651E-01	1.6797	.3116947E-01
2.3047	.230352E-01	1.7188	.2854612E-01
2.3438	.2394717E-01	1.7578	.3514961E-01
2.3828	.2398075E-01	1.7969	.2408404E-01
2.4219	.2671705E-01	1.8359	.2847206E-01
2.4609	.3092459E-01	1.8750	.2664573E-01
2.5000	.2949189E-01	1.9141	.2991973E-01
		1.9531	.2602818E-01
		1.9922	.2111585E-01
		2.0313	.2447086E-01
		2.0703	.2554371E-01
		2.1094	.2189980E-01
		2.1484	.1749072E-01
		2.1875	.3466255E-01
		2.2266	.2096707E-01
		2.2656	.2287831E-01
		2.3047	.2143503E-01
		2.3438	.1595903E-01
		2.3828	.2233711E-01
		2.4219	.2581138E-01
		2.4609	.2196430E-01
		2.5000	.2767664E-01

SUM OF THE PSD OF( UY )S= .1413042E+03

END OF FILE

SUM OF THE PSD OF( UZ )S= .8708381E+03

FREQUENCY	POWER SPECTRUM
.0000	.4910821E+02
.0391	.2016754E+02
.0781	.5251017E+01
.1172	.2365756E+01
.1563	.1620577E+01
.1953	.9669718E+00
.2344	.6585728E+00
.2734	.6639867E+00
.3125	.4445584E+00
.3516	.3142210E+00
.3906	.4005908E+00
.4297	.3685486E+00
.4688	.3684053E+00
.5078	.4969580E+00
.5469	.6630746E+00
.5859	.1274137E+01
.6250	.2100307E+01
.6641	.3123941E+01
.7031	.2578653E+01
.7422	.1575120E+01
.7813	.6152442E+00
.8203	.3063874E+00
.8594	.4205281E+00
.8984	.2710570E+00
.9375	.1969253E+00



## APPENDIX II.A. PADÉ APPROXIMATION FOR MOVING AVERAGE PROCESS

Consider the linear model given by

$$y(t) = \frac{1}{T} \int_{t-T}^t x(\tau) d\tau$$

Differentiating gives

$$\dot{y} = \frac{1}{T} [x(t) - x(t - T)]$$

Laplace transforming gives

$$sY(s) = \frac{1}{T} [X(s) - e^{-Ts}X(s)]$$

The transfer function is thus

$$T(s) = \frac{Y(s)}{X(s)} = \frac{1 - e^{-Ts}}{Ts}$$

Forming the Padé approximation with first order numerator and second order denominator

$$T(s) \approx \frac{a_0 + a_1 s}{b_0 + b_1 s + b_2 s^2} \quad (b_0 = 1)$$

Expanding  $T(s)$  in a power series

$$T(s) = 1 - \frac{1}{2} (Ts) + \frac{1}{6} (Ts)^2 - \frac{1}{24} (Ts)^3 + \dots$$

Dividing the rational approximation and equating like powers of  $s$  gives

$$b_1 = \frac{T}{2}$$

$$b_2 = \frac{T^2}{12}$$

$$a_0 = 1$$

$$a_1 = 0$$

Thus,

$$T(s) = \frac{1}{1 + \frac{T}{2}s + \frac{T^2}{12}s^2} = \frac{\frac{12}{T^2}}{s^2 + \frac{6}{T}s + \frac{12}{T^2}}$$

## APPENDIX II.B

The discrete time transfer function for a sample data system is given by

$$G_t(z) = \frac{z-1}{z} \sum [g(t)|_{t=kT}]$$

where  $g(t)$  is the continuous time unit step response for the turbine given as

$$g(t) = L^{-1} \left[ \frac{T_t(s)}{s} \right]$$

where  $T_t(s)$  is the turbine transfer function between input blade pitch angle and output torque.

For the wind turbine system

$$\begin{aligned} g(t) &= L^{-1} \left[ \frac{TQ_0}{s} + \frac{b_1 s + b_2}{s (s^2 + 2\zeta\omega_n s + \omega_n^2)} \right] \\ &= L^{-1} \left[ \frac{TQ_0}{s} + \frac{b_1 (s + \sigma_1)}{s ((s + \sigma_d \pm j\omega_d))} \right] \\ &= TQ_0 + b_1 \left\{ \frac{\sigma_1}{\omega_n^2} + \frac{a_1}{\omega_n \omega_d} e^{-\sigma_d t} \sin (\omega_d t + \alpha_1 - \alpha) \right\} \end{aligned}$$

where

$$a_1 = \sqrt{\omega_d^2 + (\sigma_1 - \sigma_d)^2}$$

$$\alpha = \tan^{-1} \frac{\omega_d}{-\sigma_d}$$

$$\alpha_1 = \tan^{-1} \frac{\omega_d}{(\sigma_1 - \sigma_d)}$$

$$\sigma_1 = \frac{b_2}{b_1}$$

$$\begin{aligned} g(t) &= TQ_0 + \frac{b_2}{\omega_n^2} + \frac{b_1 a_1}{\omega_n \omega_d} d^{-\sigma_d t} \sin(\omega_d t + \sigma_1 - \sigma) \\ &= A + B e^{-\sigma_d t} \sin(\omega_d t + \phi) \end{aligned}$$

where

$$A = TQ_0 + \frac{b_2}{\omega_n^2}$$

$$B = \frac{b_1 a_1}{\omega_n \omega_d}$$

$$\phi = \alpha_1 - \alpha$$

$$g(t) = A + B e^{-\sigma_d t} (\sin \omega_d t \cos \phi + \cos \omega_d t \sin \phi)$$

$$G_t(z) = \frac{z-1}{z} z [g(t)|_{t=kT}]$$

$$= \frac{z-1}{z} \left\{ \frac{z}{z-1} A + \left( \frac{z e^{-\sigma_d T} \sin \omega_d T}{z^2 - 2z e^{-T} \cos \omega_d T + e^{-2\sigma_d T}} \right) B \cos \phi \right\}$$

$$\begin{aligned}
& + \left( \frac{z (z - e^{-\sigma_d T} \cos \omega_d T)}{z^2 - 2ze^{-T} \cos \omega_d T + e^{-2\sigma_d T}} \right) B \sin \phi \} \\
= & A + \left( \frac{(z-1) e^{-\sigma_d T} \sin \omega_d T}{z^2 - 2ze^{-T} \cos \omega_d T + e^{-2\sigma_d T}} \right) B \cos \phi \\
& + \left( \frac{(z-1) (z - e^{-\sigma_d T} \cos \omega_d T)}{z^2 - 2ze^{-T} \cos \omega_d T + e^{-2\sigma_d T}} \right) B \sin \phi \\
= & \{ A(z^2 - 2ze^{-T} \cos \omega_d T + e^{-2\sigma_d T}) \\
& + B(z-1) e^{-\sigma_d T} \cos \phi \sin \omega_d T \\
& + B(z-1) \sin \phi (z - e^{-\sigma_d T} \cos \omega_d T) \} \\
& \{ z^2 - 2ze^{-T} \cos \omega_d T + e^{-2\sigma_d T} \}^{-1} \\
= & \{ (A+B \sin \phi) z^2 + (-2Ae^{-T} \cos \omega_d T + B \cos \phi e^{-\sigma_d T} \sin \omega_d T \\
& - B \sin \phi e^{-\sigma_d T} \cos \omega_d T - B \sin \phi) z + (Ae^{-2\sigma_d T} \\
& - B \cos \phi e^{-\sigma_d T} \sin \omega_d T \\
& + B \sin \phi e^{-\sigma_d T} \cos \omega_d T) \} \{ z^2 - 2ze^{-T} \cos \omega_d T + e^{-2\sigma_d T} \}^{-1} \\
= & \{ (A+B \sin \mu) z^2 + [-2Ae^{-T} \cos \omega_d T
\end{aligned}$$

$$+Be^{-\sigma_d T} \sin(\omega_d T - \phi)]z + [Ae^{-2\sigma_d T} - Be^{-\sigma_d T} \sin(\omega_d T - \phi)]]\}$$

$$\{z^2 - 2ze^{-T} \cos \omega_d T + e^{-2\sigma_d T}\}^{-1}$$

$$G(z) = \frac{C_2 z^2 + C_1 z + C_0}{z^2 + D_1 z + D_0}$$

where

$$C_2 = A + B \sin \phi$$

$$C_1 = -2Ae^{-T} \cos \omega_d T - B \sin \phi + Be^{-\sigma_d T} \sin(\omega_d T - \phi)$$

$$C_0 = Ae^{-2\sigma_d T} - Be^{-\sigma_d T} \sin(\omega_d T - \phi)$$

$$D_1 = -2ze^{-T} \cos \omega_d T$$

$$D_0 = e^{-2\sigma_d T}$$